UNIVERSITEIT VAN PRETORIA
UNIVERSITY OF PRETORIA
YUNIBESITHI YA PRETORIA

Design, Modelling and Construction of a Scalable Dual Fluidised Bed Reactor for the Pyrolysis of Biomass

by

S.D. Swart

A dissertation submitted in partial fulfilment of the requirements for the degree

Magister Scientiae in Chemical Engineering

in the

Department of Chemical Engineering

Faculty of Engineering, the Built Environment and Information Technology

University of Pretoria

Pretoria

South Africa

January 2012

Promoter: Professor Mike Heydenrych

CVD 800

DECLARATION

I declare that this dissertation is my own unaided work. It is being submitted for the Degree of Magister Scientiae at the University of Pretoria, Pretoria. It has not been submitted before for any degree or examination to any other university.

(Signature of Candidate)

On this 3 day of February year 2012

Design, Modelling and Construction of a Scalable Dual Fluidised Bed Reactor for the Pyrolysis of Biomass

S. D. Swart

ABSTRACT

The pyrolysis of biomass is a thermochemical process in which woody biomass is converted to several high-value products such as bio-oil, bio-char and syngas. The forestry sector has shown particular interest in this process as a large quantity of biomass is produced as an underutilised by-product in this sector annually. Dual fluidised beds (DFBs) have been identified as a feasible reactor system for this process. However, little attention has been given to the optimisation or to the design of a scalable DFB for the pyrolysis of biomass process. Therefore, the objective of the current project was the design, modelling and construction of a scalable dual fluidised bed system for the pyrolysis of biomass.

In order to achieve this objective, several tasks were performed, which included the following:

- A literature study was done in order to obtain a theoretical foundation for the current project.
- A novel dual fluidised bed reactor system was designed, which included the block flow diagram and the process and instrumentation diagram for the system.
- A cold unit of the system was built in order to test the performance of the system.
- A comprehensive model for the system was developed, which included mass and energy balance considerations, hydrodynamics and reaction kinetics.
- A complete pilot-scale system of the proposed design was built and tested at the University of Pretoria.

Solids are heated by means of combustion reactions in one of the fluidised beds in the proposed dual fluidised bed design. An overflow standpipe is then used to transport the solids to a second fluidised bed in order to provide the energy required for the endothermic pyrolysis reactions. The cooler solids are then fed back to the combustion fluidised bed by means of a screw-conveyor, creating a circulating system. A two-stage model was used to model the pyrolysis reactions. In this model, the wood is converted to bio-char, syngas and tar compounds. The tar compounds are the desired product as they can be condensed to form liquid bio-oil. However, these compounds undergo a second reaction in the gas phase in which they are converted to bio-char and syngas. It is therefore necessary to quench these gases rapidly in order to maximise the yield of bio-oil obtained from the system. Bio-oil is a source of many high-value chemicals and can also be upgraded to produce liquid bio-fuels. A portion of the syngas is recycled back to the pyrolysis fluidised bed in order to fluidise the bed. In this way, oxygen is prevented from entering the pyrolysis fluidised bed, which would cause the biomass in the bed to undergo combustion rather than pyrolysis. The operating temperatures of the combustion and pyrolysis fluidised beds were optimised at 900°C and 500°C respectively.

A cold unit of the system was built at the Agricultural Research Service in Wyndmoor, Pennsylvania, USA. From the experiments performed on this unit it was found that the solid transport mechanism designed during the project is suitable for the pyrolysis of biomass process. In addition, the solids circulation rate between the two beds was easy to control, which is necessary in order to maximise the yield of bio-oil obtained from the system. A pilot-scale unit of the dual fluidised bed design was built in order to finalise the design and ensure that it could be scaled up. This system included all the downstream units, which had to be designed for the dual fluidised bed system. Several cold-run experiments were also performed on the pilot-scale system in order to ensure that it would perform as required during operation. It was found that the combustion fluidised bed could be fluidised as required and that the circulation of solids between the combustion and pyrolysis fluidised beds functioned well and could be easily controlled. Therefore, it was concluded that the proposed dual fluidised bed system is suitable for the pyrolysis of biomass process and is a feasible reactor system for the large-scale pyrolysis of biomass.

The large-scale operation of the proposed dual fluidised bed system offers several advantages, particularly within the forestry sector. These advantages have important implications, as follows:

- The current research offers the opportunity for the forestry sector to shift its focus from the production of traditional wood products, such as pulp and paper, to products such as specialised chemicals.
- The bio-oil produced in the dual fluidised bed system can be upgraded to renewable liquid fuels, which may help reduce the dependence of the infrastructure on fossil fuels.
- The dual fluidised bed system provides an opportunity for capturing and removing CO_2 from the atmosphere in the form of bio-char. It is therefore considered to be a carbon-negative process, and may help reduce the concentration of greenhouse gases.
- The bio-char produced in the dual fluidised bed system can be used to feed nutrients back to plantation floors in the forestry sector, thereby aiding the growth of further plantations.

ACKNOWLEDGEMENTS

The author would like to acknowledge the Paper Manufacturers Association of South Africa (PAMSA) and Sappi for providing the funding necessary for the current project, as well as Eric Verhasselt, a student intern at the USDA's Agricultural Research Service (ARS), who produced the experimental results necessary for the project under ARS non-funded Cooperative Research Agreement #1935-41000-082-03.

CONTENTS

LIST OF FIGURES

LIST OF TABLES

NOMENCLATURE

A	area (m^2)
C_i	concentration of component i ($kmol/m^3$)
C_p	specific heat capacity (J/kg K)
d	diameter (m)
d_b	average diameter of the bubbles (m
d_p	average diameter of the particles (m)
D_C	cyclone diameter (m)
E_i	activation energy for reaction i (J/kmol)
f	solid volume fraction
g	gravitational acceleration (m/s^2)
h	heat transfer coefficient (W/m^2K)
h	height (m)
h	heat transfer coefficient ($W/m^2 K$)
H	height (m)
K	mass-transfer coefficient (1/s)
k	reaction rate constant (dependant)
k	thermal conductivity ($W/m \cdot K$)
Kc	pressure difference constant (Pa)
L	thickness (m)
m	mass (kg)
N	number of discrete sections
Nu	Nusselt number
P	pressure (Pa)
Pr	Prandtl number
$P_{45\mu m}$	weight fraction of particles smaller than 45 µm
Q	energy (kJ)
Q	overall rate of heat transfer (W)
R	outer radius (m)
r	radius (m)
R	universal gas constant (J/mol K)
R	thermal resistivity ($m^2 K/W$)
Re	Reynolds number
r_i	reaction rate for component i ($kmol/m^3 s$)
T	temperature (K)
t	time (s)
u	velocity (m/s)
u_0	feed-gas superficial velocity (m/s)
u_{br}	rise velocity of a single bubble (m/s)
V	volume (m^3)

Greek letters

$\emptyset_c$	volume fraction of carbon
ϕ_s	sphericity

$\mathcal{D}_e$	effective diffusivity in the catalyst (m^2/s)
ΔH	heat of reaction ($J/kmol$)
δ	bubble fraction
ε	porosity
μ	viscosity ($Pa\ s$)
ρ	density (kg/m^3)
$\mathcal{D}$	diffusivity (m^2/s)

Subscripts

0	initial values
1	at point 1
2	at point 2
b	bubble
c	cloud/char
$conv$	convection
$cond$	conduction
CF	combustion freeboard
e	emulsion
eff	effective
g	gas
k	at turbulent fluidisation
mb	at minimum bubbling
mf	at minimum fluidisation
n	for the n^{th} element
OS	overflow standpipe
PB	pyrolysis bed
PF	pyrolysis freeboard
t	terminal velocity
$total$	total
w	wood

CHAPTER 1: INTRODUCTION

1.1 Introduction

During the pyrolysis of cellulosic biomass, such as sawdust, wood bark, maize husks and straw, the low-value woody residues are converted into high-value liquid bio-fuels (Meier & Faix, 1997). As a result, this process provides the opportunity to produce a relatively large, competitively priced, renewable fuel. Fluidised beds have been identified as a feasible reactor design for the pyrolysis process as they allow high rates of heat transfer at moderate temperatures and short residence times of the product gas in the reactor (Demirbas, 2006). This is required in order to maximise the yield of bio-oil obtained from the pyrolysis process. The forestry sector has shown particular interest in this technology because a large quantity of underutilised biomass is produced as a by-product in this sector annually.

The focus of the current study is on the use of dual fluidised beds for the pyrolysis of biomass as they offer several advantages over other fluidised bed designs in the pyrolysis process. Although many dual fluidised bed designs have been developed for the pyrolysis of biomass, little attention has been given to the development of these designs for large-scale operations. The objective of the current investigation was, therefore, the design, modelling and construction of a scalable dual fluidised bed system for the pyrolysis of biomass.

1.2 Background

The current project was undertaken at the University of Pretoria in South Africa in collaboration with the Department of Agriculture in the United States, the Paper Manufacturers Association of South Africa (PAMSA) and Sappi. The forestry sector in South Africa has shown particular interest in the pyrolysis of biomass as it offers the opportunity for converting the large quantity of underutilised biomass that is produced in the forestry sector as a by-product annually into high-value products.

Pyrolysis is an endothermic, thermochemical process in which the long polymers present in biomass are split in the absence of oxygen to form shorter polymers (Meier & Faix, 1997). The products obtained from this process include heat, syngas, bio-char and liquid bio-oils, which are a source of high-value products and may be upgraded to form liquid bio-fuels (Demirbas, 2006).

1.3 Problem Statement

A large quantity of underutilised woody biomass is produced as a by-product in the forestry sector annually. It has been suggested that this biomass could be used as a feedstock in the pyrolysis process for the production of renewable liquid fuels and other high-value products. The problem is that although many reactor designs for the pyrolysis of biomass have been developed, the technology is still relatively new and little attention has been given to the design and testing of scalable reactors for the pyrolysis of biomass.

The dual fluidised bed reactor has been identified as a feasible reactor design for the large-scale pyrolysis of biomass. However, most dual fluidised bed reactors used for the pyrolysis of biomass are only slightly modified forms of the reactors used in other processes, such as the gasification of biomass. Little attention has been given to the optimisation of the dual fluidised bed reactor design for the pyrolysis of biomass.

1.4 Objectives

The main objective of this project was the design, modelling and construction of a scalable dual fluidised bed system, which would be optimised for the pyrolysis of biomass process. Several sub-objectives were considered during the project, as follows:

- A comprehensive model for the dual fluidised bed system must be developed, and should include mass and energy balance considerations, the hydrodynamics of the system and reaction kinetics.
- The model must be evaluated in order to determine the steady-state conditions required for the system. This objective will require the optimisation of the model.
- A scalable dual fluidised bed reactor must be designed and optimised for the pyrolysis of biomass process.
- A cold model of the dual fluidised bed system must be built in order to test the performance of the design and its applicability to the pyrolysis of biomass process.
- A pilot-scale system of the dual fluidised bed design must be designed and built in order to investigate all considerations required for the construction of the system and to ensure that the design can be scaled up for large-scale operations.
- The downstream processes required for the dual fluidised bed system must also be designed and built in order to optimise the design of these units for the pyrolysis of biomass process.

1.5 Importance of Research

The combustion of fossil fuels, such as coal and petroleum, is one of the main processes used for the production of energy in the world. This process has been identified as a large contributor towards greenhouse gas emissions (Zhang, Xu, Champagne, 2010). Concern about the impact of the process on the environment and its sustainability has prompted most countries to seek alternative, renewable sources of energy (Zhang *et al.*, 2010). The pyrolysis of biomass has been identified as a feasible process for the production of energy and other high-value products (Demirbas, 2006). Therefore this process is important as it offers several advantages, as follows:

- The combustion of fossil fuels, such as coal and petroleum, for the production of energy is not sustainable and the pyrolysis of biomass process may help minimise the world's dependence on these sources of energy.
- The bio-oil obtained from the pyrolysis of biomass is a source of many high-value chemicals.
- Bio-char is produced during the pyrolysis of biomass, which can be fed back to forestry floors to return nutrients to the soil. In this way, the pyrolysis of biomass process offers the opportunity to remove carbon from the atmosphere and is therefore considered to be a carbon-negative process. This is important as is may help reduce the concentration of greenhouse gases in the environment.

In order to realise these advantages, a feasible reactor system needs to be developed for the pyrolysis of biomass, which can be scaled up for large-scale operations. This research project provides an overview of the modelling, design and construction of such a system.

1.6 Methodology

In order to achieve the objectives of the current project, the project was divided into several phases:

1. A literature study was performed to identify feasible systems for the pyrolysis of biomass and the modelling techniques used for these systems.
2. With the use of the information gathered during the literature study, a feasible system was designed for the pyrolysis of biomass, which could be scaled up for large-scale operations.
3. A cold model of the designed system was built in order to test the performance of the system.
4. A model for the system was developed and optimised to determine important design considerations and the required steady-state values for the system.
5. A complete three dimensional (3D) model of a pilot-scale system for the process was developed with the use of the information gathered during the modelling phase of the project.
6. A pilot-scale system was built in order to identify all considerations required for the construction of the system.

1.7 Scope of Study

The scope of the study was the design, modelling and construction of a scalable dual fluidised bed system for the pyrolysis of biomass. A cold model of the system was built to test the performance of the dual fluidised bed design.

1.8 Conclusions

The pyrolysis of biomass allows the conversion of cellulosic biomass into high-value products such as bio-oil and bio-char (Demirbas, 2006). The forestry sector has shown particular interest in this technology due to the large quantity of underutilised biomass that is produced as a by-product in this sector annually. The dual fluidised bed reactor has been identified as a feasible reactor system for the pyrolysis of biomass, but little attention has been given to the design of a scalable system for the pyrolysis of biomass.

This project was undertaken at the University of Pretoria and focused on the design, modelling and construction of a scalable dual fluidised bed system for the pyrolysis of biomass. Included in the objectives of this project were the construction of a cold model of the system, which was used to test the performance of the system, and a pilot-scale unit.

The bio-oil obtained from the pyrolysis of biomass process could be used as an alternative source of fuel to fossil fuels. This process also offers several advantages over the combustion of fossil fuels, such as being environmentally friendly and sustainable (Zhang *et al.,* 2010). The current research is therefore important as it provides an overview of a novel dual fluidised bed design for the pyrolysis of biomass process, which may be scaled up for large-scale operations.

CHAPTER 2: THEORETICAL FOUNDATION

2.1 Introduction

The pyrolysis of biomass is a thermochemical process in which the long polymers present in the biomass are split to form compounds of lower molecular weight. These long polymers include cellulose, hemicelluloses and lignin (Fengel & Wegener, 1989: 26). Fluidised beds have been identified as a favourable type of reactor for the pyrolysis process as they allow high rates of heat transfer at moderate temperatures and excellent control over the temperature in the reactor (Demirbas, 2006), which is important as the yields obtained from the pyrolysis process are very temperature dependent (Papadikis, Gu & Bridgwater, 2009). In addition, these types of reactor allow the separation of the endothermic reactions in the pyrolysis process from the exothermic reactions. In this way, the compounds involved in the two types of reaction do not interfere with one another.

The pyrolysis of biomass is a relatively new area of study and involves several other branches of study, including the composition of biomass, thermochemical conversion techniques and fluidisation. To obtain the maximum benefit from the remainder of this dissertation, a background of these areas of study is required is provided in this chapter.

2.2 Biomass

2.2.1 Overview

Biomass refers to any biological material that is obtained from living or recently living organisms. It consists mostly of carbon, hydrogen and oxygen-based compounds such as oils, fats and other polysaccharides (Fengel & Wegener, 1989: 26). The forestry sector has a large quantity of underutilised biomass in the form of cellulosic material. Biomass can be upgraded to high-value products such as syngas and bio-oil by means of thermochemical conversion techniques (Zhang *et al.*, 2010). The term biomass is therefore used in the remainder of this document to refer to cellulosic material, also called woody biomass. Woody biomass is biomass obtained from woody plants, such as trees, in which the main compound is cellulose. Other major compounds found in woody biomass are lignin and hemicelluloses (Bowyer, Shmulsky & Haygreen, 2007: 48).

2.2.2 Cellulose

Cellulose is a polysaccharide consisting of a linear chain of up to 10 000 glucose units linked together by β-glycosidic bonds. Cellulose is the most abundant organic compound found in nature and makes up 40% to 44% of the organic constituents of both hardwood and softwood trees (Bowyer *et al.*, 2007: 49). The schematic structure of cellulose is illustrated in Figure 2.1.

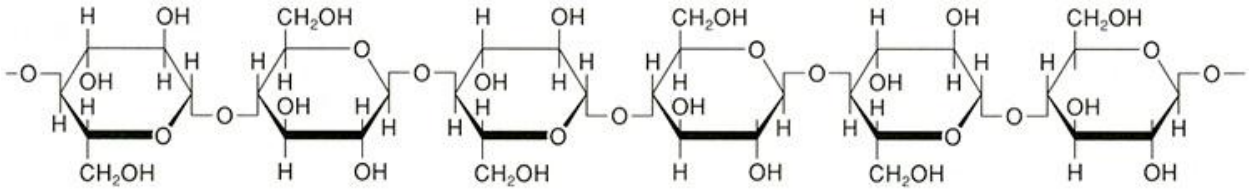

Figure 2.1: The schematic representation of the chemical structure of cellulose consisting of β-(1→4)-linked glucose units (Fengel & Wegener, 1989: 68)

2.2.3 Hemicelluloses

Hemicelluloses, also called polyoses, are branched-chain polymers of six-carbon sugars, such as galactose and mannose, and five-carbon sugars, such as xylose and arabinose. The number of monomeric units in hemicelluloses is substantially lower than in cellulose with a degree of polymerisation in the hundreds rather than the thousands, such as in the case of cellulose. An example of a polyose is mannan, which is a heteropolymer consisting of mannose and glucose units. The structure of mannan is shown in Figure Figure **2.2** (Fengel & Wegener, 1989: 106).

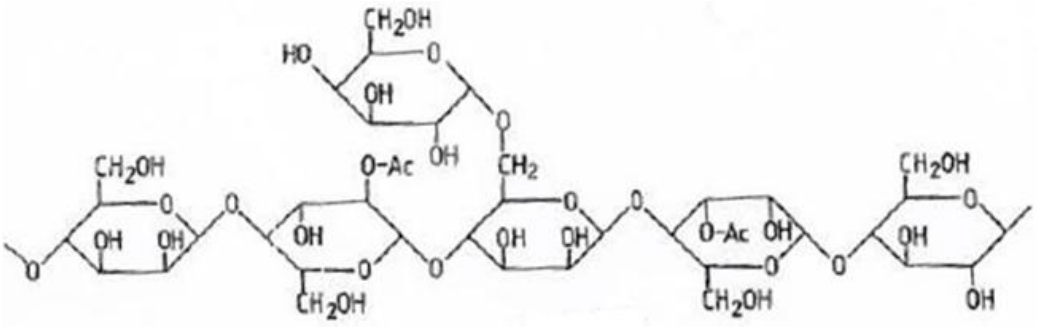

Figure 2.2: The schematic representation of the partial chemical structure of O-acetyl-galactoglucomannan (Fengel & Wegener, 1989: 116)

2.2.4 Lignin

Lignin is the second most abundant organic compound found in nature. It is a complex polymer of high molecular weight, built from phenyl-propane units. Three types of phenylpropanoid compound form the building blocks of lignin, which are shown in Figure 2.3. Lignin is a very stable compound and is found in a variety of forms. For this reason, lignin often poses a challenge during the thermochemical conversion of biomass. Unlike cellulose and hemicelluloses, lignin is not a carbohydrate but is instead phenolic in nature (Fengel & Wegener, 1989: 132).

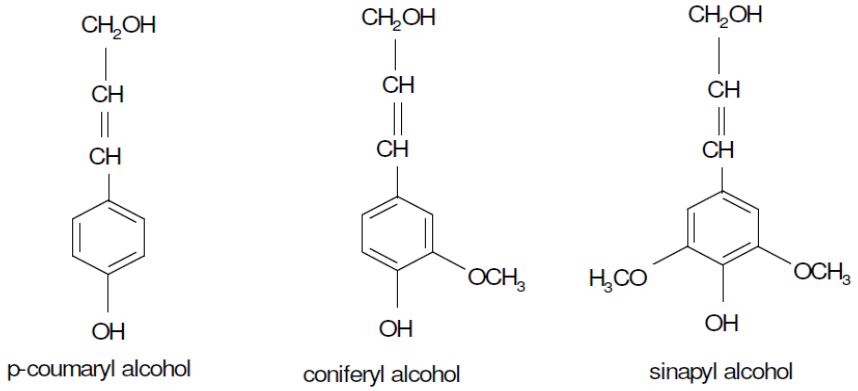

Figure 2.3: The building units of lignin, namely p-coumaryl alcohol, coniferyl alcohol and sinapyl alcohol (Fengel & Wegener, 1989: 133)

2.3 Thermochemical Conversion of Biomass

2.3.1 Overview

Thermochemical conversion processes are temperature-dependent reactions which are used for the conversion of biomass to high-value products (Demirbas, 2006). There are several thermochemical processes for the conversion of biomass, which are shown in Figure 2.4 (Robbins *et al*, 2012). These processes are divided into two groups, namely those that require the presence of oxygen and those that require the absence of oxygen or an oxygen-limited environment.

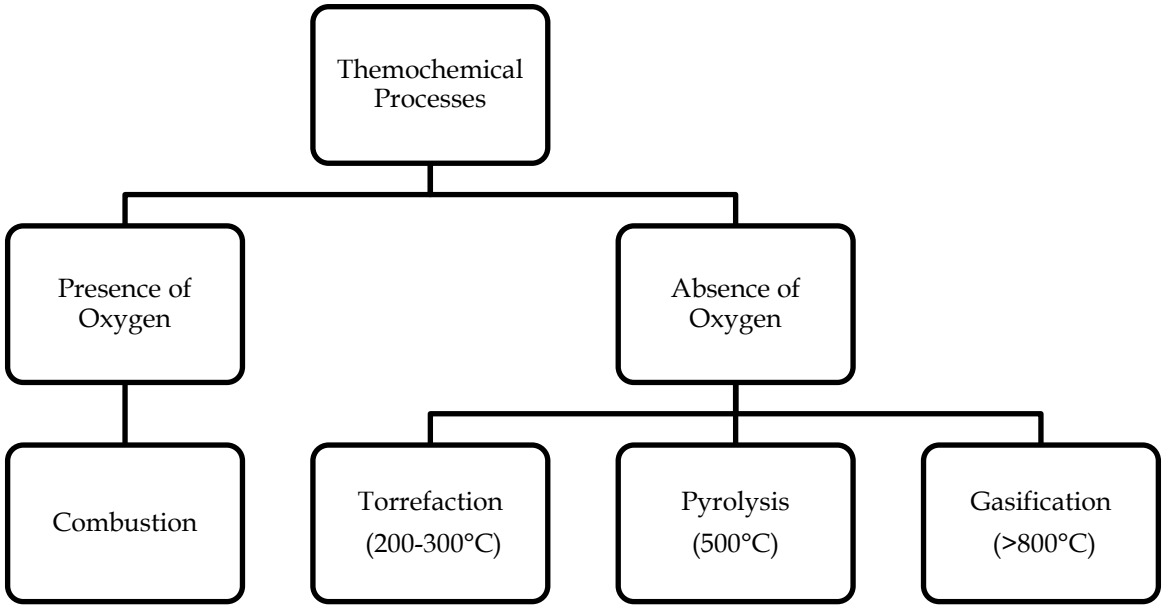

Figure 2.4: The main thermochemical processes for the conversion of biomass, namely combustion, torrefaction, pyrolysis and gasification.

The thermochemical conversion of biomass leads to the formation of four important products, namely heat, bio-char, bio-oil and syngas (Demirbas, 2006). Each one of the four conversion processes shown in Figure **2.4** is used to maximise the yield of one of these products. The combustion of biomass is exothermic, whereas torrefaction, pyrolysis and gasification are all endothermic processes. These last three processes differ according to the temperature at which they occur (Robbins *et al*, 2012). All three processes produce bio-char, bio-oil and syngas. However, the yields of these three products vary greatly, depending on the temperature of the process. The typical yields obtained for the three endothermic thermochemical processes in Figure **2.4** and the uses for the main product from each process are shown in Table 2.1 (Robbins *et al*, 2012).

Table 2.1: Product yields and uses from the thermochemical conversion of biomass

Conversion Process	Yields			Uses
	Bio-char	Syngas	Bio-oil	
Torrefaction	85%	15%	< 1%	Fuel for boilers
Pyrolysis	12%	13%	75%	Production of high-value chemicals and fuels
Gasification	< 1%	95-99%	1-5%	Generation of electricity

2.3.2 Pyrolysis

Pyrolysis is the degradation of biomass at elevated temperatures and in an oxygen-free environment. During pyrolysis, the macromolecular compounds present in biomass, such as cellulose and hemicelluloses, are split to form compounds of lower molecular weight (Meier & Faix, 1997). The products from pyrolysis include liquids and gaseous products, as well as a solid residue of charcoal, known as bio-char (Demirbas, 2006). The main product produced during pyrolysis is bio-oil, which is a source of many different types of organic compounds. Bio-oil may also be used as a source of renewable fuel, such as bio-diesel (Robbins *et al*, 2012). In addition, the bio-oil obtained from pyrolysis is more convenient to transport and store than biomass.

The pyrolysis of biomass may be modelled with the use of a two-stage pyrolysis model, which is shown in Figure 2.5 (Papadikis *et al.*, 2009). In this model, the woody biomass is converted into three types of product, namely char, tar and gas products. The char product is the solid bio-char, while the tar and gas compounds include all of the gaseous compounds formed during pyrolysis. Unlike the gas compounds, which include all of the incondensable gases (syngas), the tar gases are liquids at room temperature (bio-oil). Therefore the objective of pyrolysis is to maximise the yield of the tar compounds. However, the pyrolysis model also includes a second stage in which the gaseous tar compounds react to form char and gas compounds (Papadikis *et al.*, 2009). It is therefore important to minimise the residence time of this second stage. This is achieved through a process called fast pyrolysis, in which small wood particles are heated rapidly to the desired temperature and the gases that are formed are quenched rapidly once they leave the reactor. Slow pyrolysis with larger wood particles produces mostly bio-char (Meier & Faix, 1997). In addition, the two-stage pyrolysis model takes account of the fact that the moisture in the wood must also be converted into vaporised water, which affects the energy balance of the reactor.

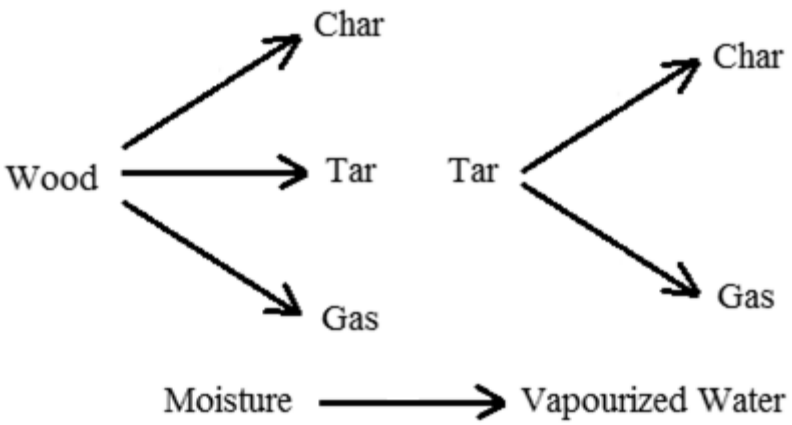

Figure 2.5: The two-stage pyrolysis model, illustrating the conversion of woody biomass into char, tar and gas products (Papadikis *et al.*, 2009)

Although the objective of this research is to maximise the yield of bio-oil from the system, the bio-char and syngas produced from the pyrolysis of biomass also have several uses. The bio-char in particular has received much attention for its uses in environmental management. Apart from the generation of heat through combustion, the high-grade bio-char obtained from the pyrolysis of biomass can also be returned to forestry floors for soil amendment to enhance the nutrition of the soil. The pyrolysis of biomass allows the sequestration of carbon as the bio-char produced during pyrolysis is first captured from the environment in the form of carbon dioxide. The syngas produced during pyrolysis consists mostly of hydrogen and carbon monoxide, which can be combusted to produce heat. The syngas may also be used in the Fischer-Tropsch process to produce liquid hydrocarbons, which may be used in fuel replacement (Robbins *et al*, 2012).

2.4 Fluidisation

During the fluidisation of a bed of solid particles, a fluid is passed upwards through the bed, which exerts an upward physical drag force on the particles. At a certain fluid velocity, this upward drag force is equal to the downward gravitational force on the particles. At this point, the bed is said to be fluidised and takes on the properties and appearance of a fluid (Kunii & Levenspiel, 1991: 1). As the fluid velocity increases, the bed takes on different appearances, called fluidisation regimes. An overview of the different fluidisation regimes is shown in Figure 2.6. If the velocity of the fluid is increased beyond the bubbling fluidised regime, the solid particles become entrained from the bed and must therefore be circulated back to the bed.

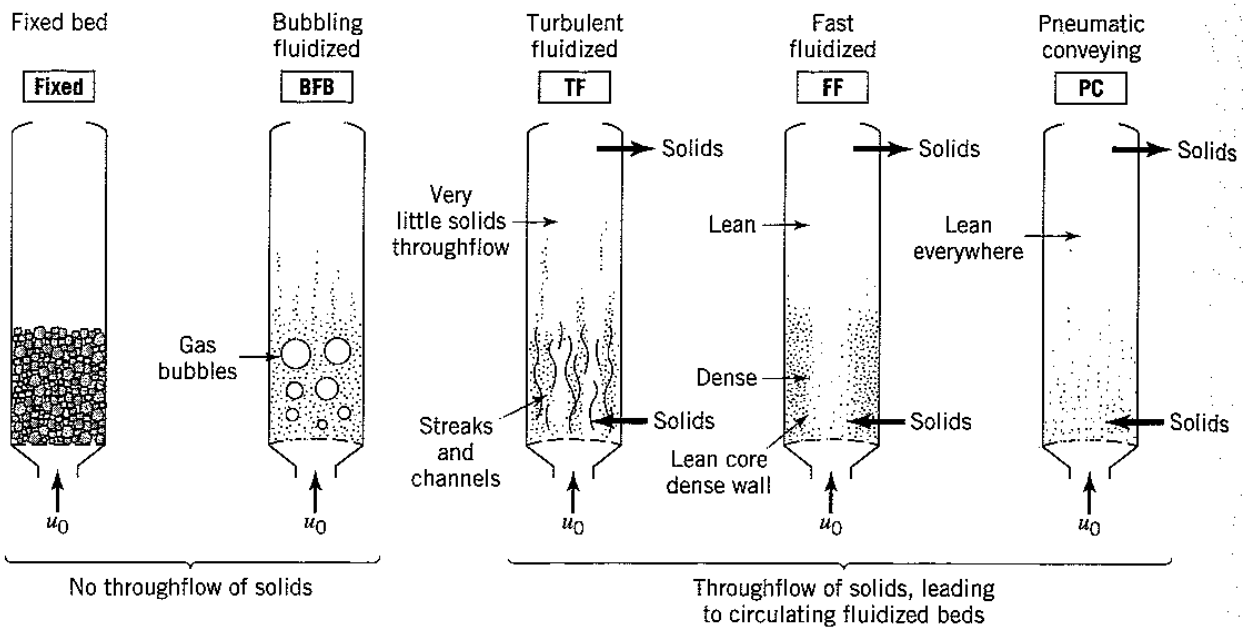

Figure 2.6: The regimes found in fluidised beds, from low to high fluid velocity (Levenspiel, 1999: 448)

In the bubbling fluidised regime, the bed takes on the appearance of a boiling liquid with large bubbles rising rapidly through the bed. A bubbling fluidised bed consists of two distinct zones, namely a bubble phase and an emulsion phase. In fine particle beds, gas circulates within the bubble and a thin cloud surrounding the bubble. Therefore three phases exist within the vicinity of a bubble, namely the bubble itself, a cloud and the emulsion phase. The gas flow in the vicinity of a rising gas bubble with all three phases is illustrated in Figure 2.7. These three phases introduce mass transfer limitations and must be considered during the development of a model of the system (Levenspiel, 1999: 451-454).

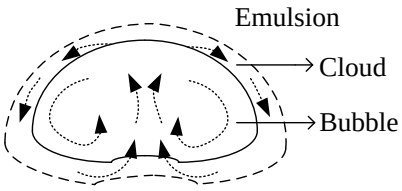

Figure 2.7: A model illustration of the three phases of a rising bubble, namely bubble, cloud and emulsion (Levenspiel, 1999: 454)

Bubbling fluidised beds consist of multiple zones, as shown in Figure 2.8 (Kunii & Levenspiel, 1991: 166). The change in the volume fraction of solids with the height of a bubbling fluidised bed is also shown in Figure 2.8. The zones in a bubbling fluidised bed are the following:

- *Freeboard:* Region between the bed surface and the gas outlet.
- *Splash zone:* Region just above the bed surface into which the particles fall back down.
- *Disengagement zone:* Region above the splash zone in which the volume fraction of solids decreases with height.
- *Dilute transport zone:* Region above the disengagement zone in which all particles are carried upwards. The volume fraction of solids remains constant in this region.

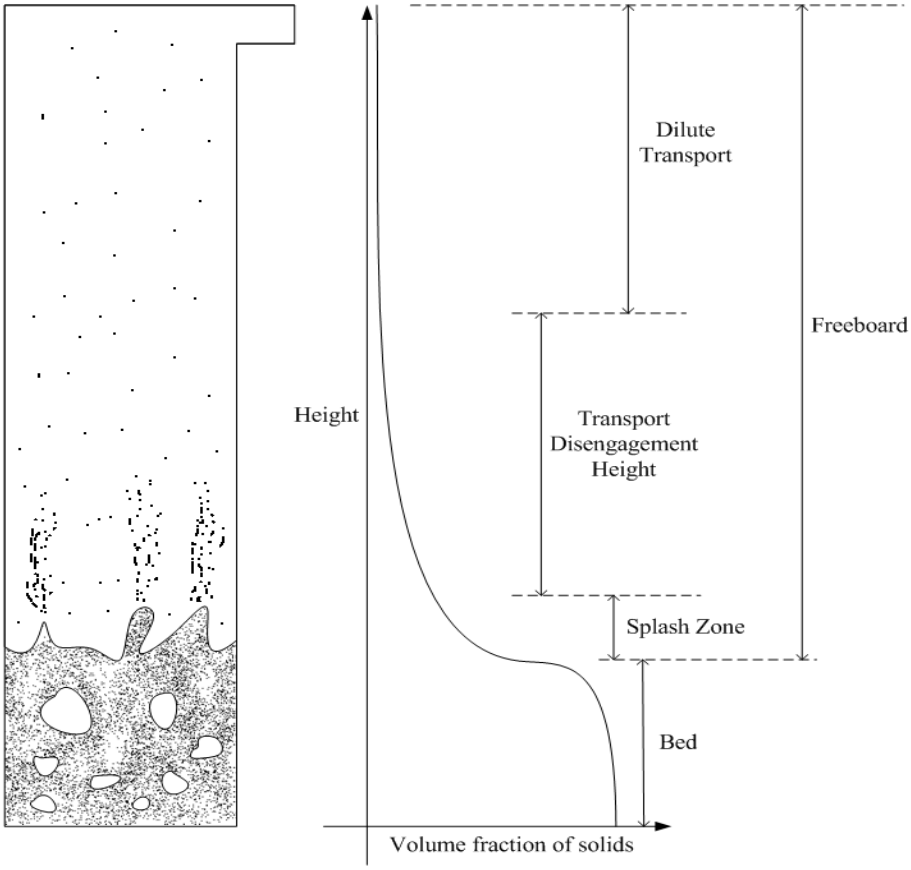

Figure 2.8: The different zones in a bubbling fluidised bed, which include the bed, splash zone, transport disengagement height and dilute transport zones

2.5 Conclusions

Biomass is obtained from living or recently living organisms, and consists of three types of polymeric compounds, namely cellulose, hemicelluloses and lignin. During pyrolysis these compounds are split to form lower molecular weight products that are of a higher value. The feedstock used in the current project is woody biomass, which is biomass obtained from woody plants, such as trees, in which the main compound is cellulose.

Pyrolysis, like other thermochemical processes, is a temperature-dependent process in which only heat is used to drive the pyrolysis reactions. Other examples of thermochemical processes in which biomass is used as the feedstock are combustion, torrefaction and gasification. The combustion of biomass differs from the other types of thermochemical process in that it takes place in the presence of oxygen. Torrefaction, pyrolysis and gasification differ according to the temperature used and the primary product formed during each process. The primary product of torrefaction is bio-char, which is obtained at a temperature between 200 and 300°C. Pyrolysis yields mainly condensable gases at a temperature of approximately 500°C, which can be condensed to form bio-oil. Incondensable gases, also called syngas, are mostly formed during gasification, which occurs at temperatures above 800°C.

An upward drag force is exerted on a bed of solids when a fluid is passed upwards through the bed. When this upward drag force is greater than the force of gravity on the particles, the particles begin to exhibit the same properties as a fluid. At this point, the bed is said to be fluidised. Fluidised beds offer several advantages compared with other types of reactor, such as near-isothermal temperatures throughout the bed due to the rapid mixing of particles in the bed. Through flow of solids is observed in fluidised beds when the flow rate of the fluid in the bed is high enough to entrain particles from the bed. Below this flow rate, the bed of solids has the appearance of a boiling liquid and is called a bubbling fluidised bed. This is because the bulk of the fluid in the reactor passes through the bed in the form of bubbles.

CHAPTER 3: DUAL FLUIDISED BED SYSTEM DESIGN

3.1 Introduction

The pyrolysis of biomass is an endothermic process during which the long polymers present in wood are split to form products of lower molecular weight (Meier & Faix, 1997). To reduce operating costs, the heat required for the endothermic pyrolysis reactions may be provided by combustion reactions. In this way, the pyrolysis process is composed of two reactors, namely a combustion reactor and a pyrolysis reactor. In the dual fluidised bed system, fluidised beds are used for both of these reactors. The medium used to transfer heat between the two beds is an inert solid.

Although many dual fluidised beds have been designed for the pyrolysis of biomass, these designs are usually only slightly modified forms of those used for the gasification of biomass. Little attention has been given to the optimisation of these designs for the pyrolysis of biomass process or to the development of scalable designs (Kaushal *et al*., 2007). An overview of the dual fluidised bed system that was designed during the current project for the pyrolysis of biomass is provided in this chapter. Included in this overview is the block flow diagram and process flow diagram of the system, the design of the downstream units from the dual fluidised bed system, the design of the control system used and material and energy balances over the system. The equations used to size and design the various components required for a pilot scale unit of the dual fluidised bed system is also discussed.

3.2 Block Flow Diagram

A block flow diagram of the proposed dual fluidised bed system is shown in Figure 3.1. The solids are heated in one fluidised bed by means of exothermic combustion reactions. The hot solids are then fed to a second fluidised bed in order to provide the heat required for the endothermic pyrolysis reactions. The colder solids and a fraction of the bio-char produced by the pyrolysis reactions are then fed back to the combustion fluidised bed, creating a circulating system. In this way, the oxygen required in the combustion fluidised bed for the combustion reactions is prevented from entering the pyrolysis fluidised bed, in which an oxygen-free environment is required. This design also allows the separation of the exothermic reactions from the endothermic reactions, which provides more control over the heat in the system and therefore the products formed in the system.

Two products are formed in the pyrolysis fluidised bed, namely pyrolysis gas and solid bio-char. The bio-char can be separated from the pyrolysis gases and collected as a second product. The pyrolysis gases, which include both the tar and gas compounds as shown in Figure 2.5, are fed to a quencher and separator where the tar compounds are rapidly quenched to form bio-oil and are separated from the incondensable gases. A fraction of the incondensable gases, also known as syngas, is purged from the system and the remaining gas is fed back to the pyrolysis fluidised bed in order to fluidise the bed. Because the syngas does not contain any pure oxygen, no oxygen enters the pyrolysis fluidised bed, and therefore no combustion occurs in the bed.

Liquid Petroleum Gas (LPG) was selected as the main fuel source in the pilot-scale system for the combustion reactions in the combustion fluidised bed. A small fraction of the char from the pyrolysis fluidised bed is also combusted, which is fed to the combustion fluidised bed with the cold solids. In full-scale operation, it is possible to replace the LPG with the purged syngas from the pyrolysis fluidised bed. Therefore the system does not require additional fuel and is said to be a self-sufficient process. Liquid Petroleum Gas was selected for the pilot-scale system in order to simplify the construction of the system. Ash and hot flue gas are produced in the combustion fluidised bed. The hot flue gas is a source of high-value heat and can be used to dry the biomass before it is fed to the pyrolysis fluidised bed.

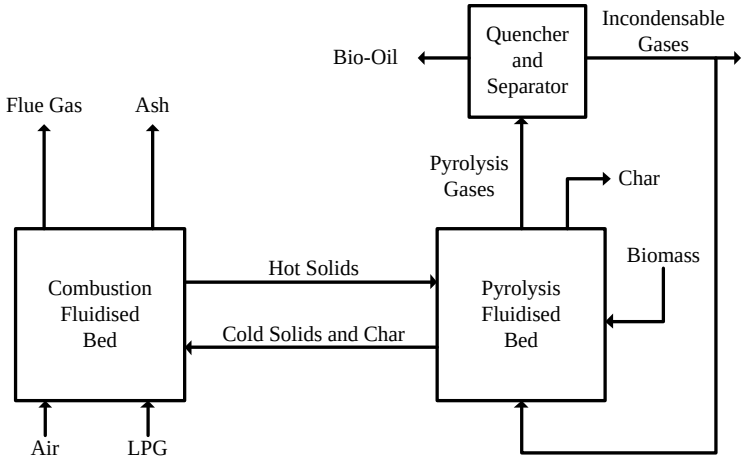

Figure 3.1: The block flow diagram of the dual fluidised bed system in which a solid is used to transport heat from the combustion bed to the pyrolysis bed

3.3 Pyrolysis Fluidised Bed

A more detailed overview of the pyrolysis fluidised bed design, as well as the design of the biomass feeder system, is shown in Figure 3.2. The pyrolysis fluidised bed was designed to be operated in the bubbling fluidised bed regime in order to minimise the entrainment of solids from the bed and to ensure a constant temperature throughout the bed. Hot solids from the combustion fluidised bed enter the pyrolysis fluidised bed by means of an overflow standpipe. The colder solids and a fraction of the char are fed back to the combustion fluidised bed by means of a screw-conveyor positioned at the bottom of the pyrolysis fluidised bed. This allows for the control of the rate at which the colder solids are fed back to the combustion fluidised bed. The gases and bio-char produced during the pyrolysis of biomass are fed to a cyclone in order to separate the bio-char from the gases before the gases are fed to the quencher system. This design therefore allows bio-char to be collected as a secondary product.

The particle size of the biomass must be less than 2 mm in order to maximise the yield of bio-oil obtained from the system. This gives the biomass the appearance of sawdust. The sawdust is kept in a hopper which is continuously agitated by means of a motor to prevent any clumps from forming in the hopper. This is required to prevent structural arching in the hopper and thereby ensure that the sawdust flows freely out of the hopper. The sawdust enters a screw-conveyor from the hopper, which is used to control the rate at which the sawdust is fed to the pyrolysis fluidised bed. A portion of the recycled incondensable gases produced by the pyrolysis reactions is fed directly to the pyrolysis fluidised bed at two different points in order to fluidise the bed. The remaining incondensable gases are fed to the end of the sawdust screw-conveyor in order to inject the sawdust pneumatically into the pyrolysis fluidised bed. This is done to prevent the backflow of heat from the pyrolysis fluidised bed to the hopper.

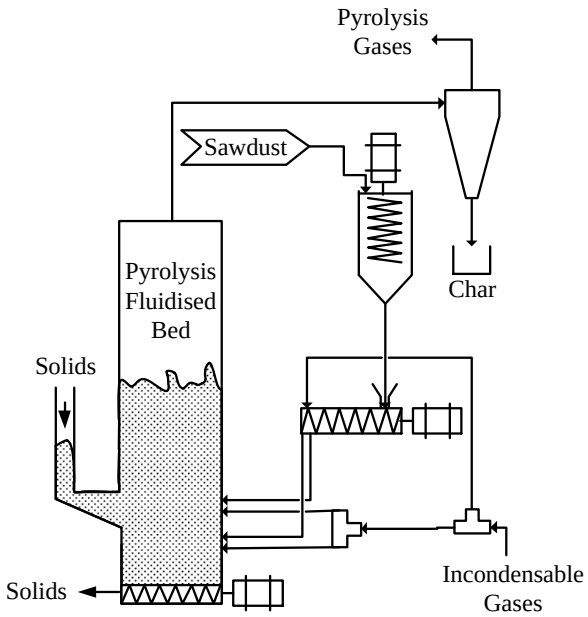

Figure 3.2: An illustration of the pyrolysis fluidised bed, which includes an illustration of the solid feed system to the bed, namely a hopper and a pneumatic injector

3.4 Combustion Fluidised Bed

An overview of the physical design of the combustion fluidised bed is shown in Figure 3.3. The combustion fluidised bed will also be operated in the bubbling fluidised bed regime to minimise the entrainment of solids from the bed. The entrance of the overflow standpipe to the pyrolysis fluidised bed is positioned at the splash zone of the combustion fluidised bed. This allows hot solids in the combustion fluidised bed to spill over continuously into the overflow standpipe and therefore, into the pyrolysis fluidised bed. The screw-conveyor used to transport bio-char and colder solids from the pyrolysis fluidised bed is positioned at the bottom of the combustion fluidised bed.

Air is used to fluidise the combustion fluidised bed and to combust the LPG fed to the bed. The air and LPG are fed to a distributor positioned near the bottom of the bed. Air is fed in excess to ensure complete combustion of the fuel and to ensure that oxygen is present along the entire height of the bed. This is required to prevent pyrolysis of the bio-char in the bed, which would result in heat losses. The flue gas formed in the combustion fluidised bed is separated from the ash that enters the bed with the bio-char. This flue gas is a source of high-value heat and can be used to dry the biomass before it is fed to the pyrolysis fluidised bed.

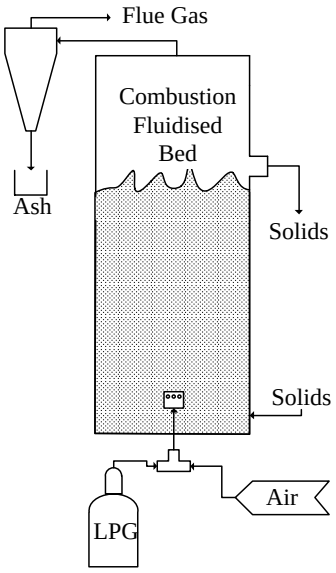

Figure 3.3: An illustration of the combustion fluidised bed, which will be operated in the bubbling regime

3.5 Quencher System

The pyrolysis gases obtained from the pyrolysis fluidised bed must be quenched rapidly to increase the yield of bio-oil obtained from the system. This is because the condensable gases produced by the pyrolysis reactions react quickly in the gas phase to form incondensable gases and bio-char. The quencher section is therefore a crucial part of the dual fluidised bed system. The physical design of the quencher section of the system is shown in Figure 3.4. Included in this section is a liquid cyclone, a demister and an electrostatic precipitator (ESP).

The gases from the pyrolysis fluidised bed first enter the quencher where they are sprayed with cold bio-oil to cool them rapidly. Most of the gases are condensed in the process, forming liquid bio-oil. The gas and bio-oil mixture is then fed to a liquid cyclone, which separates most of the bio-oil from the incondensable gases. The liquid bio-oil is collected at the bottom of the liquid cyclone, while the incondensable gases and small droplets of bio-oil move upwards through a demister. The bio-oil droplets collect in the demister, which is composed of tightly packed stainless steel wool, until the droplets are large enough to fall back into the liquid cyclone. However, after the demister, the incondensable gases still contain a fine mist of bio-oil. In order to remove this mist, the incondensable gases are fed to an ESP, where a high voltage creates a charge on the small bio-oil droplets. The charged bio-oil droplets are then attracted to grounded plates on the side of the ESP. The bio-oil droplets collect on the sides of the ESP until they become large enough to fall down to the bottom of the ESP from where the bio-oil can be removed. The remaining incondensable gases leave the ESP without any bio-oil and can then be recycled back to the pyrolysis fluidised bed.

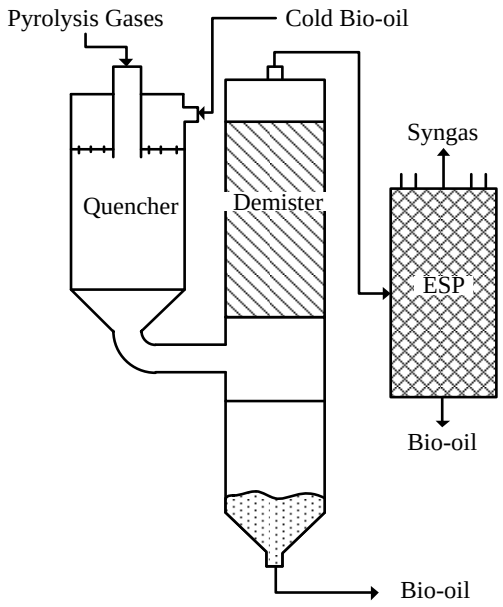

Figure 3.4: An illustration of the three sections in the quencher system of the pilot scale unit, namely the quencher, liquid cyclone, demister and electrostatic precipitator

3.6 Overall System Design

The process flow diagram for the pilot-scale system is shown in Figure 3.5. A blower is used to blow air into the combustion fluidised bed to provide the necessary pressure drop over the bed. A blower is also positioned after the ESP, which is used to drive the flow of the syngas. Part of the syngas is purged and the remaining syngas is used to fluidise the pyrolysis fluidised bed and to inject the sawdust pneumatically into the pyrolysis bed. As the syngas contains combustible, hazardous gases such as carbon monoxide and hydrogen, it was decided rather to feed the purged syngas to the freeboard of the combustion fluidised bed before it is sent to atmosphere. In this way, the syngas will undergo complete combustion before being sent to atmosphere. This will also provide additional heat in the freeboard of the combustion fluidised bed, thereby ensuring that the solids do not cool down before entering the overflow standpipe to the pyrolysis fluidised bed. The temperature of the flue gas from the combustion fluidised bed will also be increased, providing a source of high-value heat.

The hot flue gases from the combustion fluidised bed will be mixed with a large volume of air in the extraction box, thus cooling the gas before it is sent to atmosphere. An extraction fan, fitted to the extraction box, will be used to pull a slight vacuum to minimise the risk of any gas leakages from the system. Bio-oil will be collected from two points in the system, namely from the liquid cyclone and from the ESP in the quencher section. As more bio-oil will be collected from the liquid cyclone, it was decided to recycle the bio-oil from this source to the quencher. A pump will be used to move the bio-oil from the liquid cyclone, through a heat exchanger, to the quencher. An off-take valve will be positioned before the heat exchanger so that the bio-oil can be removed from the system if its level in the liquid cyclone gets too high. Tap water will be used in the heat exchanger to decrease the temperature of the bio-oil before it is fed to the quencher.

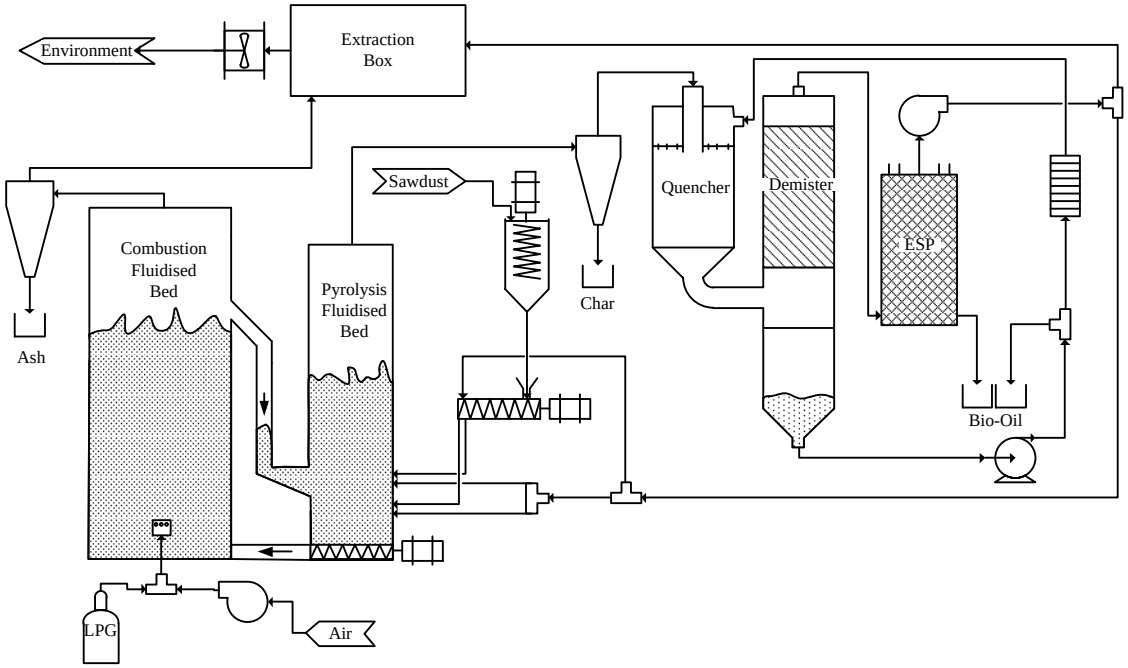

Figure 3.5: A detailed process flow diagram of the pilot scale system, including the downstream process units

3.7 Control System Design

The design of the control system used in the pilot-scale system is graphically illustrated in the piping and instrumentation diagram shown in Appendix 1. In total, five automatic controllers are used in the system, namely PIC 1, PIC 2, PIC 3, TIC 1 and TIC 2. The variables that are controlled by these controllers, the measured variables and the source of the set-point for these controllers are shown in Table 3.1. PIC 1 and PIC 2 are used to control the flow rate of the air and recycled pyrolysis gas streams respectively. The measured variables used for these controllers are the pressure drops over the orifice plates positioned on both pipelines. PIC 3 is used to control the pressure in the freeboard of the pyrolysis fluidised bed by adjusting the control valve positioned on the pyrolysis gas purge line. The last two controllers (TIC 1 and TIC 2) are used to control the temperature in the combustion fluidised bed and pyrolysis fluidised bed respectively. The manipulated variable used by TIC 1 is the control valve positioned on the LPG pipeline to the combustion fluidised bed, while the manipulated variable used by TIC 2 is the speed of the motor used to drive the screw-conveyor positioned at the bottom of the pyrolysis fluidised bed. As the temperature of the pyrolysis bed decreases, TIC 2 will increase the feed rate of solids back to the combustion fluidised bed. This will increase the spill rate of hot solids into the overflow standpipe, which will increase the temperature of the pyrolysis fluidised bed.

Table 3.1: Variables selected for the automatic controllers used in the pilot-scale system

Controller	Controlled Variable	Measured Variables	Set-point Variable
PIC 1	Air blower speed	Pressure drop over air orifice plate	Temperature of the air stream
PIC 2	Pyrolysis gas blower speed	Pressure drop over pyrolysis gas recycle stream	Temperature of the pyrolysis gas recycle stream
PIC 3	Flow rate of pyrolysis gas purge stream	Pressure in the freeboard section of the pyrolysis bed	Manual
TIC 1	Flow rate of LPG to combustion bed	Temperature in the combustion bed	Manual
TIC 2	Speed of solids screw-conveyor	Temperature in the pyrolysis bed	Manual

In addition to the variables used to control the pilot-scale system, several instruments are placed throughout the pilot-scale system. These will be used to monitor the performance of the system and for safety. A list of these instruments and their purpose is shown in Table 3.2. The names of these instruments can be found on the piping and instrumentation diagram in Appendix 1.

Table 3.2: List of all instruments used in the pilot-scale unit

Name	Type	Function
IT1-01	Temperature	Used to measure temperature of combustion fluidised bed
IT1-02	Temperature	Used to measure temperature of combustion fluidised bed
IT1-03	Temperature	Used to measure temperature of pyrolysis fluidised bed
IT1-04	Temperature	Used to measure temperature of pyrolysis fluidised bed
IT1-05	Temperature	Used to measure temperature of freeboard of the pyrolysis fluidised bed
IT1-06	Temperature	Used to measure temperature of freeboard of the combustion fluidised bed
IT1-07	Temperature	Used to measure temperature of air flow to combustion bed
IT1-08	Temperature	Used to measure temperature of recycle pyrolysis gas flow to pyrolysis bed
IT1-09	Temperature	Used to measure temperature of combustion fluidised bed and heating element
IT3-01	Temperature	Used to measure temperature of recycled bio-oil before the heat exchanger
IT3-02	Temperature	Used to measure temperature of cooling water before the heat exchanger
IT3-03	Temperature	Used to measure temperature of cooling water after the heat exchanger
IT3-04	Temperature	Used to measure temperature of gas-liquid mixture after the quencher
IT3-05	Temperature	Used to measure temperature of recycled bio-oil after the heat exchanger
IT4-01	Temperature	Used to measure temperature of purge gas-air mixture before the extraction fan
IT5-01	Temperature	Used to measure ambient temperature
IP1-01	Pressure	Used to measure pressure of air stream after orifice plate
IP1-02	Pressure	Used to measure pressure of air stream before orifice plate
IP1-03	Pressure	Used to measure pressure in freeboard of pyrolysis fluidised bed
IP1-04	Pressure	Used to measure pressure in freeboard of combustion fluidised bed
IP1-05	Pressure	Used to measure pressure of recycled pyrolysis gas stream after orifice plate
IP1-06	Pressure	Used to measure pressure of recycled pyrolysis gas stream before orifice plate
IP1-07	Pressure	Used to measure pressure at bottom of combustion fluidised bed
IP1-08	Pressure	Used to measure pressure at bottom of pyrolysis fluidised bed
IP3-01	Pressure	Used to measure pressure of bio-oil after the bio-oil pump
IF1-01	Flow rate	Used to measure flow rate of LPG to combustion fluidised bed
IF3-01	Flow rate	Used to measure flow rate of cooling water to the heat exchanger
IW1-01	Weight	Used to measure the weight of the sawdust in the hopper

3.8 Material and energy balances

3.8.1 Overall results

The basis that was used for the material balances was a feed rate of 20 kg/s of wood into the pyrolysis fluidised bed. A trial-and-error method was then used to solve for the unknown variables, namely the flow rate of char and sand between the two beds. In order to perform these calculations the conversion in each bed had to be determined. The overall results for both beds are shown in Table 3.3, from which it can be seen that more char is produced from the pyrolysis reactions than is required by the combustion reactions. Heat losses to the environment were considered when performing the total energy balance over the system, which was taken as 1 kW for both the combustion and pyrolysis fluidised beds (i.e. 2 kW in total).

Table 3.3: Overall results obtained from the material and energy balances

Parameter	Value
Flow rate of sand	96 kg/h
Char required	2.9 kg/h
Char produced	4.3 kg/h
Energy from sand	13.2 kW
Energy from combustion	26.4 kW
Heat losses	2 kW
Flow rate of air	1 m/s

The energy balance over the entire system is a summation of the energy balances for the pyrolysis and combustion fluidised beds, which are described in the next two sections.

3.8.2 Combustion fluidised bed results

The inlet and outlet concentrations obtained from the material balance over the combustion fluidised bed are shown in Table 3.4. All of the carbon into the system is converted into carbon dioxide. It is important that oxygen is present along the entire length of the reactor in order to prevent gasification in the combustion fluidised bed. It can be seen in Table 3.4 that this objective has been achieved as there is oxygen leaving the reactor. Although carbon monoxide is formed in the reactor, it is instantly reacted to form carbon dioxide, which is why no carbon monoxide exits the reactor.

Table 3.4: Inlet and outlet concentrations for the combustion fluidised bed

Compounds	In (kmol/h)	Out (kmol/h)
O_2	0.31	0.07
CO_2	0.00	0.24
C	0.02	0.00
N_2	1.17	1.17

The results obtained from the energy balance over the combustion fluidised bed are shown in Table 3.5. From this table it can be seen that the energy balance has been solved correctly as no difference between the variables was calculated. The energy leaving the reactor with the flue gas is approximately equal to the energy required to heat the sand through the reactor. Therefore it is a good idea to recover some of this energy by using a waste heat boiler positioned after the combustion fluidised bed. Alternatively, the flue gas may be used to reduce the moisture content of the biomass fed to the pyrolysis fluidised bed.

Table 3.5: Energy balance over the combustion fluidised bed

Parameter	Value (kW)
In	1.1
Out	13.3
Generated	26.4
Consumed (sand)	13.2
Losses	1.0
Difference	0.0

3.8.3 Pyrolysis fluidised bed results

The inlet and outlet concentrations obtained from the material balance over the pyrolysis fluidised bed are shown in Table 3.6. A feed rate of 20 kg/s of wood was used for the material balance. At the temperature chosen for the pyrolysis fluidised bed, the conversion of the wood is close to 100%. The yield of tar from the pyrolysis fluidised bed is nearly 64% on a weight basis. This is very close to the maximum yields reported by other authors. In addition, the outlet concentration of char is relatively high, which is desired as it can be used to support the combustion reactions in the combustion fluidised bed. It can also be seen that the outlet flow rate of the incondensable gases is greater than the inlet flow rate. For this reason part of the incondensable gases will be purged, and the remaining gases will be recycled to the pyrolysis fluidised bed. The conversion of moisture and chemically bound water in the wood to vaporised water was also considered in the material and energy balance.

Table 3.6: Inlet and outlet concentrations for the pyrolysis fluidised bed

Components	In (kg/h)	Out (kg/h)
Wood	20.0	0.0
Gas	10.9	13.7
Char	0.0	4.5
Tar	0.0	12.7
Moisture (liquid)	1.0	0.0

The results obtained from the energy balance over the pyrolysis fluidised bed are shown in Table 3.7. The energy balance was found to balance as no difference was calculated. Heat losses of 1 kW was included in the energy balance over the pyrolysis fluidised bed.

Table 3.7: Energy balance over the pyrolysis fluidised bed

Parameter	Value (kW)
In	0.32
Out	9.62
Generated (sand)	13.20
Consumed	2.90
Losses	1.00
Difference	0.00

3.9 Sizing

3.9.1 Fluidised bed insulation

Rectangular fluidised beds were used for both the pyrolysis fluidised bed and the combustion fluidised bed to simplify both the construction of the system and the design of the solids transfer mechanism used between the two beds. The thickness required for the insulation for both beds was determined with the use of elementary conductive and convective heat transfer equations, where the overall heat transfer rate is shown in equation 3.1 (Çengel, 2006:136). These equations were used to determine the thickness of the insulation that is required in order to reduce the temperature from the inside of both beds to less than 50°C on the surface of the beds.

$$Q = \frac{T_1 - T_2}{R_{total}} \tag{3.1}$$

The total thermal resistance (R_{total}) is the sum of all conductive and convective thermal resistances as shown in equation 3.2. The first convective thermal resistance ($R_{conv,1}$) is the resistance from the inside of the beds to the surface of the refractory inside the beds, while the second convective thermal resistance ($R_{conv,2}$) is the resistance from the outside of the beds to the environment. The conductive resistances ($R_{cond,n}$) represent the different layers of insulation used in the fluidised beds.

$$R_{total} = R_{conv,1} + \sum_{i=1}^{n} R_{cond,n} + R_{conv,2} \tag{3.2}$$

The conductive and convective resistances are given by equation 3.3 and 3.4 respectively (Çengel, 2006:137).

$$R_{cond,n} = \frac{L_n}{k_n A} \tag{3.3}$$

$$R_{conv} = \frac{1}{hA} \tag{3.4}$$

An overview of how these equations can be used to estimate the temperature on the outer surface of the combustion fluidised bed is provided in example 3.1.

Example 3.1:

The combustion fluidised bed is composed of four layers in order to reduce the rate of heat transfer from the inside of the bed, at its operating temperature of 900°C, to the environment, at 30°C. These layers are listed in Table 3.8 with the thickness and thermal conductivity of each layer.

Table 3.8: The name, thickness and thermal conductivity of the insulating layers used in the combustion fluidised bed.

Layer	Thickness (mm)	Conductivity (W/m·K)
Refractory	25	2.3
Vermiculite	25	0.068
Steel	3	48
Insulating wool	25	0.043

The convection heat transfer coefficient of air at the temperature inside the bed and the environment is 20 and 5 W/m²K respectively. The total thermal resistance from the inside of the bed to the environment for 1m² of the bed is calculated as follows:

$$R_{total} = R_{conv,bed} + \sum R_{cond,layers} + R_{conv,environment}$$

$$= \frac{1}{20 \times 1} + \frac{0.025}{2.3 \times 1} + \frac{0.025}{0.068 \times 1} + \frac{0.003}{48 \times 1} + \frac{0.025}{0.043 \times 1} + \frac{1}{5 \times 1} = 1.2 \frac{\text{K}}{\text{W}}$$

The total rate of heat transfer for a 1m² area of the bed can then be calculated, as shown below:

$$Q = \frac{900 - 30}{1.2} = 719\text{W}$$

The outer temperature of the bed can be calculated by adding the temperature difference due to convection on the outside of the bed to the temperature of the environment. This temperature difference can be calculated using a modified form of equation 3.1 as shown below:

$$\Delta T_{environment} = Q \times R_{conv,environment}$$

$$= 719 \times \frac{1}{5 \times 1} = 143.8°\text{C}$$

The outer temperature of the bed is then calculated as follows:

$$T_{surface} = \Delta T_{environment} + T_{environment}$$

$$= 143.8 + 30 = 173.8°\text{C}$$

Similarly, the temperature after each layer of the combustion bed can be calculated. The results from these calculations are shown in Figure 3.6. The temperature of the outer surface of the combustion fluidised bed is predicted to be 173.8°C, which is too high. Therefore, additional insulation is required in order to achieve a surface temperature less than 50°C.

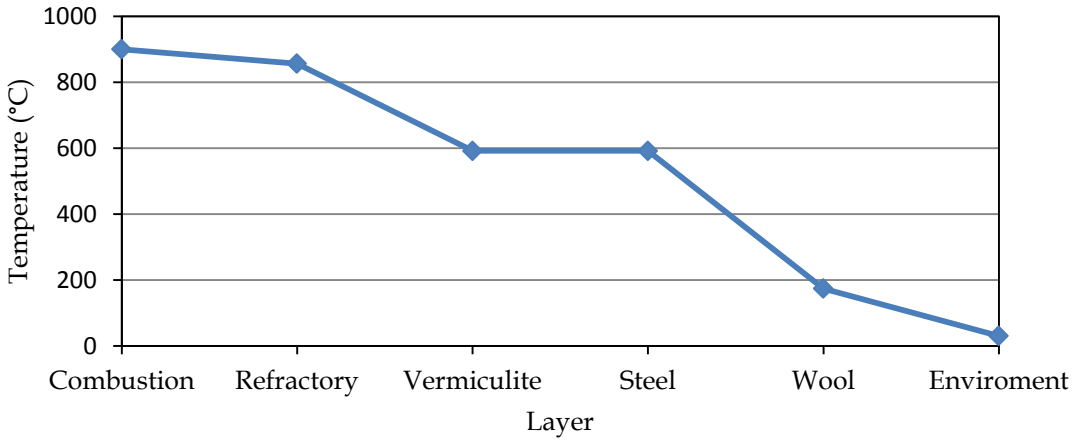

Figure 3.6: The temperature profile from the inside of the combustion fluidised bed to the environment through several layers, which include refractory, vermiculite, steel and insulating wool

3.9.2 Fluidisation gas velocity

A maximum height of 3.3 m was imposed on the dual fluidised bed system due to the environment in which the system was built. A further 0.8 m was required between the roof of the environment and the top of the dual fluidised bed system for the cyclone and for maintenance purposes. It was therefore decided to use a height of 2.5 m for the dual fluidised bed system. The disengagement height required for the solids in both beds was determined with the use of the correlations provided by Zenz & Weil (1958). The maximum height allowed for the bed of solids in each fluidised bed could then be determined, which is the difference between the maximum height of the system and the disengagement height minus the height required for the base of the system. To determine the area required for both beds, an energy balance was performed over the system and over each bed to establish the quantity of sand required in both beds. Based on the bulk density of the solids at fluidisation, the required volume of solids could then be calculated. A square area for both the combustion and pyrolysis fluidised beds was then calculated to ensure that sufficient volume was provided in each bed, within the allowable height calculated for the bed of solids, for the volume of the solids required.

The minimum bubbling gas velocity for both the pyrolysis and combustion fluidised beds was then determined with the use of equation 3.1 and 3.2 (Kunii & Levenspiel, 1991: 69).

$$\frac{1.75}{\varepsilon_{mf}^3 \phi_s}\left(\frac{d_p u_{mf} \rho_g}{\mu}\right)^2 + \frac{150(1-\varepsilon_{mf})}{\varepsilon_{mf}^3 \phi_s^2}\left(\frac{d_p u_{mf} \rho_g}{\mu}\right) = \frac{d_p^3 \rho_g (\rho_s - \rho_g) g}{\mu^2} \qquad (3.1)$$

$$\frac{u_{mb}}{u_{mf}} = \frac{2300\rho_g^{0.13}\mu^{0.52}e^{0.72P_{45\mu m}}}{d_p^{0.8}(\rho_s-\rho_g)^{0.93}} \quad (3.2)$$

The volumetric flow rate of gas required in each bed was then calculated by multiplying the minimum bubbling gas velocity in each bed by a safety factor and the area calculated for each bed. An air distributor with eight exit nozzles was designed for the combustion fluidised bed. The nozzles in this distributor were spaced evenly in order to distribute the air evenly into the bed. To prevent the flow of solids into the distributor, the diameter of the nozzles was designed to ensure that the velocity of air through each nozzle was above 50 m/s during normal operation.

3.9.3 Overflow standpipe height

The pressure balance over the overflow standpipe and the pyrolysis bed in the proposed dual fluidised bed system is shown in equation 3.3.

$$P_{CF}+\Delta P_{OS}=P_{PF}+\Delta P_{PB} \quad (3.3)$$

If the pressures at the top of the combustion and pyrolysis fluidised beds are constant and the difference between the pressures is equal to Kc, then the pressure balance can be represented as:

$$\Delta P_{OS}=Kc+\Delta P_{PB} \quad (3.4)$$

In addition, the pressure drops over the overflow standpipe and the pyrolysis fluidised bed are given in equation 3.5 and 3.6 respectively.

$$\Delta P_{OS}=H_{OS}\times\rho_{OS}\times g \quad (3.5)$$

$$\Delta P_{PB}=H_{PB}\times\rho_{PB}\times g \quad (3.6)$$

By substituting equations 3.5 and 3.6 into equation 3.4 and solving for the height of solids in the overflow standpipe, the following equation is obtained:

$$\Delta H_{OS}=\frac{Kc+H_{PB}\times\rho_{PB}}{\rho_{OS}} \quad (3.7)$$

As a result, the height of the solids in the overflow standpipe will increase if any of the following occurs:

- The height of the solids in the pyrolysis fluidised bed increases.
- The pressure in the freeboard of the pyrolysis bed increases relative to the pressure in the freeboard of the combustion fluidised bed.
- The density of the solids in the overflow standpipe is reduced relative to the density of the solids in the pyrolysis fluidised bed.

With the use of equation 3.7, the maximum possible height of the solids in the overflow standpipe can be determined. The height of the overflow standpipe must then be designed accordingly to prevent the flow of solids backwards through the pipe.

3.9.4 Cyclone design

The dimensions for both the pyrolysis and combustion gas cyclones were obtained from Stairmand's high-efficiency cyclone design (Sinnott, 2005: 450), which is shown in Figure 3.7.

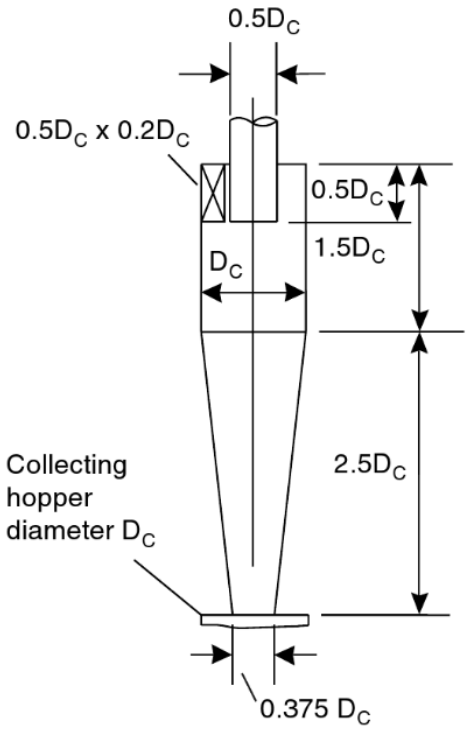

Figure 3.7: Stairmand's high-efficiency cyclone design with dimensions

The variable D_C in Figure 3.2 can be obtained by sizing the inlet duct in order to obtain an inlet gas velocity of 15 m/s (Sinnott, 2005: 450). An example of this calculation is given in Example 3.2 for an inlet gas volumetric flow rate of 0.0384 m^3/s.

Example 3.2:

The required cross-sectional area of the inlet duct can be obtained by dividing the inlet gas volumetric flow rate by the required linear flow rate as shown below:

$$A=\frac{0.0384}{15} = 0.00256 \text{ m}^2$$
$$= 2560 \text{ mm}^2$$

The area of the inlet duct is given as the following equation from Figure 6.2:

$$A=0.5D_C \times 0.2D_C$$

Substituting the required area of the duct and solving for D_C, we obtain the following:

$$0.1D_C^2 = 2560$$
$$D_C = \sqrt{25600}$$
$$D_C = 160 \text{ mm}$$

3.10 Conclusions

An overview of the dual fluidised bed system that was designed during the current project for the pyrolysis of biomass was provided in this chapter. Inert solids are circulated between the combustion and pyrolysis fluidised beds to transfer heat from the combustion fluidised bed to the pyrolysis fluidised bed. The combustion and pyrolysis fluidised beds are kept separate to prevent the oxygen present in the combustion fluidised bed from entering the pyrolysis fluidised bed. The products obtained from the pyrolysis fluidised bed are bio-char and pyrolysis gases. As a result, the current design allows the separation of bio-char as a secondary product. The pyrolysis gases are fed to a quencher and separator section where the condensable gases are condensed to form bio-oil. A fraction of the incondensable gases is purged and the remaining incondensable gases are fed back to the pyrolysis fluidised bed to fluidise the bed. The fuel used in the combustion fluidised bed for the combustion reactions is liquid petroleum gas (LPG). However, it is possible to replace the LPG with a small portion of the bio-char that is formed in the pyrolysis fluidised bed and the incondensable pyrolysis gases that are purged. In this way, the system would not require an external source of fuel and is said to be a self-sufficient system.

An overflow standpipe is used to transport the hot solids in the combustion fluidised bed to the pyrolysis fluidised bed, and a screw-conveyor is used to transport the cold solids back to the combustion fluidised bed. As a result, the rate of solids circulation between the beds can be controlled by manipulating the speed of the screw-conveyor. This is important as it provides a means of controlling temperature in the pyrolysis fluidised bed, thereby allowing optimisation of the yield of bio-oil from the system. A cyclone is used to separate the bio-char formed in the pyrolysis fluidised bed from the pyrolysis gases. A screw-conveyor is used to control the rate at which the biomass is fed from the hopper to the pyrolysis fluidised bed. To prevent backflow of heat to the hopper, the biomass is pneumatically injected from the end of the biomass screw-conveyor to the pyrolysis fluidised bed. The pyrolysis gases from the pyrolysis fluidised bed are rapidly quenched by mixing them with a spray of cold bio-oil. This is necessary to maximise the yield of bio-oil from the system. The bio-oil is then separated from the incondensable gases by means of a liquid cyclone, a demister and an electrostatic precipitator (ESP). After the ESP, the incondensable gases are fed to a blower, which is used to blow the gases back to the pyrolysis fluidised bed. Cool water is used to decrease the temperature of the bio-oil in a heat exchanger before the bio-oil is recycled back to the quencher section.

Five automatic control loops will be used in the dual fluidised bed system. The flow rate of air to the combustion fluidised bed and incondensable gases to the pyrolysis fluidised bed will be controlled by manipulating the speed of both the air blower and the pyrolysis gas blower. The pressure in the pyrolysis fluidised bed will be controlled by manipulating the control valve position on the pyrolysis gas purge line. The temperature in the combustion fluidised bed will be controlled by manipulating the flow rate of LPG to the combustion fluidised bed and the temperature in the pyrolysis fluidised bed will be controlled by adjusting the speed of the screw-conveyor used to transport solids back to the combustion fluidised bed.

Mass and energy balances were also performed over the combustion and pyrolysis fluidised beds. It was found that more bio-char is formed in the pyrolysis fluidised bed than is required by the combustion reactions. All material and energy balances were found to balance and all unknown variables in the system, including the flow rate of char and sand between the fluidised beds, were determined.

The design equations for several parts of the pilot scale dual fluidised bed system were also discussed in the current chapter with example calculations

CHAPTER 4: SOLIDS TRANSPORT MECHANISM

4.1 Introduction

Although many dual fluidised bed designs have been developed for the pyrolysis of biomass, little attention has been given to the mechanisms used for the transfer of solids between the two fluidised beds. The objectives of this investigation were to select a solids transfer mechanism for dual fluidised bed systems, to undertake an experimental evaluation of its performance and to assess the solids transfer mechanism with respect to its applicability to the pyrolysis of biomass process. The following properties of the solids transfer mechanism were required for it to be suitable for the pyrolysis of biomass process:

- The mechanism should not allow gas to be transported from the combustion fluidised bed to the pyrolysis fluidised bed.
- The mechanism should allow easy control over the solids transfer rate and therefore over the rate of heat transfer between the two beds.
- The construction of the solids transfer mechanism should not be too complicated or require a large amount of space.
- The solids transfer mechanism should not introduce large heat losses into the system.

A cold model of the proposed dual fluidised bed system was built to evaluate the performance of the solids transfer mechanism.

4.2 Background

Dual fluidised bed systems have been used extensively in the field of pyrolysis for the pyrolysis of biomass. This system makes use of two fluidised beds in order to separate the endothermic pyrolysis reactions from the exothermic combustion reactions. The inert solids are then circulated between the two beds to transfer heat from the combustion fluidised bed to the pyrolysis fluidised bed. This is done to prevent the flow of reactants between the fluidised beds and to control the rate of heat transfer between the beds.

A literature study was performed to determine the common mechanisms that have been used to transfer solids in dual fluidised bed systems for either the pyrolysis or gasification of biomass. It was found that non-mechanical solids flow devices, such as L-valves, loop seals and standpipes, are preferred for the transport of solids both from the combustion bed to the pyrolysis bed and from the pyrolysis bed to the combustion bed. The solids flow mechanisms selected by several authors for this purpose are shown in Table 4.1. It can be seen that L-valves and loop seals are the most popular solids flow devices.

Table 4.1: Solids flow devices used in dual fluidised bed systems for the pyrolysis of biomass

Reference	Combustion bed to pyrolysis bed	Pyrolysis bed to combustion bed
Karmakar & Datta (2010)	Cyclone →L-valve	Connection pipe →L-valve
Göransson, Söderlind & Zhang (2010)	Cyclone →loop seal	Connection pipe
Murakami *et al* (2010)	Connection pipe	Connection pipe
Kaushal, Pröll & Hofbauer (2007)	Cyclone →L-valve	Connection pipe
Kaushal, Pröll & Hofbauer (2011)	Cyclone →L-valve	Connection pipe

4.3 Solids Transport Mechanism Design

An overview of the physical design of the mechanism used to transport solids between the two fluidised beds is shown in Figure 4.1. An overflow standpipe will be used to transport solids from the combustion fluidised bed to the pyrolysis fluidised bed, while screw-conveyor, which is positioned at the bottom of both fluidised beds, will be used to transport solids back to the combustion fluidised bed. The entrance of the overflow standpipe will be positioned at the splash zone of the combustion fluidised bed. This will allow the solids to spill over continuously into the entrance of the overflow standpipe.

The design allows for the unaided transport of solids from the combustion fluidised bed to the pyrolysis fluidised bed. An advantage of this design is that the overflow standpipe may be built from the refractory separating the two fluidised beds. Therefore the space required for this design is relatively small compared with common fluidised bed designs. As the speed of the screw-conveyor is increased, more solids will enter the combustion fluidised bed, which will increase the height of the solids in this bed. This will cause more solids to spill over into the overflow standpipe and therefore into the pyrolysis fluidised bed. The rate at which the solids are circulated between the beds, and therefore the rate of heat transfer from the combustion fluidised bed to the pyrolysis fluidised bed, can therefore be easily controlled by manipulating the speed of the screw-conveyor. This in turn provides better control over the products obtained from the pyrolysis fluidised bed.

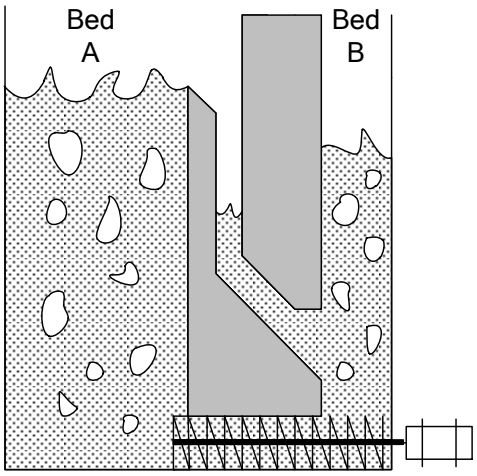

Figure 4.1: An illustration of the mechanism used to transport solids between the combustion fluidised bed (Bed A) and the pyrolysis fluidised bed (Bed B)

4.4 Experimental

A two dimensional (2D) cold model of the dual fluidised bed system was built at the Agricultural Research Service in Wyndmoor, Pennsylvania, USA, which is shown in Figure 4.2. The cold unit was built from transparent Perspex sheets in order to view the height of the sand in the combustion and pyrolysis fluidised beds, as well as in the overflow standpipe.

Figure 4.2: A picture of the cold unit system built at the Agricultural Research Service in USA, which is made from transparent Perspex sheets

In order to investigate the performance of the cold unit, several parameters were altered during the operation of the system and the resultant effects on the steady-state values of the system were recorded. The following manipulated parameters were considered during the investigation:

- The speed of the screw-conveyor
- The flow rate of the gas fed to the pyrolysis fluidised bed
- The flow rate of the air fed to the combustion fluidised bed
- The amount of sand in the dual fluidised bed system

Four different steady-state values were considered during the experiments:

- The pressure drop over the combustion bed
- The pressure drop over the pyrolysis bed
- The height of the sand in the pyrolysis bed
- The rate of spills or overflow of the sand into the standpipe per minute

4.5 Results and Discussion

4.5.1 Screw-conveyor Speed Results

The consequences of varying the screw-conveyor speed on the circulating flow of the cold flow model were found to give sufficiently accurate results and allowable assumptions from a statistical point of view. The effects on the pressure drop over the combustion and pyrolysis fluidised beds and the height of the medium in the pyrolysis fluidised bed are shown in Figure 4.3, and the effects on the rate of spills to the overflow standpipe are shown in Figure 4.4. The experiment led to the following conclusions:

- The pressure drop over the combustion bed increased slightly as the speed of the screw-conveyor increased (Figure 4.3). This is due to an increase in the amount of sand in the combustion bed as the speed of the screw-conveyor increases. However, this increase in pressure drop is not substantial.
- The pressure drop over the pyrolysis bed remained approximately constant as the speed of the screw-conveyor increased, despite a larger quantity of sand being removed from the bed. It is believed that this is because of the standpipe that connects the pyrolysis bed to the combustion bed. The pressure drop over the pyrolysis bed is therefore dependent on the gas flow in the combustion bed, rather than on the quantity of sand in the pyrolysis bed.
- The height of the sand in the pyrolysis bed was directly influenced by the speed of the screw-conveyor. An increase in the speed of the screw-conveyor would decrease the height of the sand in the pyrolysis bed. This is due to an increase in the amount of sand being removed from the pyrolysis bed by the screw-conveyor.
- The rate of spills into the overflow standpipe from the combustion bed was found to be dependent on the speed of the screw-conveyor. This rate peaked at a speed between 115 and 125 r/min (Figure 4.4).

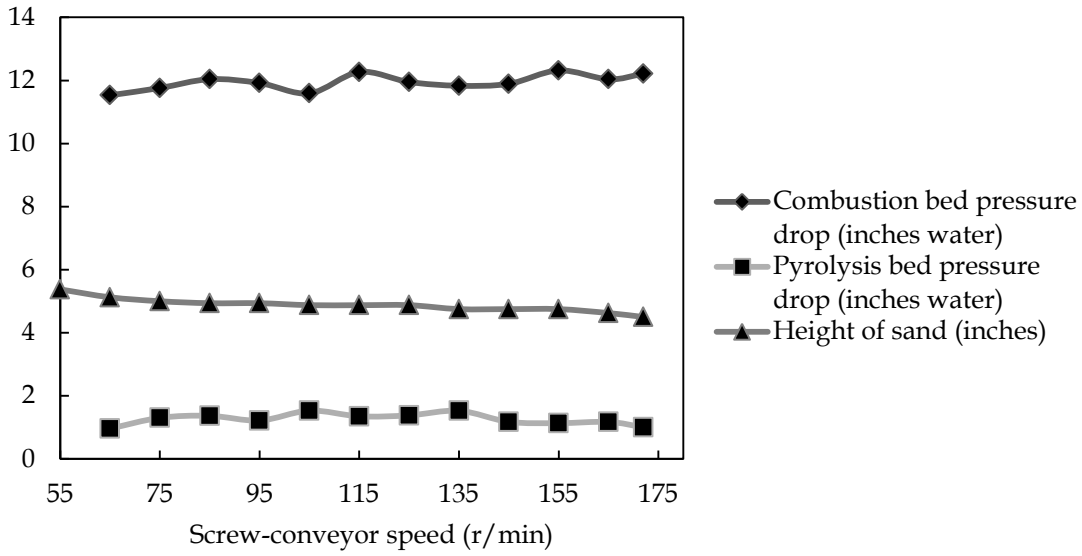

Figure 4.3: Experimental results of the pressure drop over the combustion and pyrolysis bed, and the height of the sand in pyrolysis bed versus the speed of the screw-conveyor

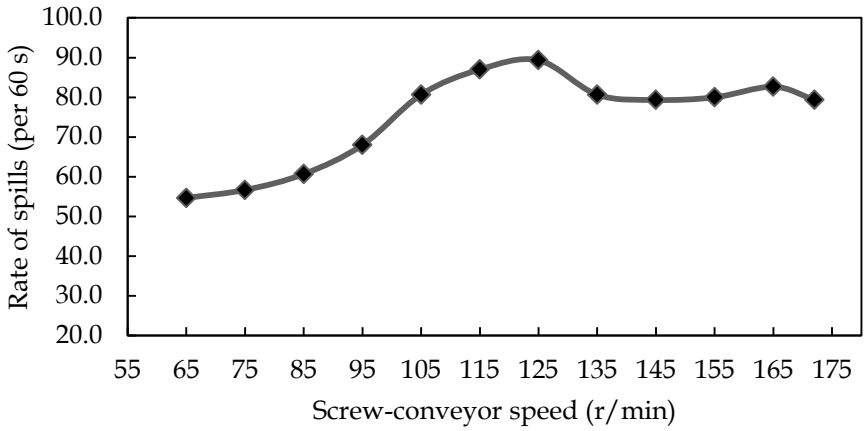

Figure 4.4: Experimental results of the rate of spills to overflow standpipe per minute versus the speed of the screw-conveyor

4.5.2 Pyrolysis Gas Flow Rate Results

The objective of this experiment was to investigate the effects of varying the flow of gas to the pyrolysis bed on the circulating flow of the cold flow model. The results obtained for the pressure drop over the combustion and pyrolysis fluidised beds, as well as the height of the sand in the pyrolysis fluidised bed, are shown in Figure 4.5, and the rate of spills to the overflow standpipe is shown in Figure 4.6. The conclusions drawn from this experiment are as follows:

- The pressure drop over the pyrolysis bed was not affected substantially by the flow rate of gas to it. This may be due to the gas flow through the overflow standpipe connecting the pyrolysis bed to the combustion bed, i.e. the pressure drop over the pyrolysis bed is dependent rather on the gas flow in the combustion bed because of its much higher flow rate.
- Similarly, the pressure drop over the combustion bed was not influenced substantially by changes in the flow rate of gas to the pyrolysis bed.
- It can be seen in Figure 4.5 that the height of the pyrolysis bed increased as the flow rate of gas to the bed increased. This is due to an increase in the voids fraction of the bed. The lack of data points in Figure 4.5 is due to difficulties in accurately measuring the height of the bed at high gas flow rates.
- The rate of spills to the overflow standpipe decreased as the gas flow rate to the pyrolysis bed increased. This is because the gas flow reduced the amount of sand that entered the screw-conveyor and therefore the combustion bed.

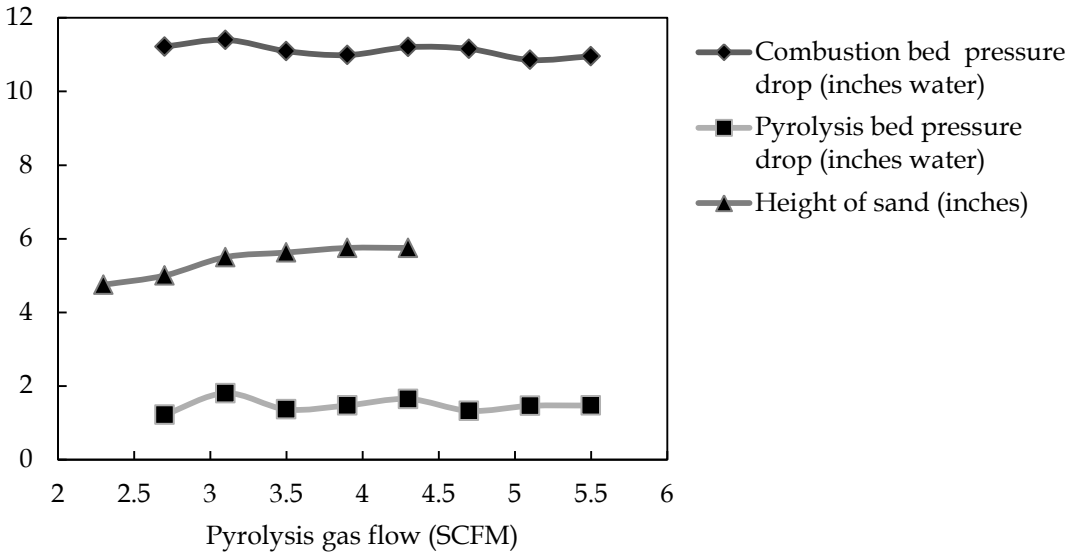

Figure 4.5: Experimental results of the pressure drop over the combustion and pyrolysis bed, and the height of the sand in pyrolysis bed versus the flow rate of gas to the pyrolysis bed

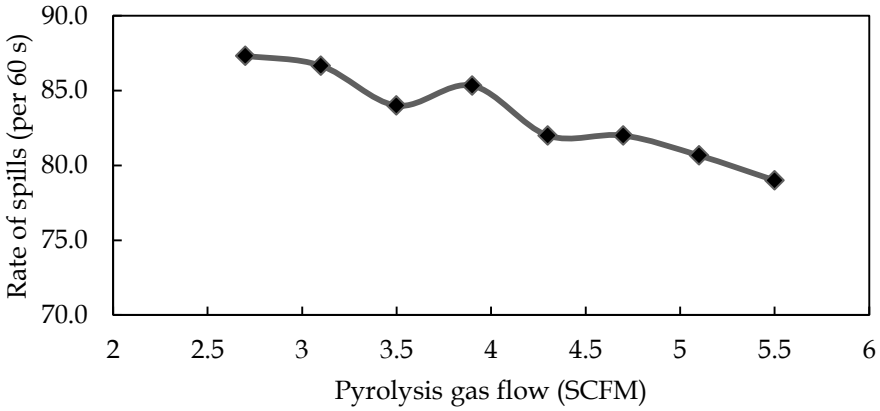

Figure 4.6: Experimental results of the rate of spills to overflow standpipe per minute versus the flow rate of gas to the pyrolysis bed

4.5.3 Combustion Gas Flow Rate Results

The objective of this experiment was to determine the effects of varying the gas flow rate to the combustion fluidised bed on the steady-state values in the cold model. The results obtained for the pressure drop over the combustion and pyrolysis fluidised beds, as well as the height of the medium in the pyrolysis fluidised bed, are shown in Figure 4.7, and the rate of spills to the overflow standpipe is shown in Figure 4.8. All measurements were taken after the minimum fluidisation velocity as the screw-conveyor would not operate until the bed was fluidised. The conclusions drawn from this experiment are as follows:

- The pressure drop over the combustion fluidised bed decreased as the flow rate of the gas to the bed increased. This may be due to an increase in the flow rate of gas from the pyrolysis bed to the combustion bed through the standpipe.
- The pressure drop over the pyrolysis fluidised bed increased as the flow rate of the gas to the combustion bed increased. However, it began to decrease at a volumetric flow rate of 9.5 standard cubic feet per minute (SCFM). This is because the standpipe was filled with sand at this point, which reduced the flow of gas to the combustion fluidised bed.
- The height of the sand in the pyrolysis fluidised bed increased as the combustion gas flow rate increased. This increase in height followed the same trend as the pressure drop over the pyrolysis bed.
- The rate of spills into the overflow standpipe increased rapidly until a gas flow rate of approximately 9 SCFM. This is because the height of the combustion fluidised bed increased as the gas flow rate increased. However, above 9 SCFM, the rate of spills decreased until a gas flow rate of approximately 9.5 SCFM. The decrease in the rate of spills was due to the increase in the flow rate of the gas from the pyrolysis fluidised through the standpipe, which prevented smaller clumps of sand from spilling into the standpipe. Only larger clumps of sand were able to overcome the frictional drag caused by the gas flowing through the standpipe and spill into the standpipe. Above a gas flow rate of 9.5 SCFM, the rate of spills began to increase again as the standpipe started to fill with sand, which reduced the gas flow through the standpipe, allowing smaller clumps of sand to spill over into the standpipe.

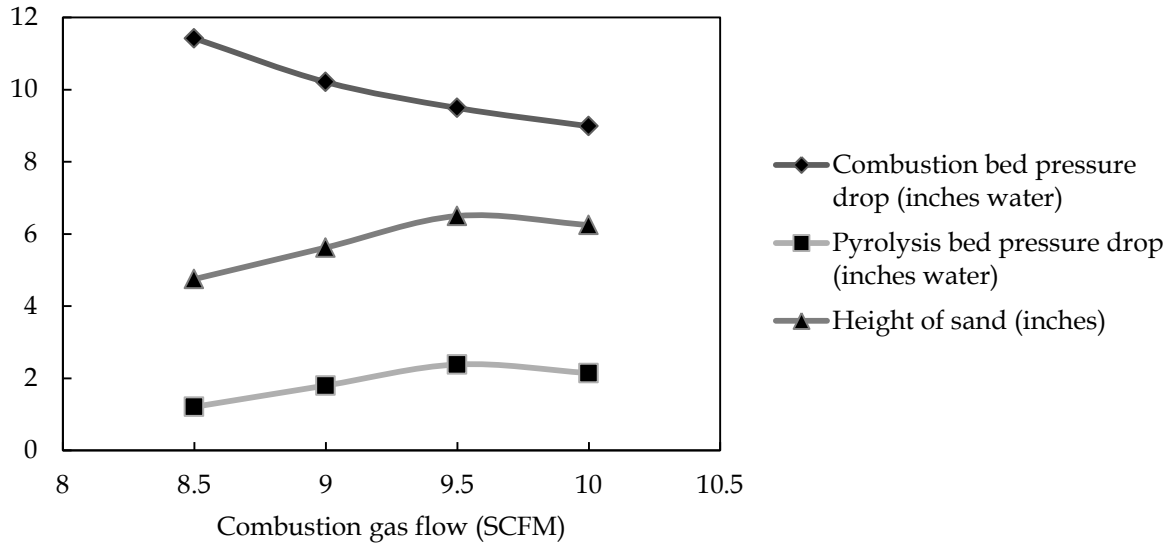

Figure 4.7: Experimental results of the pressure drop over the combustion and pyrolysis bed, and the height of the sand in pyrolysis bed versus the flow rate of gas to the combustion bed

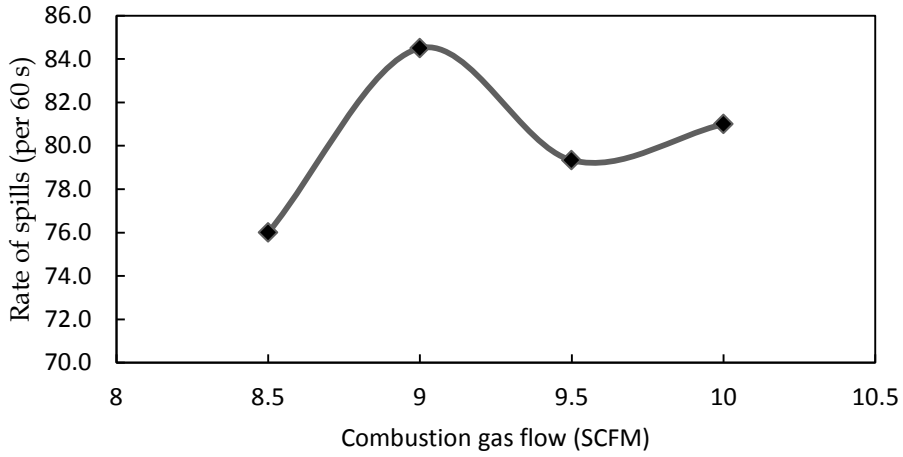

Figure 4.8: Experimental results of the rate of spills to overflow standpipe per minute versus the flow rate of gas to the combustion bed

4.5.4 Amount of Sand Charged to the System

The objective of this experiment was to determine the consequences of varying the amount of sand charged to the dual fluidised bed system. The screw-conveyor speed, pyrolysis gas flow rate and combustion gas flow rate experiments were repeated with a larger volume of sand in the dual fluidised bed system to determine the dependence of these results on the amount of sand charged to the system. The results obtained for the pressure drop over the combustion and pyrolysis fluidised beds, as well as the height of the medium in the pyrolysis fluidised bed versus the speed of the screw-conveyor, are shown in Figure 4.9, and the rate of spills to the overflow standpipe is shown in Figure 4.10. The conclusions drawn from this experiment are as follows:

- The results obtained for the pressure drop over the combustion and pyrolysis bed, and for the height of the sand in the pyrolysis bed are very similar to those obtained in the first experiment. It was therefore concluded that a change in the amount of sand charged to the system does not substantially affect the outcomes of varying the screw-conveyor speed with regard to these parameters.
- The rate of spills to the overflow standpipe went through a peak at approximately the same speed of the screw-conveyor as in the first experiment. However, this peak was less substantial than in the first experiment. Therefore it is believed that an increase in the amount of sand charged to the system has a dampening effect on the rate of spills.

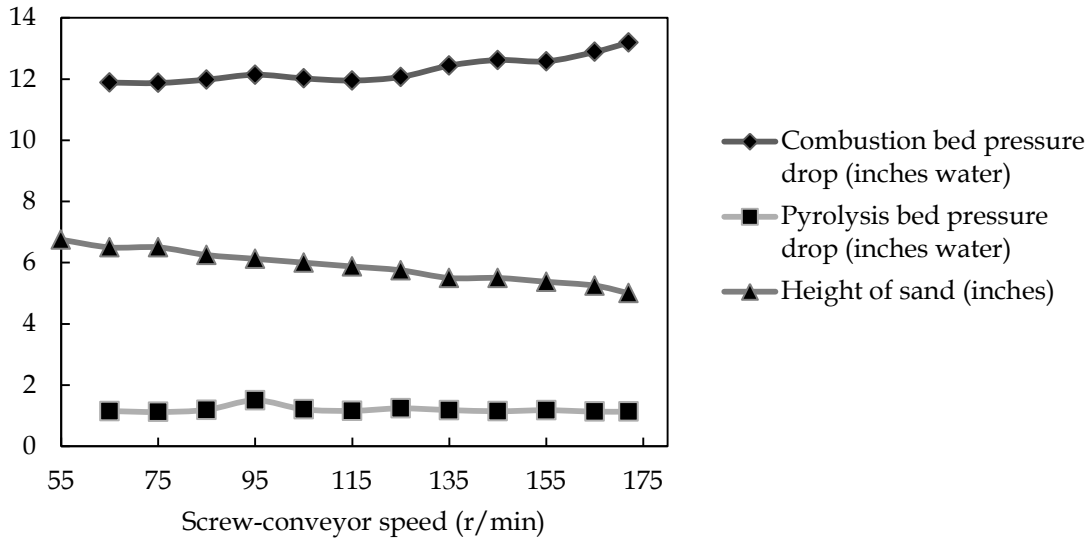

Figure 4.9: Experimental results of the pressure drop over the combustion and pyrolysis bed, and the height of the sand in pyrolysis bed versus the speed of the screw-conveyor with a larger volume of sand in the system

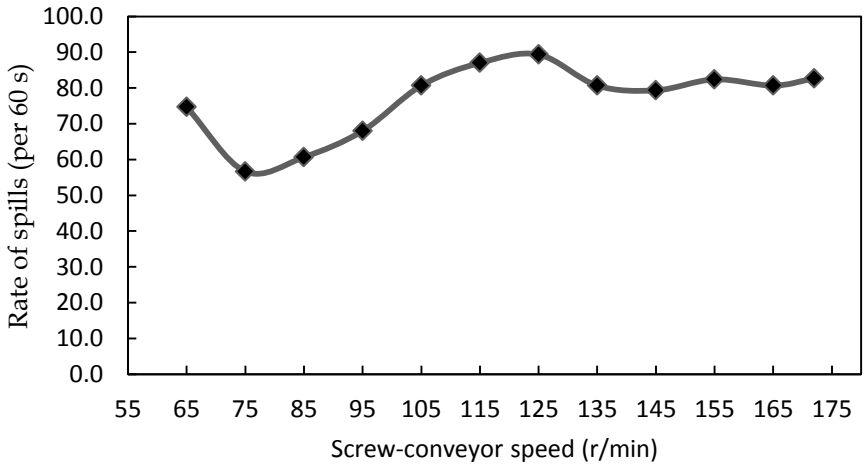

Figure 4.10: Experimental results of the rate of spills to overflow standpipe per minute versus the speed of the screw-conveyor with a larger volume of sand in the system

The results obtained for the pressure drop over the combustion and pyrolysis fluidised beds, as well as the height of the sand in the pyrolysis fluidised bed versus the pyrolysis gas flow rate, are shown in Figure 4.11, and the rate of spills to the overflow standpipe is shown in Figure 4.12. The conclusions obtained from this experiment are as follows:

- The results obtained for the pressure drop over the combustion and pyrolysis beds, and the height of the sand in the pyrolysis bed are very similar to those obtained in the first experiment. It was therefore concluded that a change in the amount of sand charged to the system does not substantially affect the outcomes of varying the gas flow rate to the pyrolysis fluidised bed with regard to these parameters.

- The rate of spills into the overflow standpipe showed a slight downward trend, similar to the first experiment. However, the decrease in the rate of spills was much lower than in the first experiment. This is because the weight of the additional sand in the pyrolysis reactor overcame the upward drag force exerted on the particles by the pyrolysis gas flow.

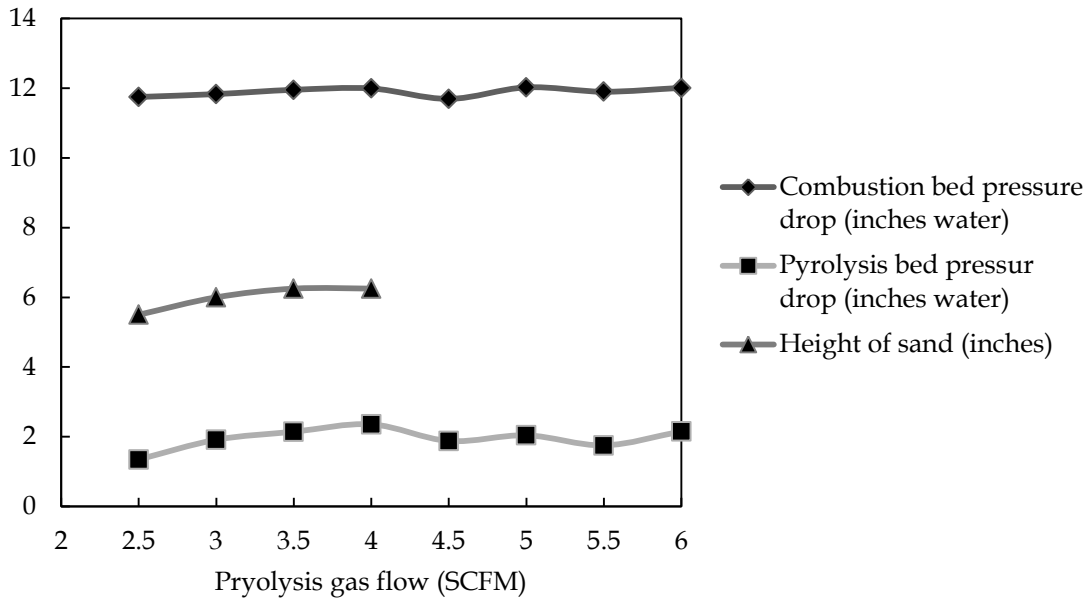

Figure 4.11: Experimental results of the pressure drop over the combustion and pyrolysis bed, and the height of the sand in pyrolysis bed versus the flow rate of gas to the pyrolysis bed with a larger volume of sand in the system

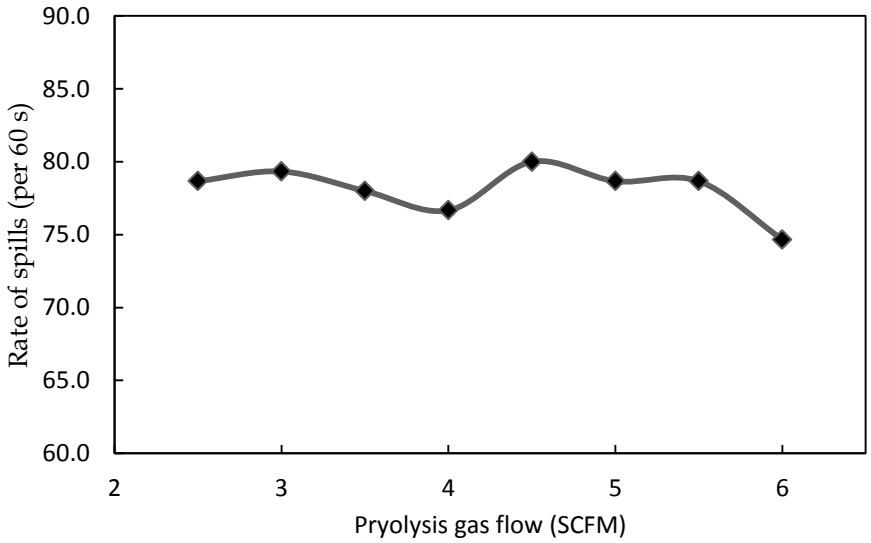

Figure 4.12: Experimental results of the rate of spills to overflow standpipe per minute versus the flow rate of gas to the pyrolysis bed with a larger volume of sand in the system

The results obtained for the pressure drop over the combustion and pyrolysis fluidised beds, as well as the height of the sand in the pyrolysis fluidised bed versus the combustion gas flow rate, are shown in Figure 4.13, and the rate of spills to the overflow standpipe is shown in Figure 4.14. The conclusions that drawn from this experiment are as follows:

- The results obtained for the pressure drop over the combustion and pyrolysis beds, and the height of the sand in the pyrolysis bed are very similar to those obtained in the first experiment. It was therefore concluded that a change in the amount of sand charged to the system does not substantially affect the outcomes of varying the gas flow rate to the combustion fluidised bed with regard to these parameters.
- On the other hand, the rate of spills shows a very clear linear correlation with the increase in the gas flow rate to the combustion bed. This is because the larger quantity of sand in the combustion bed easily overcame the frictional drag force exerted by the pyrolysis gas in the overflow standpipe. Therefore we can conclude that an increase in the amount of sand charged to the reactor has a stabilising effect on the rate of spills into the standpipe.

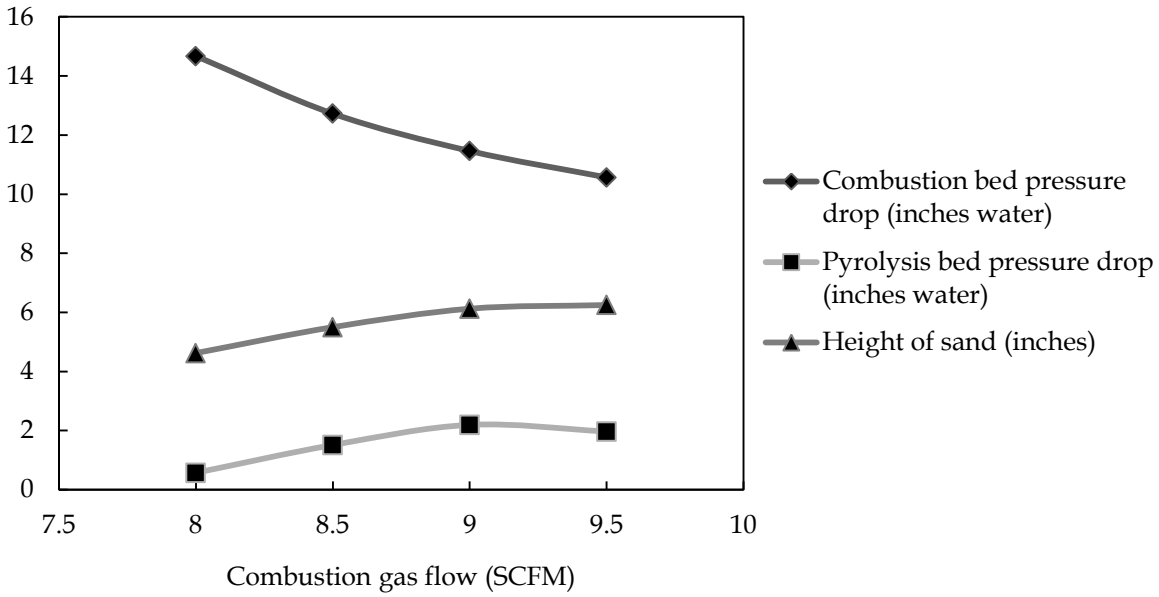

Figure 4.13: Experimental results of the pressure drop over the combustion and pyrolysis bed, and the height of the sand in pyrolysis bed versus the flow rate of gas to the combustion bed with a larger volume of sand in the system

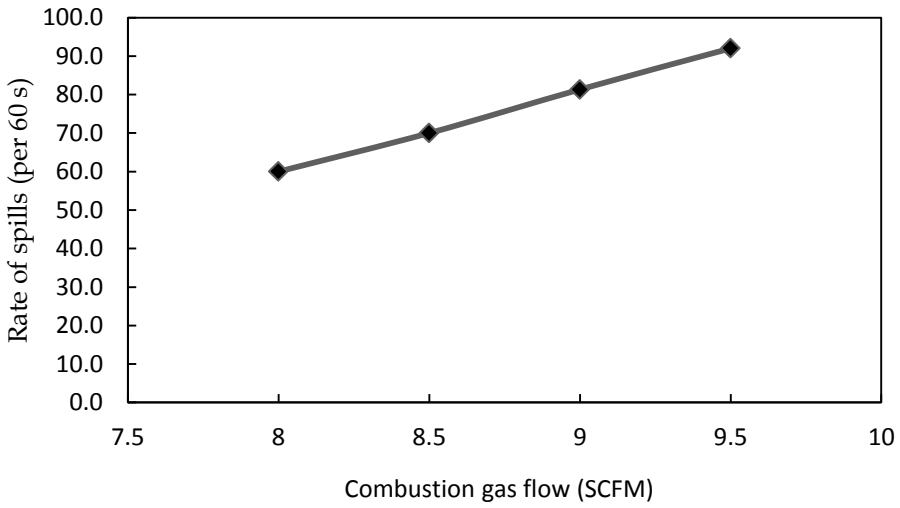

Figure 4.14: Experimental results of the rate of spills to overflow standpipe per minute versus the flow rate of gas to the combustion bed with a larger volume of sand in the system

4.5.5 Applicability to Pyrolysis of Biomass Process

Four requirements for the solids transfer mechanism were identified in order for the mechanism to be considered suitable for the pyrolysis of biomass process. The results obtained from the above experiments were used to determine whether or not the solids transfer mechanism selected in the current investigation met these requirements. The results of this evaluation are shown in Table 4.2. It was found that the solids transfer mechanism selected met all the requriements identified for the pyrolysis of biomasss process. It is therefore a suitable mechanism for this process.

Table 4.2: Conformation to the requirements for the pyrolysis process

Requirement	Conforms	Discussion
The flow of gas from the combustion bed to the pyrolysis bed should be prevented.	Yes	It was possible to ensure that the flow of gas through the standpipe was from the pyrolysis bed to the combustion bed.
The solids transfer rate should be easy to control.	Yes	The flow rate of sand to the pyrolysis bed was dependent on the speed of the screw-conveyor.
Construction of the mechanism should not be complicated or require large amounts of space.	Yes	The standpipe could be built from the refractory separating the combustion bed and the pyrolysis bed.
The solids transfer mechanism should not introduce large heat losses into the system.	Yes	The solids transfer mechanism does not require additional gas inlets to drive the movement of the solids, thereby reducing heat losses.

4.6 Conclusions

A feasible solids transport mechanism in a dual fluidised bed system for the pyrolysis of biomass was selected. In this mechanism, an overflow standpipe is used to transport solids from the combustion fluidised bed to the pyrolysis fluidised bed, and a screw-conveyor is used to transport solids back to the combustion bed. Most dual fluidised bed designs for the pyrolysis or gasification of biomass use only non-mechanical solids flow devices to transport solids between the fluidised beds, such as L-valves and loop seals. The solids transfer mechanism selected in this project is therefore a new approach to the transport of solids in dual fluidised bed systems for the pyrolysis of biomass.

Several experiments were performed on a cold model of the dual fluidised bed system to test the performance of the solids transfer mechanism. During these experiments, the response of the steady-state parameters to changes in several input parameters was observed. These parameters were the speed of the screw-conveyor, the flow rate of the gas fed to the pyrolysis and combustion fluidised beds, and the amount of solids charged to the system. The steady-state parameters that were considered in these experiments were the height of the solids in the pyrolysis bed, the pressure drop over the pyrolysis and combustion beds, and the rate of spills into the overflow standpipe per minute. The following important observations and conclusions were obtained from these experiments:

- It was found that the pressure drop over the combustion and pyrolysis fluidised beds was not influenced by the speed of the screw-conveyor.
- The flow rate of gas to the pyrolysis fluidised bed had a negligible effect on the pressure drop over this bed. This is believed to be because of the gas flow through the overflow standpipe. The pressure drop over the pyrolysis bed is therefore dependent mostly on the flow of gas in the combustion fluidised bed due to its relatively higher flow rate.
- As the flow rate of gas to the combustion fluidised bed increased, the pressure drop over this bed decreased and the pressure drop over the pyrolysis fluidised bed increased. This may be due to an increase in the flow rate of gas from the pyrolysis fluidised bed to the combustion fluidised bed through the standpipe.
- A change in the amount of solids charged to the system had a negligible effect on the response of the pressure drop over the combustion and pyrolysis fluidised beds, and the height of the solids in the pyrolysis bed to changes in the combustion and pyrolysis gas flow rate and the screw-conveyor speed.
- The height of the solids in the pyrolysis fluidised bed increased with increases in the pyrolysis and combustion gas flow rates and decreased with increases in the screw-conveyor speed.
- An increase in the amount of solids charged to the system had a dampening effect on the rate of spills into the overflow standpipe. It also stabilised the response of the rate of spills to changes in the combustion gas flow rate.

Four requirements of the solids transfer mechanism were identified which would favour its suitability for the pyrolysis of biomass process. It was found that the solids transfer mechanism selected in the current investigation met these requirements. The proposed dual fluidised bed design is therefore a feasible design for the pyrolysis of biomass.

CHAPTER 5: MATHEMATICAL MODELING OF THE PYROLYSIS OF BIOMASS

5.1 Introduction

The study of dual fluidised beds (DFBs) is not new and a number of different models have been developed and reviewed. However, most of these models have been developed for coal combustion, and little attention has been given to the processing of biomass in DFBs (Kaushal *et al*., 2007). A brief review of the use of DFBs for the conversion woody biomass to bio-oil is provided in this chapter. In addition, a complete model of the system is presented and discussed. The objectives for the model were as follows:

- A comprehensive model for the dual fluidised bed system was required and should include the hydrodynamics of the system and reaction kinetics.
- An evaluation of the model was required in order to determine the steady-state conditions and variables for the system. This objective will require the optimisation of the model.
- A method was required for the rapid quenching and separating the product gas from the pyrolysis reactions.
- All assumptions were required to be reasonable and model decisions well supported.

The discussion and model presented in this chapter are based on a literature study only. All the parameters used in the model that was developed for the dual fluidised bed system were also obtained from the literature. To simplify the current model, char was used as the only source of fuel to the combustion fluidised bed.

5.2 Theory

5.2.1 Three-phase bubbling fluidised bed model

A three-phase model will be used to model a bubbling fluidised bed. This model is given as equation 5.1, equation 5.2 and equation 5.3, and incorporates the assumption that gas flows in the bubble, cloud and emulsion phase.

$$u_b^* \frac{dC_{Ab}}{dh} = -\delta K_{bc}(C_{Ab} - C_{Ac}) - f_b r_{Ab} \tag{5.1}$$

$$u_c^* \frac{dC_{Ac}}{dh} = \delta K_{bc}(C_{Ab} - C_{Ac}) - \delta K_{ce}(C_{Ac} - C_{Ae}) - f_c r_{Ac} \tag{5.2}$$

$$u_e^* \frac{dC_{Ae}}{dh} = \delta K_{ce}(C_{Ac} - C_{Ae}) - f_e r_{Ae} \tag{5.3}$$

The above differential equation must be solved simultaneously over the height of the bed. An approximation for K_{bc} and K_{ce} can be obtained with the use of equation 5.4 and equation 5.5 respectively (Levenspiel, 1999:457).

$$K_{bc} = 4.5\left(\frac{u_{mf}}{db}\right) + 5.85\left(\frac{\mathcal{D}^{0.5} g^{1/4}}{{d_b}^{5/4}}\right) \tag{5.4}$$

$$K_{ce} = 6.77\left(\frac{\varepsilon_{mf}\mathcal{D}u_{br}}{{d_b}^3}\right)^{1/2} \tag{5.5}$$

The bubble fraction (δ) can be obtained with the following equation:

$$\delta = \frac{u_0 - u_{mf}}{u_b + u_{mf}} \tag{5.6}$$

The bubble rise velocity (u_b) can be obtained with the use of equation 5.7.

$$u_b = u_0 - u_{mf} + u_{br} \tag{5.7}$$

The value for u_{br} in the above equation can be obtained with the use of the following equation (Levenspiel, 1999:456):

$$u_{br} = 0.711(g d_b)^{1/2} \tag{5.8}$$

Industrial reactors are often operated as bubbling fluidised beds with gas velocities (u_0) typically around 5 to 30 times the minimum fluidisation velocity (u_{mf}). The minimum fluidisation velocity can be is shown in equation 5.9. The dimensionless quantities d_p^* and u^* in equation 5.9 can be obtained with the use of equation 5.10 and 5.11 respectively (Levenspiel, 1999:449).

$$\frac{150(1-\varepsilon_{mf})}{\varepsilon_{mf}^3}u_{mf}^* + \frac{1.75}{\varepsilon_{mf}^3}(u_{mf}^*)^2 d_p^* = (d_p^*)^2 \tag{5.9}$$

$$d_p^* = d_p\left[\frac{\rho_g(\rho_s-\rho_g)g}{\mu^2}\right]^{1/3} \tag{5.10}$$

$$u^* = u\left[\frac{\rho_g^2}{u(\rho_s-\rho_g)g}\right]^{1/3} \tag{5.11}$$

5.2.2 Combustion fluidised bed model

Due to the complexity of the process, the model of the combustion fluidised bed involves several steps, which are described in the following paragraphs.

Step1: Perform an energy balance over the pyrolysis fluidised bed:

Given the flow rate of biomass to the reactor, the energy required to drive the endothermic pyrolysis reactions can be calculated. This is done through the use of experimentally determined heats of reaction and average conversion data found in the literature. According to Papadikis *et al.* (2009), the overall heat of reaction of the pyrolysis reactions can be estimated to be 255 kJ/kg.

Step 2: Determine the total amount of char and oxygen required in the combustion fluidised bed:

The flow rate of sand between the combustion and pyrolysis fluidised beds can be calculated with the use of the energy required by the pyrolysis reactions, which was calculated in the first step. This is done with the use of the heat capacity of the sand and the temperature over which the sand is cooled in the pyrolysis fluidised bed. The total amount of char that needs to be combusted to heat this flow rate of sand in the combustion fluidised bed can be calculated by performing a simple energy balance over the bed. To perform this energy balance, it was assumed that all of the char in the reactor is combusted and that 5% of the oxygen entering the reactor exits the reactor with the flue gas. The second assumption was made to ensure that oxygen is present throughout the entire height of the bed so that no pyrolysis will occur in the combustion fluidised bed. In this way, the total amount of char in the bed and the flow rate of air to the combustion fluidised bed could be calculated. Heats of reactions for the combustion reactions are given by Perry, Green & Maloney (1997). The average composition of the char is shown in Table 5.1.

Table 5.1: Average composition of char (Kaushal *et al.*, 2007)

Component	Composition (weight %)
Carbon	82
Hydrogen	4
Oxygen	14

Step 3: Determine the concentration profiles along the height of the combustion fluidised bed:

The three-phase model was used to determine the concentration profiles in the bubble, cloud and emulsion phase throughout the height of the reactor. This was done by using the results obtained in Step 2, and the average composition of char shown in Table 5.1. Seven reactions were considered in the model; these are shown in Table 5.2 (Weimer & Clough, 1981).

Table 5.2: Reactions considered in the model for the combustion fluidised bed with reaction rates

Number	Reaction	Reaction rate
1	$C + O_2 \rightarrow CO_2$	$R_1 = k_1[O_2]$
2	$C + CO_2 \rightarrow 2CO$	$R_2 = k_2[CO_2]$
3	$C + H_2O \rightarrow CO + H_2$	$R_3 = k_3[H_2O]$
4	$CO + H_2O \rightarrow H_2 + CO_2$	$R_4 = k_4[CO][H_2O]$
5	$H_2 + CO_2 \rightarrow CO + H_2O$	$R_5 = k_5[CO_2][H_2]$
6	$CO + 1/2O_2 \rightarrow CO_2$	$R_6 = k_6[CO][O_2]$
7	$H_2 + 1/2O_2 \rightarrow H_2O$	$R_7 = k_7[H_2][O_2]/[CO]$

The kinetic and thermodynamic parameters for the reactions listed in Table 5.2 were obtained from Weimer & Clough (1981). These kinetic parameters are in close agreement with those provided by Kaushal *et al* (2007) and are shown in Table 5.3, along with the thermodynamic parameters. The rate constants (k_i) for the reactions are expressed by the Arrhenius equation:

$$k_i = k_{oi} \times \exp\left(\frac{-E_i}{RT}\right) \tag{5.12}$$

Table 5.3: Kinetic and thermodynamic parameters

Reaction Number	k_{oi}	E_i (J/kmol)	$(-\Delta H)$ (J/kmol)
1	1.55×10^7 m/s	1.247×10^8	3.87×10^8
2	1.6×10^7 m/s	2.469×10^8	-1.73×10^8
3	656 m/s	1.473×10^8	-1.31×10^8
4	$30\times\varepsilon_{mf}$ m^3/kmol s	6.027×10^7	4.2×10^7
5	$1362\times\varepsilon_{mf}$ m^3/kmol s	9.492×10^7	-4.2×10^7
6	3.09×10^8 m^3/kmol s	9.976×10^7	2.83×10^8
7	8.83×10^8 m^3/kmol s	9.976×10^7	2.38×10^8

A trial-and-error method was used to determine the required dimensions and total quantity of sand in the reactor. This was done to ensure that the heat produced in the reactor was similar to that calculated in Step 2, that all of the char was combusted and that oxygen was present throughout the entire height of

the bed. The effects due to the shrinking of the char particles were also considered with the use of equation 5.13. However, these effects are predicted to be negligible due to the small particle size of the char particles from the pyrolysis fluidised bed.

$$t = \frac{\rho_c r_0^2 \emptyset_c}{6 \mathcal{D}_e C_{A0}} \left[1 - 3\left(\frac{r}{r_0}\right)^2 + 2\left(\frac{r}{r_0}\right)^3\right] \tag{5.13}$$

5.2.3 Pyrolysis fluidised bed model

Unlike the combustion fluidised bed, the pyrolysis reactions occur in the solid phase. In addition, the gas used to fluidise the bed does not take part in the reactions either. Therefore the three-phase model described in Section 2.4.2 cannot be used to model the pyrolysis fluidised bed. A plug flow reactor (PFR) or continuous stirred-tank reactor (CSTR) model could not be used for the pyrolysis bed either due to the fact that the particles only leave the reactor when they are small enough to be entrained from the bed. It was therefore decided to model a single wood particle in the bed and then use those results to predict the conversion of the entire reactor. Several important assumptions were used in the development of this model, as follows:

- The wood particles are assumed to be completely spherical.
- The particles in the pyrolysis fluidised bed are assumed to be perfectly mixed.
- The gaseous phase does not influence the solid-phase reactions. This assumption agrees well with the results obtained by Papadikis *et al.* (2009).

A two-stage model was used to model the reaction kinetics of the biomass pyrolysis reactions. This model is illustrated in Figure 5.1 with kinetic rate symbols, and includes the reaction of chemically bound water in the wood to released water vapour (Papadikis *et al.*, 2009). The model includes four main grouped components (wood, char, tar and gas) and is composed of both primary reaction paths (1, 2 and 3) and secondary reaction paths (4 and 5). The tar compounds are gaseous compounds that can be quenched to form bio-oil, such as phenols, levoglucosan and condensed aromatics. The gas compounds consist mostly of incondensable gases, which will be used to fluidise the pyrolysis fluidised bed. The tar splitting reactions are grouped together in reaction 4 and 5, which alters the composition of the gas and has little effect on the solid-phase reactions (Chan, Kelbon & Krieger, 1985).

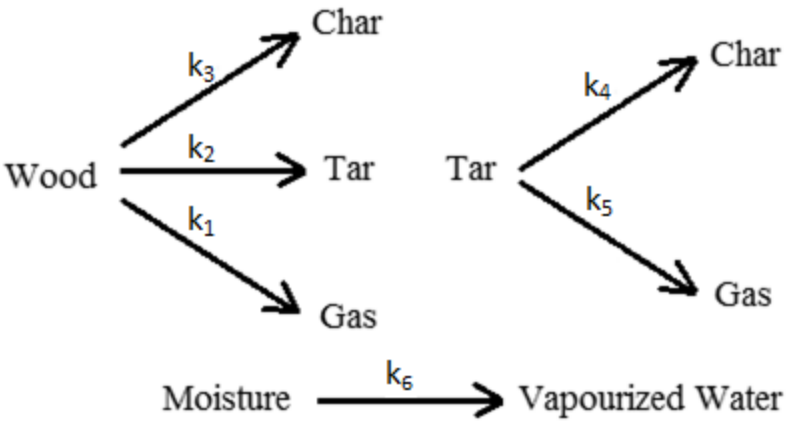

Figure 5.1: The two-stage pyrolysis model, illustrating the conversion of woody biomass into char, tar and gas products with kinetic rate symbols (Papadikis *et al.*, 2009)

The rate constants (k_i) for the reactions in Figure 5.1 are also expressed by the Arrhenius equation given as equation 5.12. Chan *et al.* (1985) suggested kinetic parameters for pine wood pyrolysis, which are shown in Table 5.4. It is difficult to obtain accurate kinetic parameters for a particular wood species in literature due to the widely varying property values among different types of wood. For this reason, the kinetic parameters in Table 5.4 were used as a rough estimate of the temperature and residence time required for the pyrolysis reactions. More accurate kinetic parameters will be obtained for different wood species during the experimental evaluation of the pilot scale unit.

Table 5.4: Kinetic parameters for pine wood pyrolysis reactions

Reaction Number	k_{oi} (s^{-1})	E_i (kJ/mol)
1	1.3×10^{8}	140
2	2.0×10^{8}	133
3	1.08×10^{7}	121
4	1.48×10^{6}	144
5	1.48×10^{6}	144
6	5.13×10^{6}	87.9

The effects of heat transfer along the radius of the wood particles and the shrinking of the particles were considered in the model for the pyrolysis fluidised bed. The heat diffusion equation for an isotropic particle is given as equation 5.14.

$$\frac{\partial}{\partial t}\left(\rho C_{peff} T\right) = \frac{1}{r^2}\frac{\partial}{\partial r}\left(k_{eff} r^2 \frac{\partial T}{\partial r}\right) + (-\Delta H)\left(-\frac{\partial \rho}{\partial t}\right) \tag{5.14}$$

The boundary conditions at the surface and centre of the particle are given as equation 5.15 and equation 5.16 respectively.

$$h(T_\infty - T_s) = -k_{eff}\left.\frac{\partial T}{\partial r}\right|_{r=R} \tag{5.15}$$

$$\left.\frac{\partial T}{\partial r}\right|_{r=0} = 0 \tag{5.16}$$

The heat transfer coefficient can be obtained from the Ranz-Marshall correlation, which is given as equation 5.17.

$$Nu = \frac{hd_p}{k} = 2 + 0.6{Re_d}^{1/2}Pr^{1/3} \tag{5.17}$$

Char formation during pyrolysis takes place mainly on the surface of the wood particles, as shown in Figure 5.2.

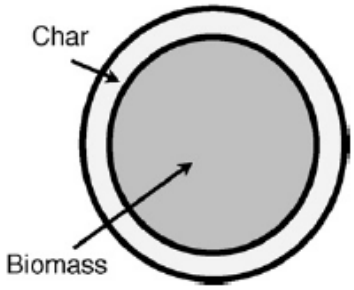

Figure 5.2: Illustration of the formation of char on the outer surface of a biomass particle the during pyrolysis process (Papadikis *et al.,* 2009)

The volume of the wood particles is assumed to decrease linearly with wood mass and increase linearly with char mass. The volume of the wood particle is given by equation 5.18.

$$\frac{V_s}{V_{w0}} = \frac{m_w}{m_{w0}} + \frac{m_c}{M_{w0}} \tag{5.18}$$

Hagge & Bryden (2002) reported that predicted tar yields increase for shrinking particles due to the effect of shrinking on the rate of heat transfer along the radius of the particles. This is due to the change in the density of the particles caused by particle shrinking. The change in the density of the particle with the change in particle volume can be predicted with the use of equations 5.19 to 5.22 (Papadikis *et al.,* 2009).

$$dV_k = \frac{4}{3}\pi(r_k^3 - r_{k-1}^3) for k = 1, \dots, N \tag{5.19}$$

$$dm_k = \frac{(\psi_{kw}+\psi_{k-1_w})+(\psi_{kc}+\psi_{k-1_c})}{2}\frac{m_p}{N} for k = 1, \dots, N \tag{5.20}$$

$$d\rho_{pk} = \frac{dm_k}{dV_k} \tag{5.21}$$

$$\rho_{p_{av}} = \frac{1}{N}\sum_{k=1}^{N} d\rho_{pk} \tag{5.22}$$

The above equations predict the average particle density from the average densities of the discrete volumes. The discretisation of the particle is illustrated in Figure 5.3 where the radius of the particle is divided into N number of grid points numbered from k = 0 to k= N.

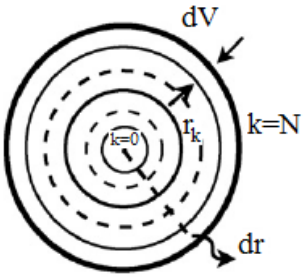

Figure 5.3: Particle discretization of a biomass particle from the inner grid at k=0 to the outer grid at k=N (Papadikis *et al.,* 2009)

Reaction 4 and 5 in Figure 5.1 is the only gas-phase reaction. In order to maximise the production of tar, the residence time of the gaseous tar in the reactor must be as short as possible. In this way, the extent of reaction 4 and 5 will be minimised before the gaseous tar is condensed. The residence time for this reaction will be calculated using the flow rate of the fluidising gas through the reactor and the average distance of the bed from the gas outlet.

Unlike PFR or CSTR reactors, the particles do not leave the reactor after a particular residence time but rather when the gas velocity in the bed exceeds the terminal settling velocity of the particles. At this velocity, the particles are blown out of the bed. The terminal settling velocity for a certain particle size can be calculated with the use of equation 5.23. The dimensionless quantities d_p^* and u_t^* in equation 5.23 can be obtained with equation 5.10 and equation 5.11 respectively.

$$u_t^* = \left[\frac{18}{(d_p^*)^2} + \frac{2.335 - 1.744\phi_s}{(d_p^*)^{1/2}}\right]^{-1} \tag{5.23}$$

The gas velocity in the pyrolysis fluidised bed affects the performance of the reactor in several ways. Firstly, in order to ensure that the bed is operating in the bubbling regime, the velocity of the gas must exceed the bubbling velocity of the sand particles. Secondly, the velocity should be low enough to allow maximum conversion of the wood particles before they are entrained. Lastly, the velocity of the gas should be high enough to minimise the residence time of the gaseous tar products in the reactor in order to minimise the conversion of the tar products to incondensable gases.

5.2.4 Comparison of pyrolysis model with literature

A quantitative comparison between the model for the pyrolysis fluidised bed and experimental results is difficult because of the varying chemical composition of wood, the uncertainty of kinetic data, the simplicity of the pyrolysis model and widely varying property values among different types of wood (Hagge & Bryden, 2002; Di Blasi, 1996). Therefore, the results obtained from the pyrolysis fluidised bed model were mainly used for initial estimates of the temperature and fluidisation velocity required for the pyrolysis fluidised bed reactor in the pilot scale system. The model used for the pyrolysis fluidised bed reactor was developed from three concepts, namely the two-stage pyrolysis model shown in Figure 5.1, particle shrinkage and particle entrainment from the bed. As the commissioning and experimental evaluation of the pilot scale system did not form part of the current project, comparison of the model results with experimental data was not possible. Therefore, a literature study was performed in order to investigate the conclusions that were made by other authors who have used the same concepts in developing a model for the fast pyrolysis of biomass. Five papers were considered during the literature study. The main findings from this investigation are discussed in the following list:

- Papadikis *et al.* (2009) concluded that both primary and secondary reaction paths are affected by the shrinkage of the wood particles and that the best tar yields were predicted when particle shrinkage was included in the model.
- Chan *et al.* (1985) reported that the predictions obtained from their model did not always agree with experimental results to within the standard error presented for the replicates. However, they were all generally within 5% of the measured results for nearly all of the conditions studied in their experimental design, and exhibited the same trends as the experimental results.
- Babu & Chaurasia (2004) compared the results obtained from a different two-stage pyrolysis model to the experimental results obtained by Pyle & Zaror (1984), Shafizadeh *et al* (1979) and *Scott et al* (1988). They reported that the results obtained from their model were in excellent agreement with the experimental results. Although they used a different two-stage model, Papadikis *et al.* (2009) reported that they obtained very similar results with the same two-stage pyrolysis model used in the current study.
- Di Blasi (1996) reported that the two-stage pyrolysis model used in the current study could be profitably applied to simulate the thermal conversion of biomass. This is because it includes the description of the primary degradation of the biomass and the secondary degradation of primary pyrolysis products. They concluded that there is qualitative agreement between model predictions and experimental results. In addition, product yields show a quantitative agreement with the model results for very low radiative heat fluxes (corresponding to a kinetically controlled regime).
- Hagge & Bryden (2002) reported that in the thermal wave pyrolysis regime (when the internal heat transfer of the biomass particles is much greater than external heat transfer) the effects of particle shrinkage significantly reduce the gas product yield, increase the tar yield, and reduce the pyrolysis time.

5.3 Results and Discussion

5.3.1 Model Parameters

The important parameters that have been chosen for the system are shown in Table 5.5.

Table 5.5: Model parameters

Parameter	Choice
Inert solid used in the system	Silica sand
Classification of solid	Geldart B
Density of the sand	2 500 kg/m^3
Woody biomass used	Eucalyptus wood chips
Density of the biomass	700 kg/m^3
Operating regime for pyrolysis fluidised bed	Bubbling
Operating regime for combustion fluidised bed	Bubbling
Feed gas for combustion fluidised bed	Air
Feed gas for pyrolysis fluidised bed	Syngas
Operating temperature of the combustion fluidised bed	±900°C
Operating temperature of the pyrolysis fluidised bed	±500°C
Average diameter of the sand particles	440 µm
Average diameter of the wood particles	500 µm
Combustion reactor diameter	225 mm
Pyrolysis reactor diameter	113 mm

5.3.2 Combustion fluidised bed results

A PFR model was used to model the combustion reactions to determine the ideal conversion attainable in the combustion fluidised bed. To prevent the gasification of the char particles, the char will be fed as the limiting reagent to the reactor. This will ensure that oxygen will always be present throughout the height of the reactor. The flow rate of char to the combustion fluidised bed was optimised to ensure that the conversion of oxygen would not exceed 95%.

A graph of the mol fractions of the compounds in the combustion fluidised bed versus the height of the reactor, which was calculated with the use of a PFR model, is shown in Figure 5.4. Due to the high rates of the combustion reactions, only a small section after the bed inlet is shown in the graph. The components react rapidly until all of the carbon has been converted into gaseous compounds, at which point the concentrations in the bed remain constant. Although several reactions were included in the model, it can be seen in Figure 5.4 that the oxygen in the bed is converted mainly into carbon dioxide, while hydrogen is converted into water. The mol fraction of oxygen decreases rapidly to its final value, while the mol fraction of carbon dioxide increases at approximately the same rate to its final value. The mol fraction of hydrogen decreases almost instantly to zero, while the mol fraction of water increases to a final value approximately equal to the starting mol fraction of hydrogen. Although some carbon monoxide is formed during this process, it is instantly converted into carbon dioxide, which results in a constant mol fraction of zero for this compound.

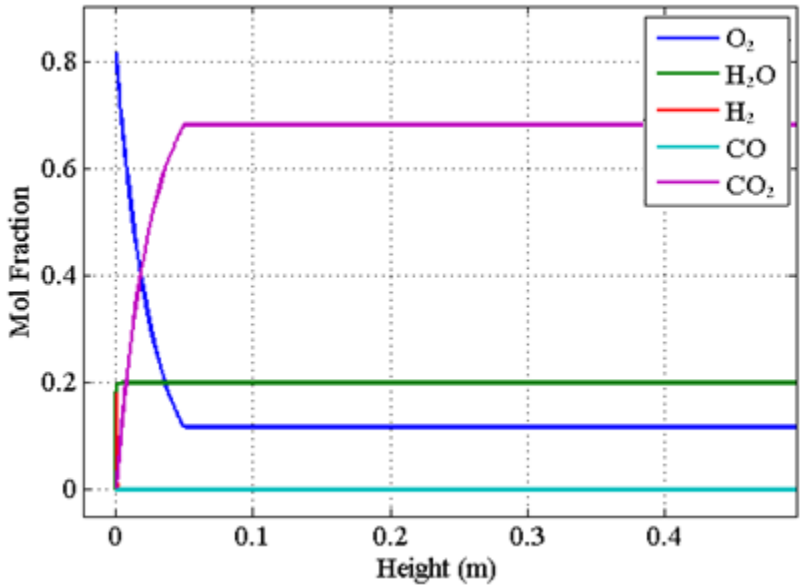

Figure 5.4: Mol fraction of the different components in the combustion fluidised bed versus height, as predicted with the use of a PFR model

The conversions obtained from the PFR model, described in the previous paragraphs, were used in a trial-and-error process to perform the energy and material balances over both the combustion and pyrolysis fluidised beds. This process was used to solve for two important variables, namely the flow rates of sand and char between the fluidised beds.

The solution of the combustion fluidised bed model in the bubbling regime proved to be difficult due to the very long solution times of the model, which were caused by the large reaction rates. Therefore to decrease the solution time, the model was evaluated at lower temperatures to predict how close the real conversions would be to the ideal conversions calculated in the PFR model. In addition, unlike in the classic PFR model, the reaction rates for reactions 1, 2 and 3 in Table 5.2 were not set to zero when the carbon had been completely reacted to improve solution times.

A graph of the concentrations in the combustion fluidised bed versus height, obtained with the bubbling fluidised bed model, is shown in Figure 5.5. These concentrations were obtained for a temperature of 500°C and at a feed-gas superficial velocity equal to the minimum bubbling velocity. Even at this lower temperature, the conversion of oxygen is equal to 100%. In addition, the concentration profiles are very similar to those shown in Figure 5.4. Therefore it is expected that similar conversions would be obtained for a bubbling fluidised bed at 900°C compared with the ideal PFR conversions if the effects of the limited carbon were included. It can also be seen in Figure 5.5 that the oxygen concentration drops suddenly at the bed inlet as it is converted into water. At slightly higher feed-gas superficial velocities, it is expected that similar conversions will still be obtained despite greater interphase mass transfer restrictions due to the high reaction rates.

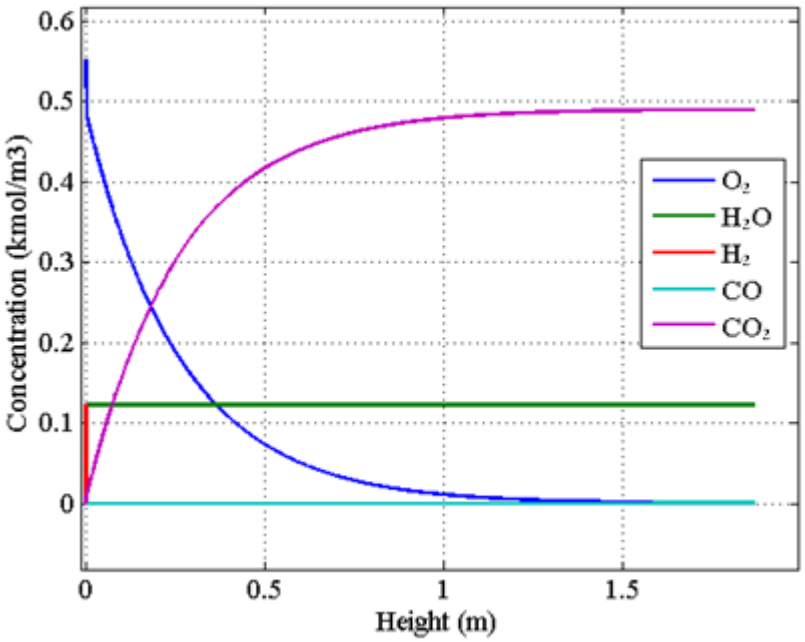

Figure 5.5: Concentration of the different components in the combustion fluidised bed versus height, as predicted with the use of the bubbling fluidised bed model

5.3.3 Pyrolysis fluidised bed results

In order to solve the model for the pyrolysis fluidised bed, the wood particles were discretised into 15 sections, as shown in Figure 5.3. In this way, the heat diffusion equation, given as equation 5.14, could be solved by means of the method of lines numerical procedure for partial differential equations. Using this procedure, the partial differential equation was used to create 15 simultaneous ordinary differential equations, which could be solved for the temperatures in the discrete sections of the wood particles. These temperatures were then used in the two-stage biomass pyrolysis model to determine the conversion of wood in the discrete sections of the wood particles. The results obtained from this procedure for the mass of wood in a single particle are shown in Figure 5.6. A three dimensional (3D) representation of the change in the mass of wood in the particle with time along the radius of the particle is shown in the top left graph in this figure. A contour map of this graph is given in the top right graph in Figure 5.6. In addition, the change in the average mass of wood compounds versus time in the particle is shown in the bottom graph of Figure 5.6. From these graphs it can be seen that the outer sections of the particle contain the largest mass of wood compounds. Approximately 10 seconds is required to obtain complete conversion of the wood compounds.

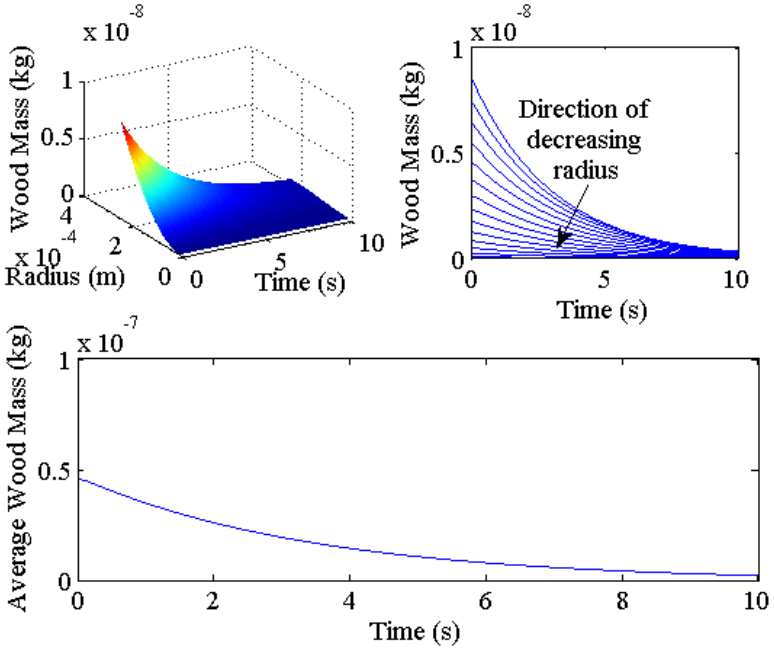

Figure 5.6: Mass of wood for a single particle in the pyrolysis fluidised bed versus time and radius

Similar to Figure 5.6, the mass of char in the wood particle is shown in Figure 5.7. From this figure it can be seen that no char exists in any of the discrete sections at the start of the process. However, as shown in the bottom graph of Figure 5.7, the mass of char in the particle increases up to 10 seconds, after which it begins to level off. The outer section of the particle contains the largest mass of char and also has the highest conversion rate. These higher conversion rates may be attributed to the higher temperate of the outer layers of the particle as given by the heat diffusion equation.

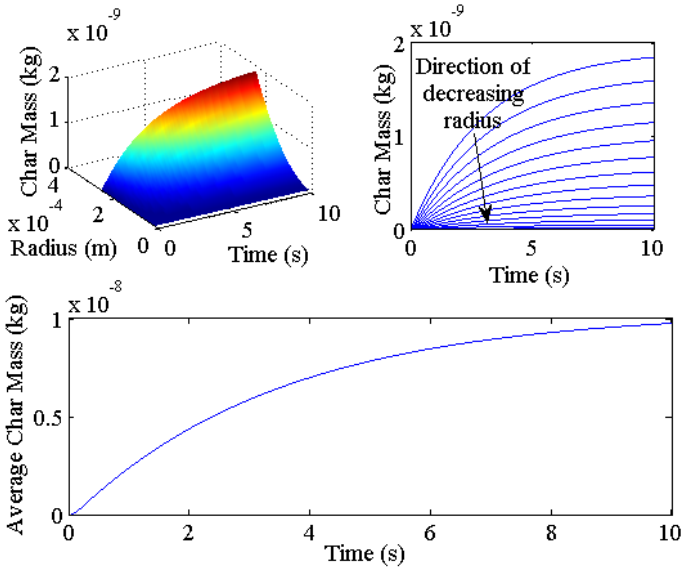

Figure 5.7: Mass of char for a single particle in the pyrolysis fluidised bed versus time and radius

A graph of the average mass of the compounds in a single particle versus time is shown in Figure 5.8. From this graph it can be seen that the wood reacts almost completely to form tar and char products. This is the ideal situation as the char can be fed to the combustion fluidised bed to support the combustion reactions, while the tar products can be quenched to form bio-oil. Only the solid compounds (i.e. wood and char) were used to determine the change in volume of the particle as the gaseous compounds are assumed to leave the particle as soon as they are formed.

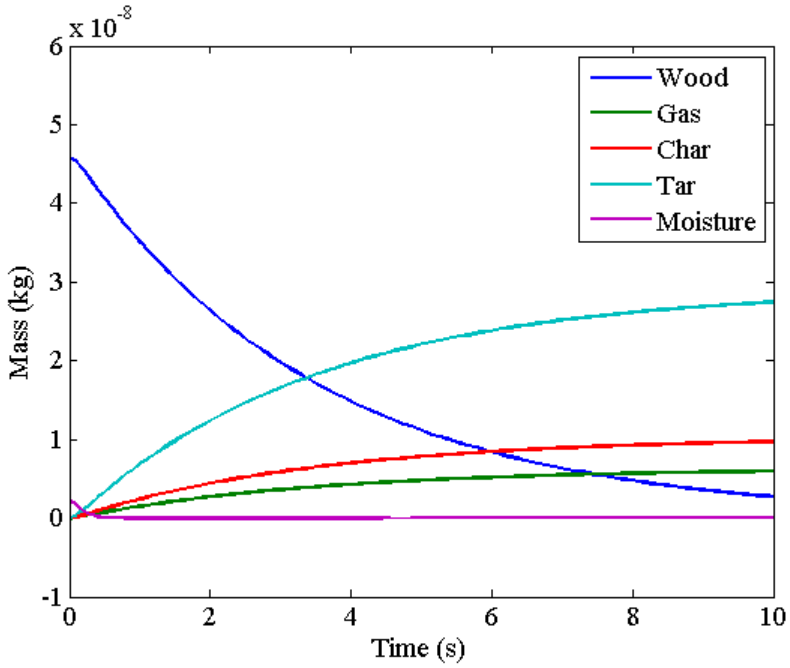

Figure 5.8: Mass of the different grouped components for a single biomass particle in the pyrolysis fluidised bed versus time, as predicted with the use of the two-stage pyrolysis model

The final mass of the compounds obtained from a single particle versus the temperature of the pyrolysis fluidised bed is shown in Figure 5.9. The main objective of this calculation was to determine at which temperature the tar outlet concentration would be at a maximum. From Figure 5.9 it can be seen that this is achieved at a temperature of approximately 500°C. This corresponds very well with the temperature range of 450-550°C suggested by Wang *et al* (2005) for maximum bio-oil yield. Therefore a temperature of 500°C was chosen for the pyrolysis fluidised bed. It can also be seen that the outlet concentration of char reaches a local maximum at this temperature, which is also desirable. Furthermore, the conversion of wood at this temperature is near 100%.

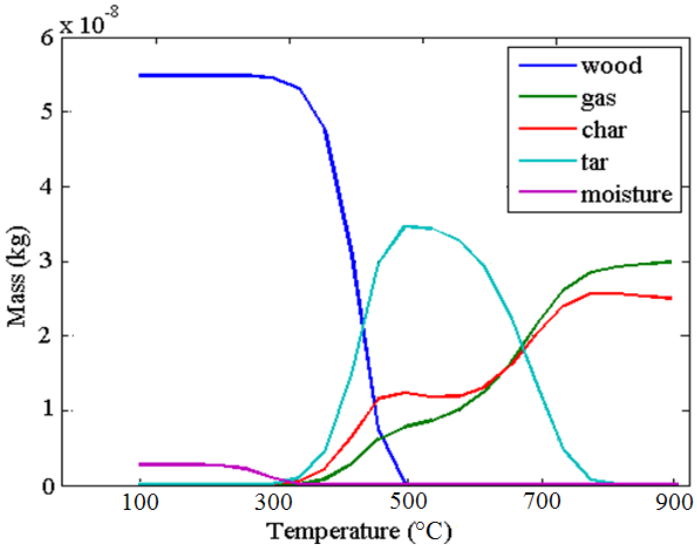

Figure 5.9: Final mass of the different grouped components for a single biomass particle in the pyrolysis fluidised bed versus temperature, as predicted with the use of the two-stage pyrolysis model

The change in the total radius of a single particle versus time is shown in Figure 5.10. Only the masses of the wood and char compounds were used in determining the radius of the particle, as shown in equation 5.18. It is important to note that the change in radius does not result in the disappearance of the outer discrete layers of the particle but is instead the result of the change in the volumes of the discrete sections. The change in the radius of the particle begins to level off towards 10 seconds. Therefore the radius of the char particles obtained from the bed is expected to be near 1.6 µm.

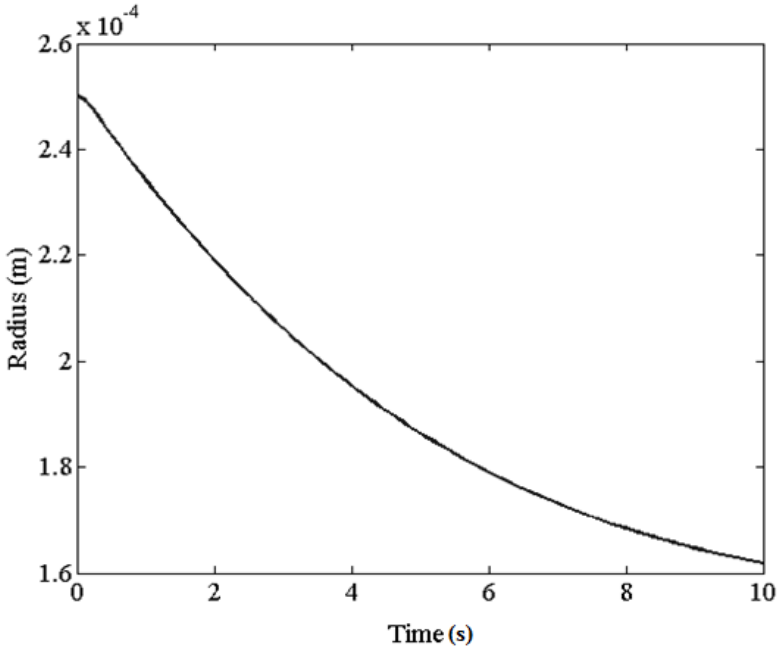

Figure 5.10: Reduction in the radius of a single biomass particle in the pyrolysis fluidised bed versus time due to particle shrinkage

The average density of a single particle versus time is shown in Figure 5.11. The density of the wood particle decreases from 700 kg/m^3 to a final value near 200 kg/m^3. Therefore the density of the char particles obtained from the pyrolysis fluidised bed is expected to be near 200 kg/m^3. This significant change in density validates the use of the heat diffusion equation, used in the model of the pyrolysis fluidised bed. The smaller the change in the density of the particle versus time, the greater is the increase in heat conduction along the radius of the particle (Papadikis *et al.,* 2009). Therefore more accurate conversions are obtained when the change in the density of the particle is considered in the model for the reactor.

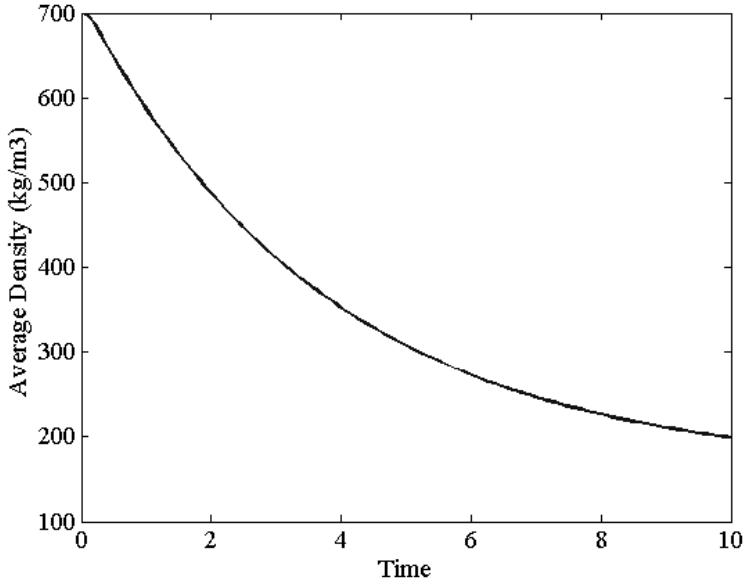

Figure 5.11: Reduction in the average density of a the biomass particles in the pyrolysis fluidised bed versus time

A 3D graph of the change in temperature of a single particle in the pyrolysis fluidised bed is shown in Figure 5.12. From this graph it can be seen that the temperature along the radius of the particle increases rapidly to the bed temperature of the pyrolysis reactor. The change in the temperature of the inner discrete layers of the particle is slower and reaches a lower final temperature compared with the outer layers, as was expected. The rapid increase in temperature is attributed mostly to the small size of the particle. Although there is some temperature variation in the particle, this may be ignored due to the small size of the particle.

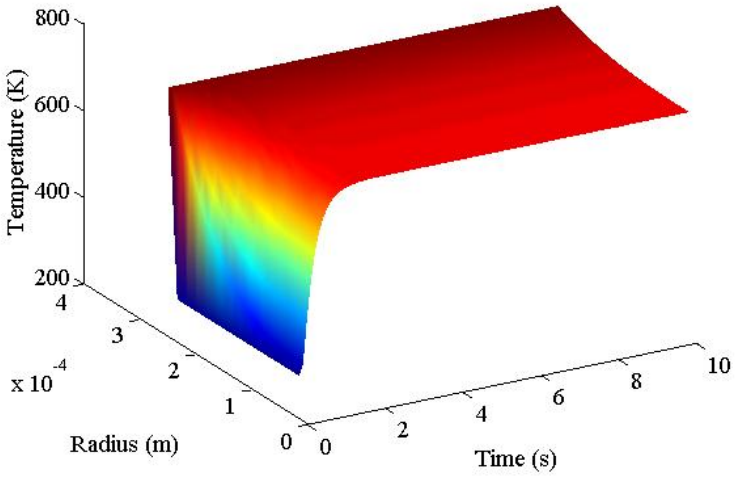

Figure 5.12: Change in the temperature of a single particle in the pyrolysis fluidised bed versus time and radius

To ensure that the wood particles are not entrained from the reactor before they are completely converted, the terminal velocity of the particles obtained after 10 seconds in the bed was calculated. This was found to be 0.28 m/s, which is above the bubbling velocity of the sand particles. Therefore the optimum flow rate of the fluidising gas to the pyrolysis bed must be determined from the conversion of the wood particles before they are entrained and from the extent of reaction 4 and 5 in the two-stage pyrolysis model. The mass of tar exiting the reactor from one biomass particle versus the inlet flow rate of gas to the pyrolysis fluidised bed is shown in Figure 5.13. From this graph it can be seen that the secondary conversion of tar due to reaction 4 and 5 in the two-stage pyrolysis model is less important than the conversion of the wood before it is entrained. Therefore the optimum gas flow rate is approximately 0.28 m/s.

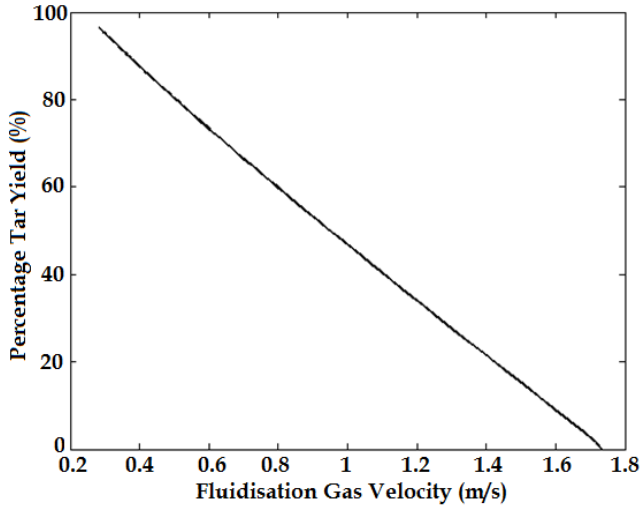

Figure 5.13: Reduction in the yield of tar from the pyrolysis fluidised bed versus the fluidization gas velocity due to particle entrainment from the bed

5.4 Conclusion

A brief description of the theory and models that were used in the design of a dual fluidised bed system for the conversion of woody biomass to bio-oil is provided in this chapter. Both the pyrolysis and combustion fluidised beds will be operated in the bubbling regime. Seven reactions were used in the model for the combustion fluidised bed and the effect of particle shrinkage was also considered. A two-stage model, suggested by Papadikis *et al.* (2009), was used to model the pyrolysis fluidised bed.

A PFR and bubbling fluidised bed model was used for the combustion fluidised bed. It was found that the conversion obtained from the combustion reactor was not significantly affected by the interphase mass transfer limitations observed in bubbling fluidised beds due to the high reaction rates of the combustion reactions. Therefore the conversion predicted by the bubbling fluidised bed model was the same as that predicted by the ideal case (i.e. the PFR model). Char will be fed to the combustion fluidised bed as a limiting reagent to prevent the gasification of the char particles.

The model for the pyrolysis fluidised bed was obtained through the development of a model for a single biomass particle in the bed. The effects of temperature and density variations in the particle over time along the radius of the particle were considered in this model. In addition, the change in the diameter of the particle over time was also considered in the model.

Three main concepts were used in the development of the pyrolysis fluidised bed model, namely the two-stage pyrolysis model, the shrinkage of the biomass particles and particle entrainment from the pyrolysis bed. A literature study was conducted in order to investigate the conclusions that were reported by other authors who had used the same concepts to develop models for the fast pyrolysis of biomass. From this investigation, it was found that the two-stage pyrolysis model used in the current study agrees well with experimental results, and can be used to simulate the fast pyrolysis of biomass process with reasonable accuracy (Di Blasi, 1996; Chan *et al,* 1985). In addition, particle shrinkage has a significant effect on the gas product yield, the tar yield, and pyrolysis time (Hagge & Bryden, 2002).

During the modelling of the pyrolysis fluidised bed, it was found that the temperature along the radius of the biomass particles increases rapidly to the bed temperature due to the small size of the particles. The wood achieved total conversion after 10 seconds in the reactor. The temperature of the pyrolysis fluidised bed was optimised to be 500°C. At this temperature the maximum yield of bio-oil is obtained, which is approximately 64% on a weight basis. It was also found that the effects of the secondary conversion of tar in the two-stage biomass pyrolysis model were far less than those obtained if the wood was not converted fully before being entrained from the bed. Therefore the velocity of the fluidising gas to the pyrolysis bed should be set low enough to ensure that complete conversion of the wood is obtained. For the pyrolysis fluidised bed modelled in this chapter, it is suggested that the set-point for this flow rate be approximately 0.28 m/s.

CHAPTER 6: PHYSICAL DESIGN

6.1 Introduction

The current project was performed in collaboration with the paper and pulp sector in South Africa. A large quantity of underutilised biomass is produced as a by-product in this sector annually. Therefore, to realise the advantages of the pyrolysis process in this sector, a reactor design for this process is required, which can be scaled up for large-scale operations. A 20 kg per hour pilot-scale version of the dual fluidised bed system designed during this project was constructed at the University of Pretoria in South Africa to finalise the design and to ensure that it could be scaled up.

The objective of this chapter is to provide an overview of the design of the pilot-scale system. Three dimensional pictures of each part of the pilot-scale system are shown, along with the dimensions used for each part.

6.2 Dual Fluidised Bed Section

6.2.1 Overview

The overall design for the dual fluidised bed section of the pilot-scale system is shown in Figure 6.1. The pyrolysis fluidised bed is the small bed on the left of Figure 6.1 and the large square bed on the right of the figure is the combustion fluidised bed. The larger size of the combustion fluidised bed is required due to the larger volumetric flow rate of gas required in this bed compared with the pyrolysis bed. It was decided to use square beds rather than round beds to simplify the construction of the system. The pilot-scale system shown in Figure 6.1 was designed to process approximately 20 kg of biomass per hour.

The pyrolysis fluidised bed is bolted to the combustion fluidised bed. This allows the pyrolysis fluidised bed to be separated from the combustion fluidised bed for maintenance purposes. A screw-conveyor is positioned at the bottom of the pyrolysis fluidised bed, which is used to convey cold sand and char back to the combustion fluidised bed. A variable speed motor is used to drive the screw-conveyor, which allows control over the solids circulation rate between the combustion and pyrolysis fluidised beds. The outlet from the overflow standpipe to the pyrolysis fluidised bed is positioned slightly above the screw-conveyor. This allows for a sufficient pressure differential between the top and bottom of the overflow standpipe to ensure that gas flow through the standpipe is only from the pyrolysis fluidised bed to the combustion fluidised bed. The cyclone for the pyrolysis gases is positioned on the side of the pyrolysis fluidised bed. This is important as it allows room to take off the lid of the pyrolysis fluidised bed in order to add additional solids to the system.

The combustion fluidised bed is composed of two sections, namely a bottom section and the freeboard section. These sections are separated near the middle of the combustion fluidised bed. The freeboard section of the combustion fluidised bed can therefore be removed for maintenance purposes. Two valves are positioned at the bottom of the combustion fluidised bed which can be used to remove solids from the dual fluidised bed system. The dual fluidised bed system is supported on four legs connected to the combustion fluidised bed. This provides space under the system for maintenance and for removing solids from the system.

Both the combustion fluidised bed and pyrolysis fluidised bed are approximately 2 m in height, despite the larger volumetric flow rate of gas in the combustion fluidised bed. This is because the disengagement height required in both beds is dependent on the superficial gas velocity in the bed rather than on the volumetric gas flow rate. Therefore the height required for the system will not increase substantially in large-scale operation.

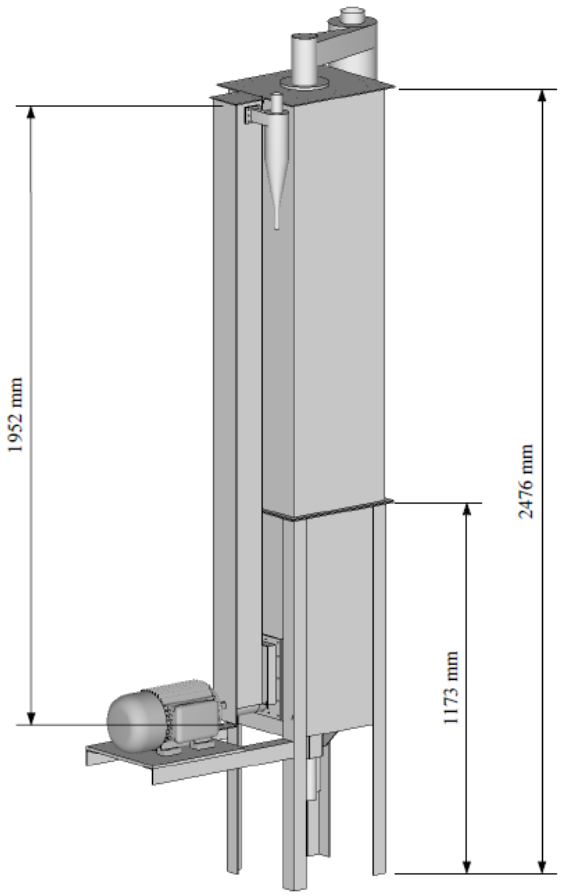

Figure 6.1: The assembled design of the dual fluidised bed section of the pilot scale system, where the combustion bed and pyrolysis bed is shown in the right and left of the figure respectively

All the components of the dual fluidised bed section is illustrated in an exploded view of system (Figure 6.2). The air inlet and distributor part includes the LPG inlet and fits through the sand outlet part of the combustion fluidised bed. The sand outlet includes two manual valves and forms the bottom of the combustion fluidised bed. This part is bolted to the bottom mild steel shell of the combustion fluidised bed. This shell houses the bottom refractory in which the combustion reactions occur. To save space, the overflow standpipe to the pyrolysis fluidised bed is made out of the bottom refractory. The combustion bed is further insulated with 25 mm of insulation wool which fits between the refractory and the shell and with another 25 mm of insulation wool fitted to the outside of the shell. This is done to reduce the temperature from 900°C in the centre of the combustion fluidised bed to approximately 50°C on the outside of the bed. The bottom shell is bolted to the mild steel shell of the freeboard section which houses the top refractory. A lid, also insulated with refractory, is bolted to the top of the combustion fluidised bed. The cyclone part for the combustion fluidised bed slides into a hole in this lid and can therefore be removed or repositioned easily.

The pyrolysis fluidised bed has three main parts, namely the pyrolysis mild steel shell, the pyrolysis cyclone and the screw-conveyor casing. Due to the lower temperature of the pyrolysis fluidised bed, it is only insulated with 25 mm of insulating wool fitted to the outside of the shell. The screw-conveyor casing is welded to the bottom of the pyrolysis fluidised bed. This allows solids and char to fall continuously into the screw-conveyor. The pyrolysis cyclone is bolted to the side of the pyrolysis fluidised bed to allow

the easy removal of the pyrolysis lid. The pyrolysis fluidised bed will be bolted to the bottom shell of the combustion fluidised bed.

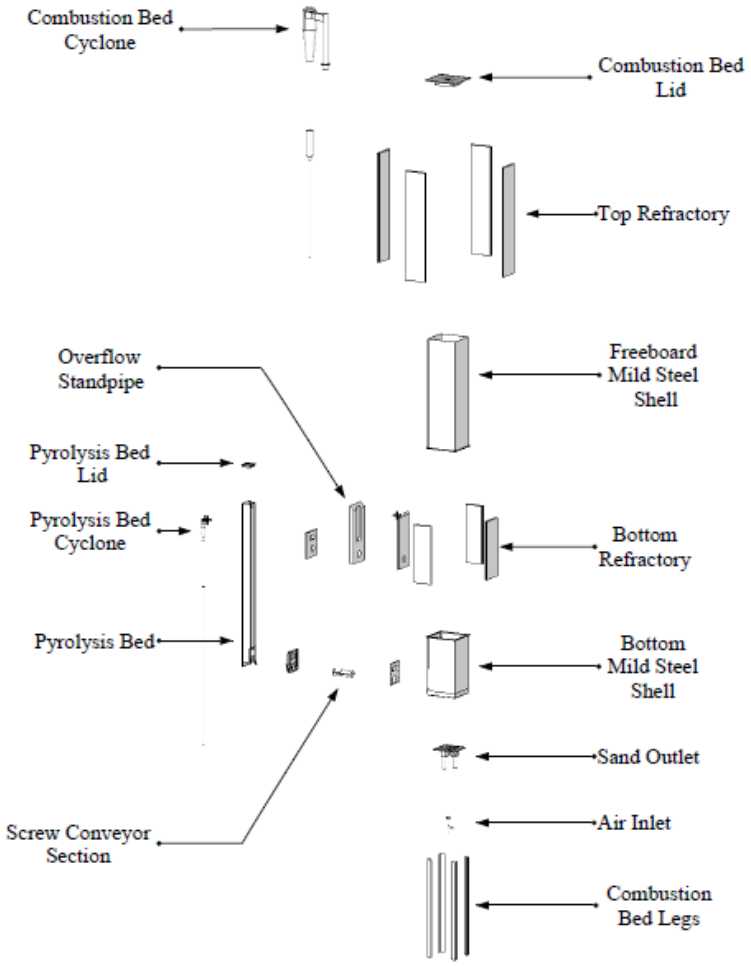

Figure 6.2: The exploded view of all the components of the dual fluidised bed section. The components that were required for the combustion fluidised bed are shown on the right, while those required for the pyrolysis fluidised bed are shown on the left

6.2.2 Combustion Fluidised Bed

The complete design of the combustion fluidised bed is shown in Figure 6.3. The total height of the bed is close to 2.5 m as shown in the figure. A mild steel plate is welded to the bottom mild steel shell of the combustion fluidised bed. The pyrolysis fluidised bed will be bolted to this plate. This plate includes two holes for the exit of the overflow standpipe to the pyrolysis bed and the exit of the screw-conveyor to the combustion bed.

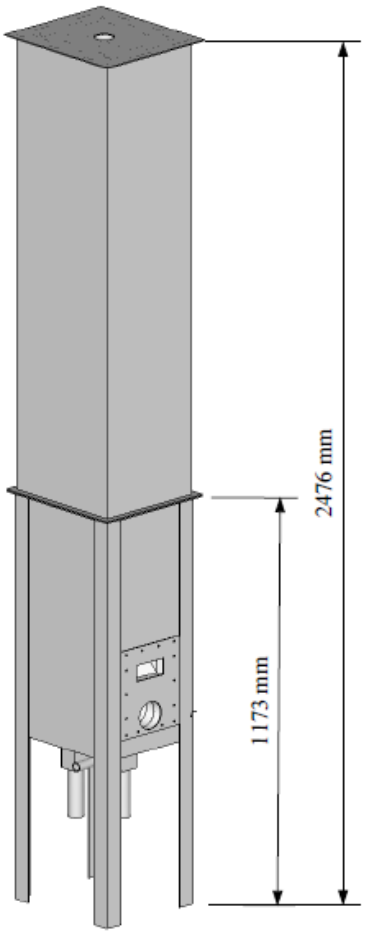

Figure 6.3: The assembled design of the combustion fluidised bed

The mild steel shell used for the freeboard section of the combustion fluidised bed is shown in Figure 6.4. The bottom of the shell includes a lip that extends into and out of the shell. The part of the lip that extends into the shell is used to support the top refractory section and the outer part of the lip is used to bolt the freeboard section to the bottom section of the combustion fluidised bed. As a result, the freeboard section of the bed can be removed with the top refractory, which allows access to the bottom section of the combustion fluidised bed for maintenance purposes.

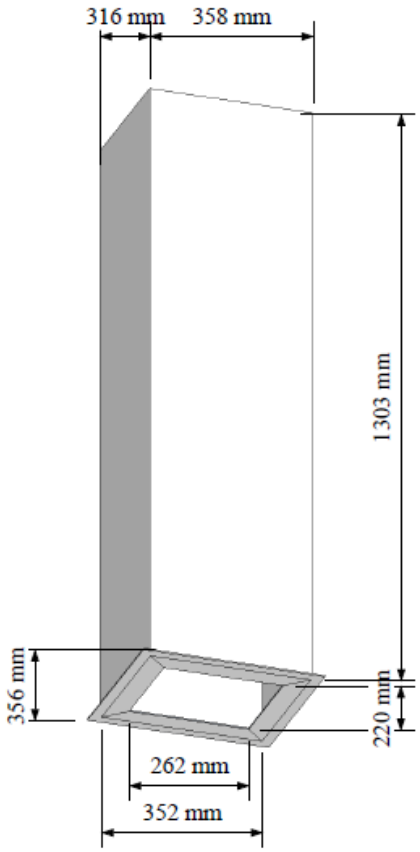

Figure 6.4: Mild steel shell for the freeboard section of the combustion fluidised bed

The bottom mild steel shell of the combustion fluidised bed is shown in Figure 6.5. A lip that extends outwards is positioned at the top of the shell and is used to bolt the freeboard section to the bottom section of the combustion fluidised bed. The large opening towards the bottom of the shell is used for the placement of the plate to which the pyrolysis fluidised bed is bolted. The four legs for the combustion fluidised bed are welded to the four corners of the bottom mild steel shell and extend to the upper lip of the shell for support. This narrows the opening left for the plate. The bottom mild steel shell also includes a lip that extends inwards at the bottom the shell. This is used to support the bottom refractory in the bed. An additional 45 mm of mild steel is welded to the bottom lip facing the front of the bed. It accommodates the thicker refractory facing the front of the bed which is required for the overflow standpipe.

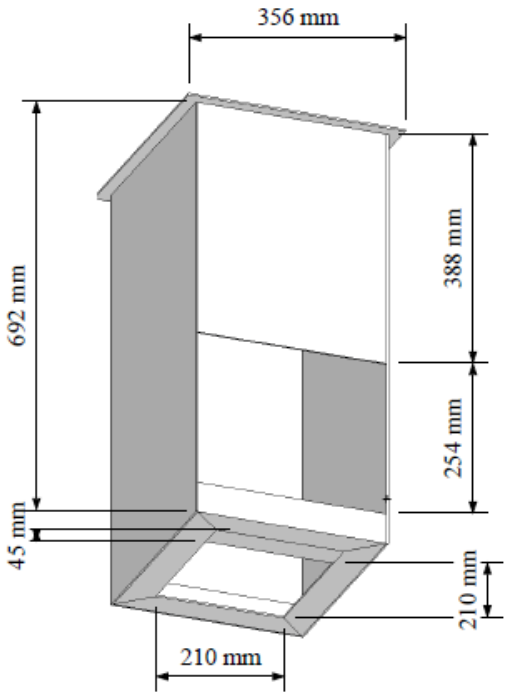

Figure 6.5: Mild steel shell for the bottom section of the combustion fluidised bed

The dimensions of the plate to which the pyrolysis fluidised bed are bolted are shown in Figure 6.6. The top and bottom of the plate are welded directly to the bottom mild steel shell, while the side of the plate is welded to the legs attached to the bottom shell. The rectangular hole in the plate is the exit of the overflow standpipe to the pyrolysis fluidised bed and the round hole is the exit of the screw-conveyor to the combustion fluidised bed.

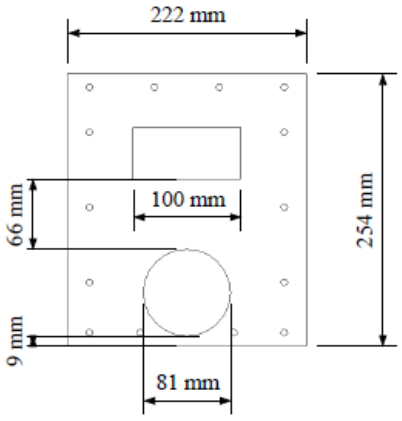

Figure 6.6: Mild steel connection plate for the pyrolysis fluidised bed

The dimensions of the legs for the combustion fluidised bed are shown in Figure 6.7. Standard 50 mm angle iron was used for these legs. They are welded to the corners of the bottom shell of the combustion fluidised bed and extend to the upper lip of the shell and to approximately 500 mm below the shell. The bottom 500 mm of the legs provides space under the dual fluidised bed system for maintenance purposes and for removing solids from the system when required.

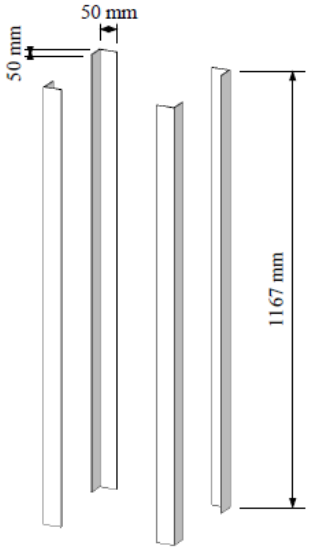

Figure 6.7: The design of the legs, which will be used for the combustion fluidised bed with dimensions

The bottom plate section of the combustion fluidised bed is shown in Figure 6.8. This part includes two outlet valves, which are used to remove solids from the bed. The valves will be fitted to the two pipes shown at the bottom of Figure 6.8. These two pipes are connected to the bottom plate of the combustion fluidised bed by means of rectangular steel boxes, which are angled at 45° to allow the unaided flow of solids to the valves. Two outlet pipes are used to provide space at the centre of the bottom plate through which the air and LPG inlet part can fit. The pipes are positioned at opposite ends of the bottom plate to allow working space at the bottom of the bed.

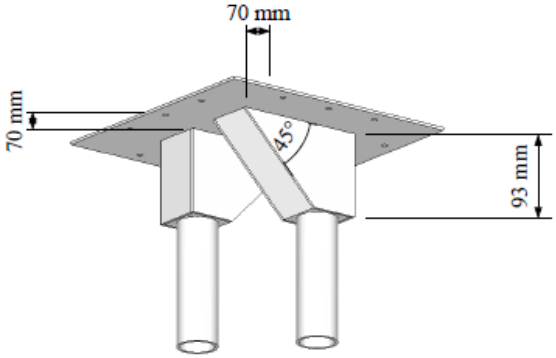

Figure 6.8: Sand outlet part on the combustion fluidised bed, which includes two outlet valves

The air and LPG distributor for the combustion fluidised bed are shown in Figure 6.9. The larger diameter pipe, which enters from the right in Figure 6.9, is the air inlet, while the smaller pipe at the bottom of the figure is the LPG inlet. The LPG inlet pipe fits through the corner of the air pipe so that it is positioned at the centre of the air pipe. The concentric pipes both end at the distributor section at the top of Figure 6.9. This is done to ensure that the LPG and air only mix as they enter the combustion fluidised bed. The air and LPG enter the bed through eight 5 mm diameter nozzles which were sized in order to ensure that the exit velocity of the gas from the distributor is above 50 m/s. This is required in order to prevent the flow of the solids from the bed into the distributor. The vertical 85 mm section of the distributor fits through the centre of the bottom plate of the combustion fluidised bed, which is shown in Figure 6.8. The length of this vertical section was designed so that the distributor section at the top of the part is positioned slightly above the screw-conveyor outlet to the combustion fluidised bed. This was done to prevent the distributor from blowing solids against the end of the screw-conveyor, which would result in excessive abrasion.

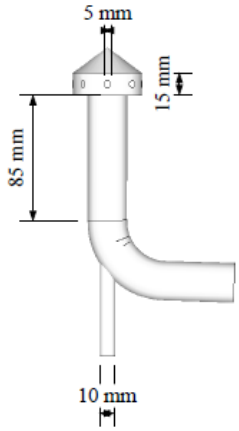

Figure 6.9: Air and LPG inlet and distributor for the combustion fluidised bed

6.2.3 Refractory

The complete design of the bottom refractory in the combustion fluidised bed is shown in Figure 6.10. To simplify the construction of the bottom refractory, several flat refractory parts were cast and were then glued together to form the complete design. The thicker refractory section on the left of Figure 6.10 includes the overflow standpipe. The other sides of the bottom refractory are each 25 mm thick and fit together to form a 200 × 200 mm square opening for the bed. The refractory is separated from the walls of the bottom mild steel shell by 25 mm which is filled with insulation wool. This is done to insulate the combustion fluidised bed further. However, a small piece of refractory, which fits against the mild steel shell, protrudes at the bottom of the bed. This piece is required for the flow of solids to and from the pyrolysis fluidised bed by means of the overflow standpipe and the screw-conveyor respectively. The top of the overflow standpipe refractory is slanted downwards to prevent solids from collecting on top of the refractory.

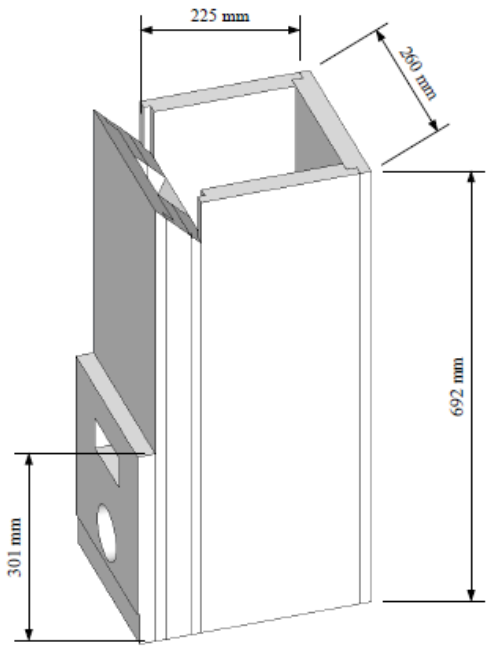

Figure 6.10: The assembled refractory for the bottom section of the combustion bed, which includes the overflow standpipe

The detailed design of the bottom piece of refractory that fits against the mild steel shell of the combustion bed is shown in Figure 6.11. The top rectangular hole in the refractory is the outlet of the overflow standpipe and the bottom round hole is for the outlet of the screw-conveyor. Although the rectangular hole is shown as horizontal in Figure 6.11, it is angled downwards to allow solids to fall through. The 3 mm notch in the bottom of the refractory is required so that it can fit tightly against the shell which includes 3 mm angle iron at the bottom to support the refractory.

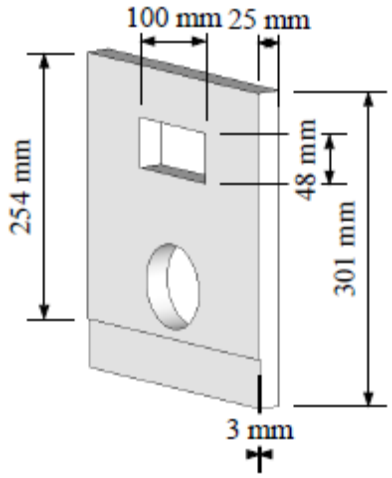

Figure 6.11: The outer combustion fluidised bed refractory piece

The design of the refractory piece that includes the overflow standpipe is shown in Figure 6.12. To simplify the construction of the standpipe, the refractory was cast with a rectangular slot which forms the vertical section of the standpipe. The open end of the standpipe is then closed with another flat piece of refractory with a slot angled in the direction of the standpipe to allow solids to spill over into the standpipe. The round hole at the bottom of the piece of refractory in Figure 6.12 is required for the screw-conveyor.

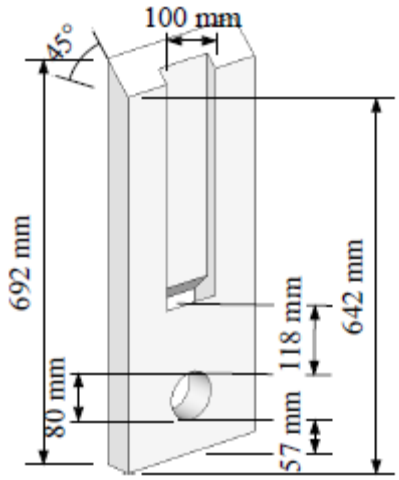

Figure 6.12: The overflow standpipe refractory piece

The assembled refractory section used for the freeboard of the combustion fluidised bed is shown in Figure 6.13. The freeboard refractory is formed from four flat pieces of refractory which slot into one another. The total height of these pieces is 1.3 m which is required for the disengagement of most of the solids in the gas before it is fed to the combustion cyclone. As with the bottom refractory, the top refractory is also separated from the mild steel shell by 25 mm which is filled with insulating wool. Unlike the bottom refractory, however, which has an internal area of 200 × 200 mm for the bed, the top refractory has an internal area of 200 × 242 mm. As a result, the flow rate of the gas in the combustion fluidised bed will decrease when it reaches the freeboard section, which will assist the disengagement of particles from the gas.

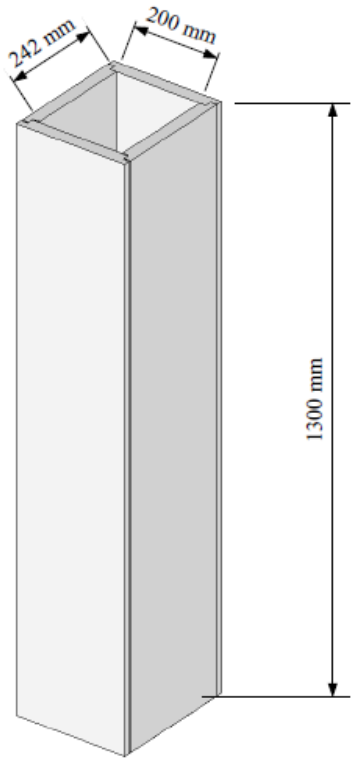

Figure 6.13: The assembled refractory section for the freeboard section of the combustion fluidised bed

6.2.4 Pyrolysis Fluidised Bed

The complete design of the pyrolysis fluidised bed is shown in Figure 6.14. The bed is composed of three main sections, namely the mild steel shell, the connection plate to the combustion fluidised bed and the screw-conveyor casing. The shell is close to 2 m in height with an internal area of 100 × 100 mm. The connection plate is used to bolt the pyrolysis fluidised bed to the combustion fluidised bed. This part is welded to the pyrolysis fluidised bed near the bottom of the bed. The screw-conveyor casing is welded to the bottom of the pyrolysis fluidised bed to allow solids to fall into the screw-conveyor. Additional solids can be added to the system through the lid of the pyrolysis fluidised bed, which can be unbolted from the bed.

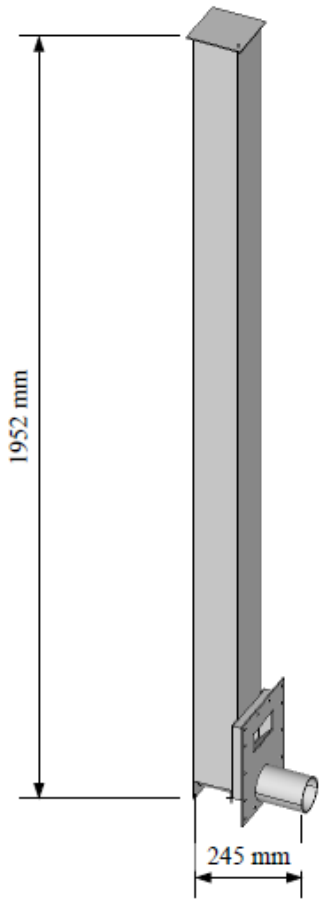

Figure 6.14: The assembled pyrolysis fluidised bed design

The mild steel section of the pyrolysis fluidised bed is shown in Figure 6.15. The connection plate used to bolt the pyrolysis fluidised bed to the combustion fluidised bed is welded to the 185 mm face of the pyrolysis bed. The large square hole in this face is the outlet of the overflow standpipe to the pyrolysis fluidised bed. To allow the pyrolysis fluidised bed to stand upright when it is unbolted from the combustion fluidised bed, an additional 47 mm of mild steel is added to the back of the bed. When the connection plate is welded to the front of the pyrolysis fluidised bed, the bottom of this piece of steel will be in line with the bottom of the connection plate, which provides a base for the bed.

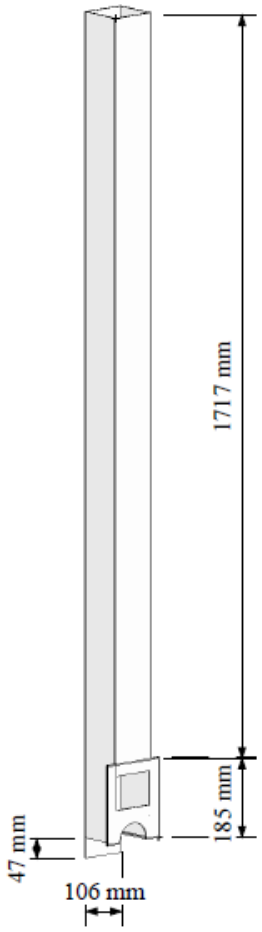

Figure 6.15: The mild steel shell design for the pyrolysis fluidised bed

The design of the connection plate section of the pyrolysis fluidised bed is shown in Figure 6.16. The back plate is where the pyrolysis bed will be bolted to the combustion bed, while the front plate is where the connection plate section will be welded to the pyrolysis bed shell. The space between the front and back of this section is required to allow space to reach the bolts connecting the pyrolysis bed to the combustion bed.

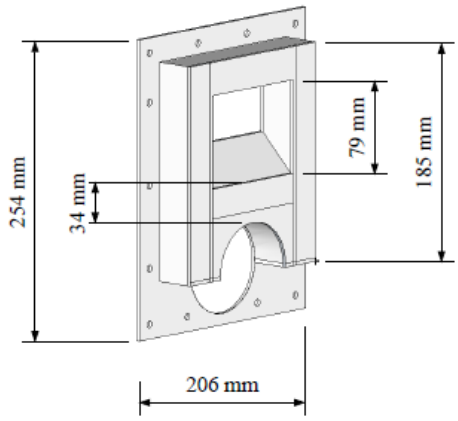

Figure 6.16: Mild steel piece, which will be used to connect the pyrolysis bed to the combustion bed

The casing for the screw-conveyor in the pyrolysis fluidised bed is shown in Figure 6.17. It has an inner diameter of 75 mm for the screw-conveyor and a length of 245 mm, which ends in the bottom refractory of the combustion fluidised bed. The opening in the casing fits below the pyrolysis fluidised bed and allows solids to fall into the screw-conveyor.

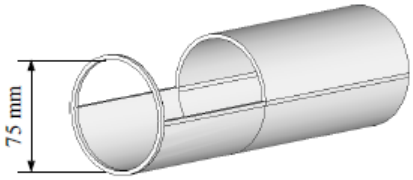

Figure 6.17: Screw-conveyor outer casing

6.3 Quencher Section

6.3.1 Overview

The complete design of the quencher section of the system is shown in Figure 6.18. This section has three parts, namely a quencher, a liquid cyclone and a demister. All three parts are made from glass pipelines so that the flow of gas and liquid in each part can be observed. The pyrolysis gases will enter the top of the quencher part, which is shown on the left of Figure 6.18. Cold bio-oil will also be fed to the quencher part for the purpose of rapidly condensing the condensable gases present in the pyrolysis gases. The pipe on the side pyrolysis gas inlet shown in Figure 6.18 is the inlet for the bio-oil. The liquid and gas mixture passes through the glass pipeline into the liquid cyclone. The cyclone drives the liquid and gas mixture to the side of a cylinder where the centrifugal force exerted on the mixture separates most of the liquid from the gases. The liquid bio-oil then travels downwards to the bio-oil outlet, while the incondensable pyrolysis gases, which contain small droplets of bio-oil, move upwards to the demister. The demister glass pipeline is packed with a dense bed of stainless steel wire, which creates a surface on which the small bio-oil droplets will collect. As the bio-oil droplets collect, the weight of the drops increases until they become heavy enough to drop down to the bio-oil outlet. The pyrolysis gases exit the demister at the pyrolysis gas outlet shown in Figure 6.18, with only a fine mist of bio-oil. This mist will be removed by using an electrostatic demister before the pyrolysis gases are recycled back to the pyrolysis fluidised bed. The pipelines are supported between the steel pieces by means of long threaded rods, as shown in the figure. These rods are tightened until the pipelines are secured in place. Enough space is left between each rod so that the glass pipelines can fit through the spacing. Therefore the rods do not have to be completely loosened in order to remove the glass pipelines.

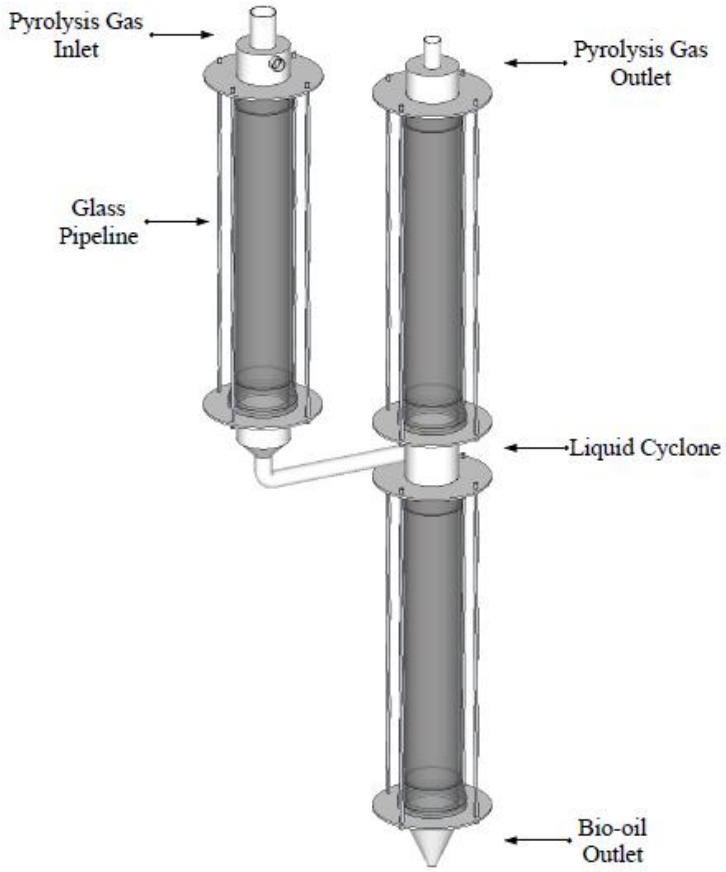

Figure 6.18: Assembled design of the quencher system, which includes the quencher, liquid cyclone and demister sections

6.3.2 Glass Pipeline

The design of the glass pipelines used for the quencher, liquid cyclone and demister is shown in Figure 6.19. The same design was used for all three sections to simplify construction and to make it easier to replace a section if damaged. A standard diameter of 75 mm was selected for the glass pipelines. To ensure that all of the condensable gases in the pyrolysis gas would be condensed before being separated from the cold bio-oil in the liquid cyclone, a length of 500 mm was selected for the glass pipelines. The ends of the pipelines are flanged for extra strength and to create a sufficiently large flat surface at each end where they can be supported on the steel parts so that the pipelines will not shift during operation.

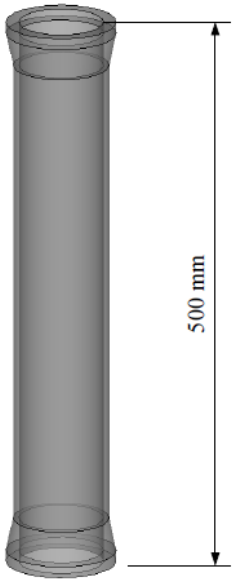

Figure 6.19: The design of the glass pipelines used in the quencher system

6.3.3 Pyrolysis Gas Inlet

The design of the steel parts used for the pyrolysis gas and cold bio-oil inlets to the quencher section is shown in Figure 6.20 and Figure 6.21. Both parts are made from stainless steel to protect them from the corrosive chemicals present in the bio-oil. The pyrolysis gas inlet shown in Figure 6.20 is made from a 3 inch threaded pipe into which the threaded unit shown in Figure 6.21 is screwed. The pipe for the pyrolysis gas inlet extends close to the bottom of the unit, as shown in Figure 6.20. As the threaded unit shown in Figure 6.21 is screwed into the pyrolysis gas inlet part, it narrows the gap at the sides of the pipe through which the bio-oil is fed. Therefore the degree to which the bio-oil is sprayed into the quencher section can be controlled by changing the vertical position of the threaded unit. The bio-oil is fed to the quencher section through the 18 mm pipe at the side of the steel part shown in Figure 6.20.

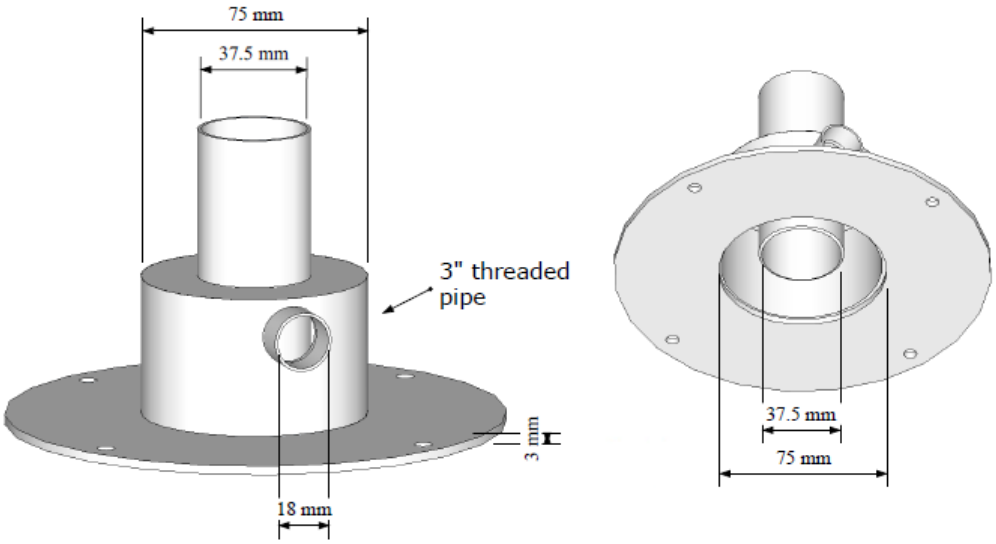

Figure 6.20: The design of the inlet section for pyrolysis gas and liquid bio-oil to the quencher system

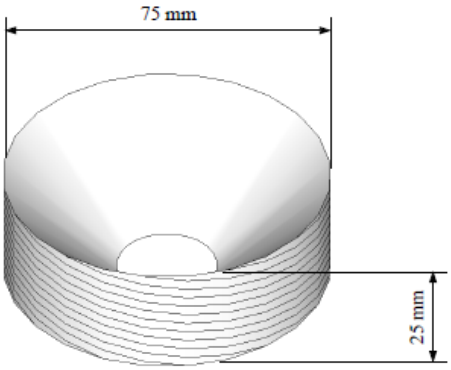

Figure 6.21: The design of the threaded unit which fits into the inlet unit for pyrolysis gas and liquid bio-oil

6.3.4 Liquid Cyclone

The design of the liquid cyclone steel part is shown in Figure 6.22. The liquid and gas mixture enters the liquid cyclone through the opening shown on the left of Figure 6.22. To improve the performance of the cyclone, the flow rate of the mixture is increased by reducing the diameter of the pipe from 75 mm to 22 mm. The mixture then travels horizontally through the 22 mm pipe to the edge of another 75 mm diameter pipe. This forces the mixture to the side of the pipe and exerts a centrifugal force on it, which helps separate the liquid from the gas. The liquid, which is pulled to the side of the pipe, moves downwards, while the gas, which moves to the centre of the pipe, moves upwards to the demister section. A perforated plate is used to prevent the stainless steel wire in the demister section from falling into the liquid cyclone section. It also helps to reduce the amount of liquid entering the demister section.

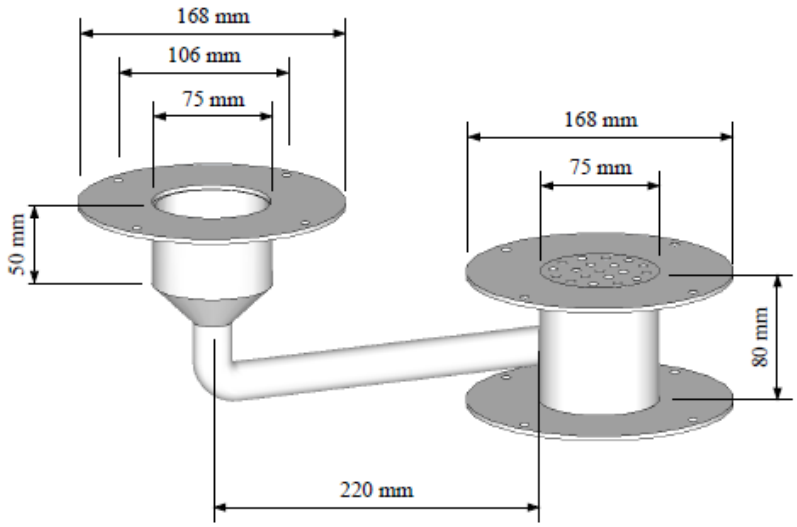

Figure 6.22: The design of the liquid cyclone section of the quencher system

6.3.5 Pyrolysis Gas Outlet

The steel unit used for the pyrolysis gas outlet is shown in Figure 6.23. This unit is positioned at the top of the demister section. It is used to hold the demister glass pipeline in place and to reduce the diameter of the pipe from 75 mm to 25 mm. A 25 mm stainless steel pipe is then used to feed the pyrolysis gases to the pyrolysis blower before they are recycled to the pyrolysis fluidised bed.

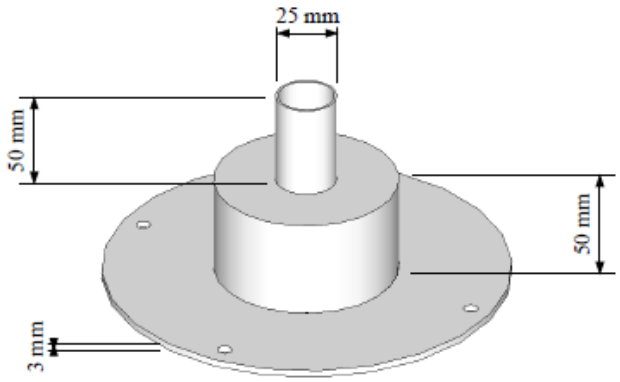

Figure 6.23: The incondensable pyrolysis gas outlet piece of the quencher system

6.3.6 Bio-oil Outlet

The steel outlet for the bio-oil from the liquid cyclone section is shown in Figure 6.24. To ensure that the bio-oil drains easily to the 12 mm diameter outlet at the bottom of the unit, the unit was built as a cone,

which is angled downwards by 60°. The bio-oil is then fed to the bio-oil pump where part of it is pumped to the heat exchanger before it is fed back to the quencher section, and part of it is pumped to an off-take valve where it is collected as a product. To ensure that bio-oil is always available to be recycled to the quencher, it is allowed to collect in the liquid cyclone. Bio-oil is therefore only taken out of the system by means of the off-take valve when the level in the liquid cyclone is too high.

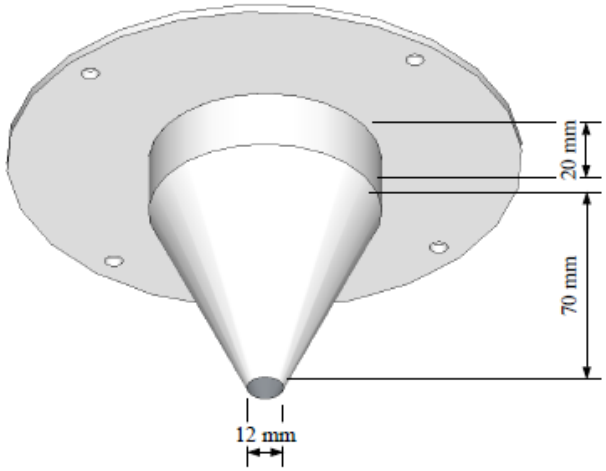

Figure 6.24: The liquid bio-oil outlet piece of the quencher system

6.4 Hopper

6.4.1 Overview

The complete design of the hopper that is used to feed the sawdust to the system is shown in Figure 6.25. The hopper is capable of storing approximately 160 kg of sawdust, which allows 8 hours of operation at a processing rate of 20 kg of biomass per hour. Sawdust can be added to the hopper by means of a small inlet on top of its lid. A screw-conveyor positioned at the bottom of the hopper is used to feed the sawdust to the pneumatic conveyor. To ensure that the flow rate of the sawdust from the hopper is correct, the hopper is suspended from the roof by means of three load cells, which are used to measure its weight. Therefore the rate at which the weight of the hopper decreases is equal to the flow rate of the sawdust to the pyrolysis fluidised bed. This parameter is used to control the variable speed motor that drives the screw-conveyor. To prevent clumping of the sawdust in the hopper, the sawdust is continuously agitated by means of a large screw positioned inside the hopper. The screw is driven by a chain attached to a motor, which is positioned near the top of the hopper on the opposite side to the screw-conveyor motor in order to balance the hopper. It was decided to use this design, rather than having the screw driven directly by the motor, to reduce the height required at the top of the hopper and to make it easier to take off the lid of the hopper for maintenance purposes.

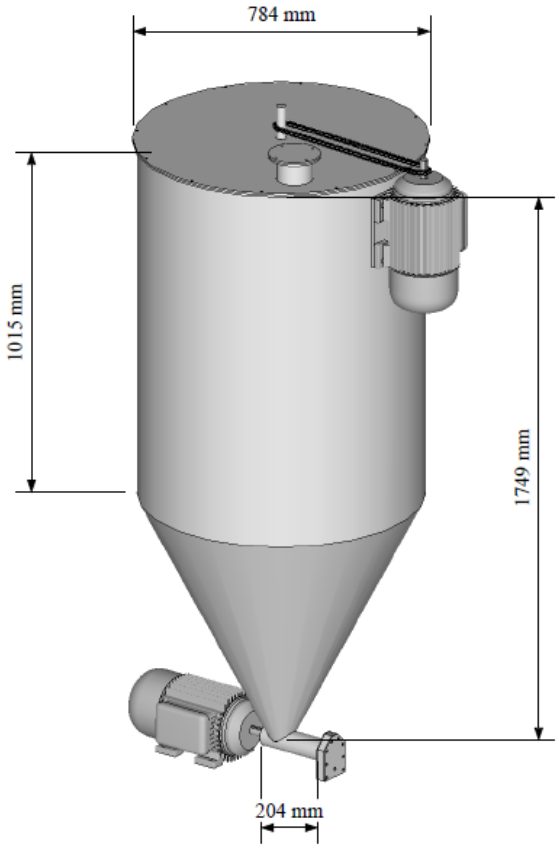

Figure 6.25: The overall design of the hopper, which includes a screw conveyor and pneumatic injector

6.4.2 Agitator

The design of the large screw used to agitate the sawdust in the hopper is shown in Figure 6.26. It was decided to use a corkscrew design to reduce the load on the motor used to agitate the sawdust. The corkscrew is attached at several points to a 610 mm steel rod, which is attached to the chain driven by the agitator motor. The total height of the screw is 1256 mm, which means that the screw ends in the cone section of the hopper. To ensure that the clumping of biomass towards the exit of the hopper is prevented, a steel corkscrew with a smaller diameter is situated in the centre of the agitator shown in Figure 6.26. This smaller corkscrew, which is not shown in Figure 6.26, extends the agitator by a further 450 mm into the cone of the hopper, which is close to the hopper exit.

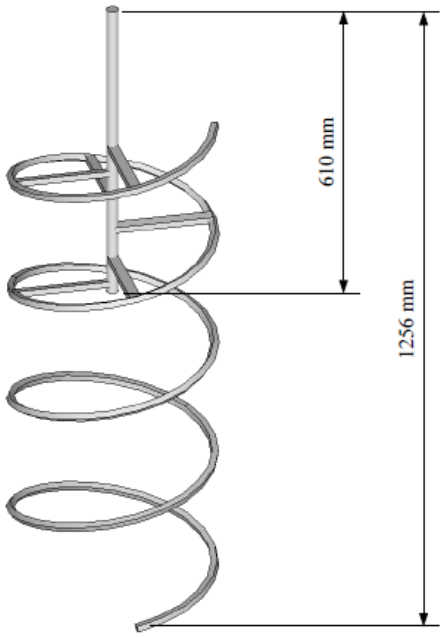

Figure 6.26: The agitator, which will be used to mix the biomass in the hopper in order to prevent clumping of the biomass in the hopper

6.4.3 Pneumatic Injector

The design of the pneumatic injector section of the sawdust hopper is shown in Figure 6.27. This section is made up of three parts. The first part, which is shown on the left of Figure 6.27, is made from mild steel and is welded to the end of the sawdust screw-conveyor. Therefore the 55 mm diameter hole in this part is the same diameter as the screw-conveyor. As the sawdust passes through this first part, it enters the second part of the pneumatic injector section, which is shown in the middle of Figure 6.27. This part is also made from mild steel and is bolted to the first part. A 10 mm diameter hole is drilled through the top of the second part. This is the hole through which the pyrolysis gases enter the pneumatic injector section. These gases force the sawdust down into two separate outlets, which are connected to 6 mm diameter

pipes. These pipes are used to feed the mixture of sawdust and pyrolysis gas to the pyrolysis fluidised bed. The final part of the pneumatic injector section is used to cover the second part and prevent any leakages from the section. To ensure that the pneumatic injector works properly during operation, a 10 mm transparent Perspex plate was used for this part. As a result, the flow of sawdust into the pneumatic injector can be observed.

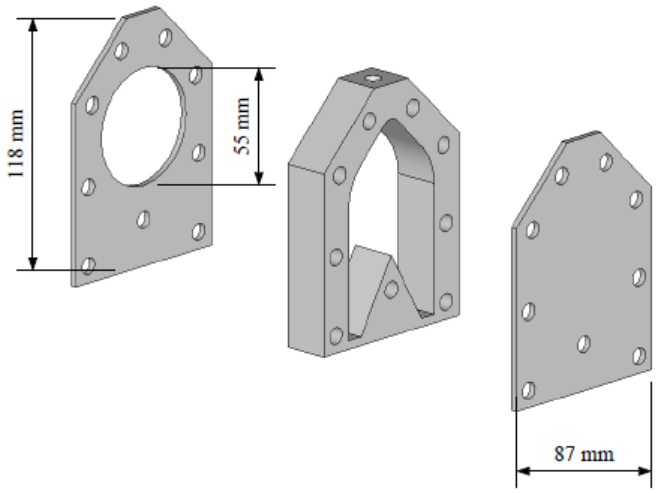

Figure 6.27: An exploded view of the three parts of the pneumatic injector

6.5 Extraction Box

The design of the extraction box is shown in Figure 6.28. The inlet to the extraction box is the hole on the side of the box shown in the figure. To decrease the temperature of the flue gas from the combustion fluidised bed before it is sent to atmosphere, it is first diluted with the air present in the extraction box – hence the large size of the extraction box. A fan positioned at the end of the extraction box is used to feed the combustion gases to atmosphere and to pull a slight vacuum in the dual fluidised bed system to reduce any gas leakages from the system.

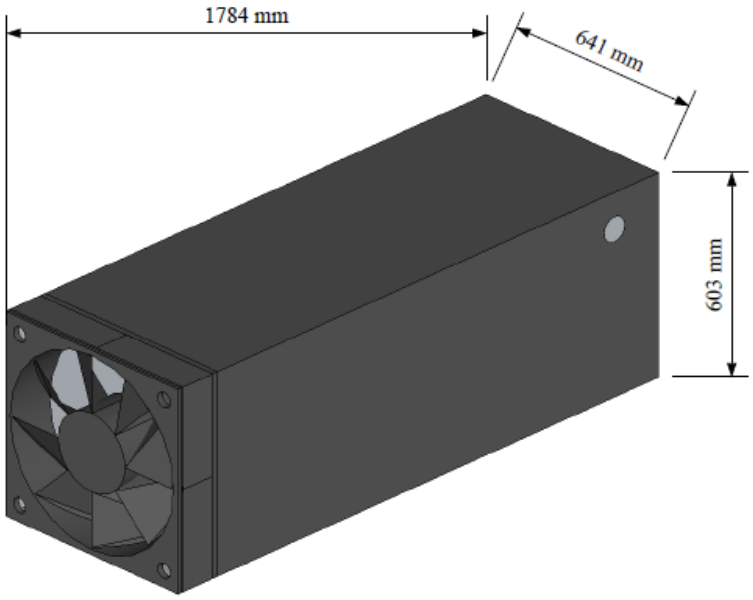

Figure 6.28: The design of the extraction box, which will be used to remove potentially dangerous gases from the pilot scale system

6.6 Electrostatic Precipitator

The design of the electrostatic precipitator (ESP), which is used to remove small bio-oil droplets from the incondensable gases produced in the pyrolysis fluidised bed, is shown in Figure 6.29. ESPs are capable of easily removing fine mists from gases without greatly impeding the flow of gas. This is done with the use of a high voltage which is usually applied over large flat plates. As the gas moves between the plates, the electrons moving from the negative plate to the grounded plate create a charge on the particles in the gas. The charged particles are attracted out of the gas to the grounded plate where they collect and fall downwards.

The pipe shown on the left of Figure 6.29 is the inlet for the incondensable gases and the pipe at the bottom of the ESP is the outlet for the bio-oil. The outlet pipe for the incondensable gases is on the right side of the ESP shown in the figure. In order to observe the operation of the ESP, its sides are made from transparent Perspex blocks held in place by stainless steel plates which are tightened together by means of threaded rods. The design uses two grounded plates and one negative plate. The grounded plates are positioned near the sides of the ESP, while the negative plate is secured in the centre of the ESP. The wiring for these plates is taken through holes in the top of the ESP which are blocked afterwards to prevent any gas leakages from the ESP.

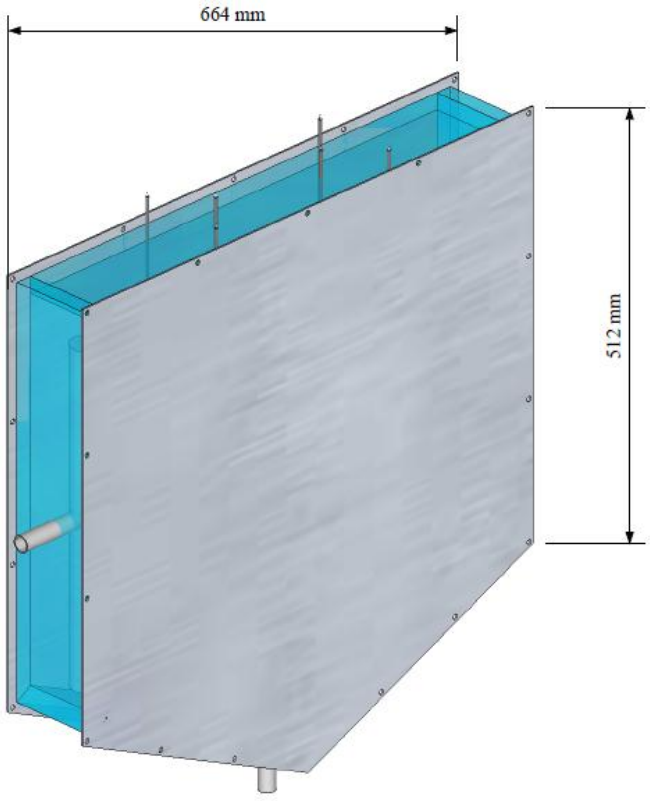

Figure 6.29: The assembled design of the electrostatic precipitator

An exploded view of the different parts used in the ESP is shown in Figure 6.30. Long vertical pipes are used both to distribute the gas evenly into the ESP and for the outlet of the incondensable gases. Several holes are drilled into both of these pipes at equal lengths from one another to ensure that the flow of gas to and from these pipes is approximately even. Both of the grounded or positive plates are made from stainless steel. Two positive plates are used in order to improve the performance of the ESP and to reduce the size of the ESP required. The negative plate in the centre of the ESP is made from a roughened stainless steel mesh. This is required to create sharp points on the negative plate where electrons can accumulate and discharge to the grounded plates, charging the particles in the gas in the process. As the bio-oil droplets collect on the positive plates, they will begin to fall down into the bottom of the ESP, which is angled downwards to allow the bio-oil to flow into the outlet pipe.

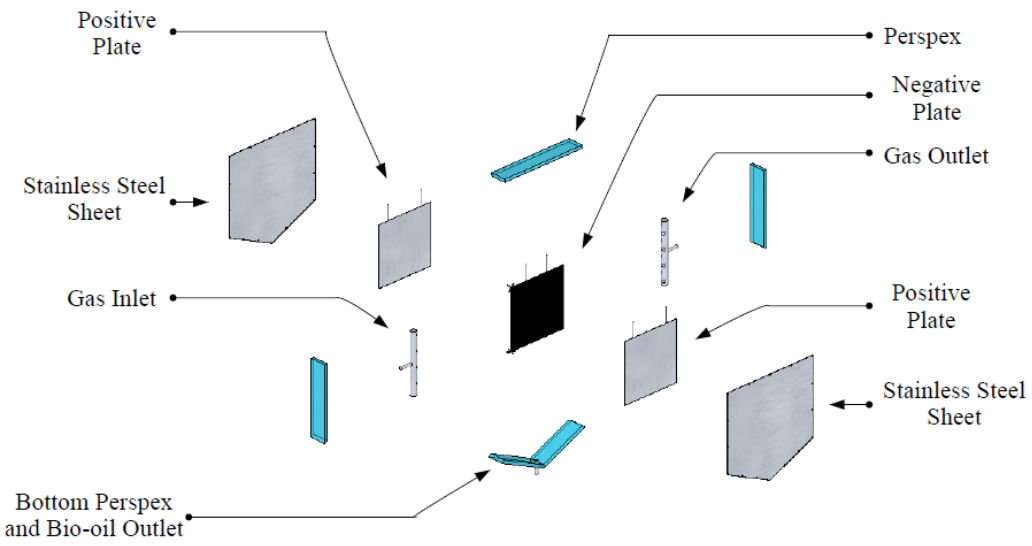

Figure 6.30: An exploded view of the electrostatic precipitator

6.7 Overall Design

6.7.1 Piping

The design of the piping used for the air flow to the combustion bed and the pyrolysis gas flow to the pyrolysis fluidised bed and pneumatic injector is shown in Figure 6.31. The blower shown at the bottom left corner of the figure is used for the air flow to the combustion fluidised bed, while the blower to the right of it is used for the pyrolysis gas flow. The pipes from both of these blowers are flanged close to the blowers. This is required for the orifice plates that are used to determine the flow rate of the gas in both of the pipes. The air from the first blower is fed directly to the combustion fluidised bed.

After the orifice plate, the pyrolysis gas stream is split into two 10 mm pipes. The first 10 mm pipe is split again into two 10 mm diameter pipes, which are used to feed the pyrolysis gas to the pyrolysis fluidised bed at opposite ends of the bed at the same vertical position. The second 10 mm diameter pipe is also split into two 10 mm diameter pipes. One of these pipes is used to purge some of the pyrolysis gases to the freeboard section of the combustion fluidised bed, where the gases are first combusted before being sent to atmosphere. The other pipe is used to feed a portion of the pyrolysis gases to the pneumatic injector for the sawdust. The sawdust pyrolysis gas mixture exits the pneumatic injector section in two 6 mm pipes. These two pipes are used to feed the sawdust pyrolysis gas mixture to the same two points used for the 10 mm pipe inlets to the pyrolysis fluidised bed.

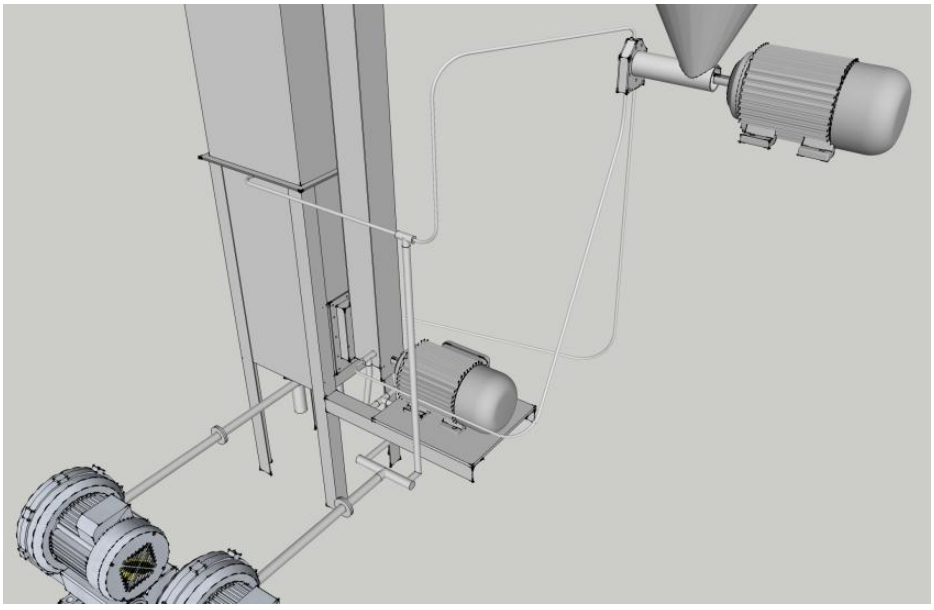

Figure 6.31: The design of the pipelines, which will be used for the fluidization gas feed to combustion and pyrolysis bed and for the pneumatic injector

6.7.2 Complete Quencher Design

The complete design of the quencher section, including piping, the bio-oil pump, the heat exchanger and the electrostatic precipitator, is shown in Figure 6.32. The wire grid shown in the figure is used as a support for these items and for the instrumentation in the system, such as the pressure sensors. After the pyrolysis gases exit the pyrolysis cyclone, they are fed to the top of the quencher section. The bio-oil that is obtained from this section is fed downwards into the bio-oil pump, which pumps the bio-oil through a brazed plate heat exchanger before it is fed back to the quencher section. Not shown in the figure is an off-take valve for the bio-oil product which is positioned after the bio-oil pump. The mixture of incondensable gas and bio-oil that is obtained from the quencher section is fed to the side of the ESP. The bio-oil that is fed to the ESP is collected at the bottom, while the incondensable gases exit on the right-hand side of the ESP, as shown in Figure 6.32. From the ESP, the incondensable gases are fed downwards to the pyrolysis blower where they are recycled to the dual fluidised bed system.

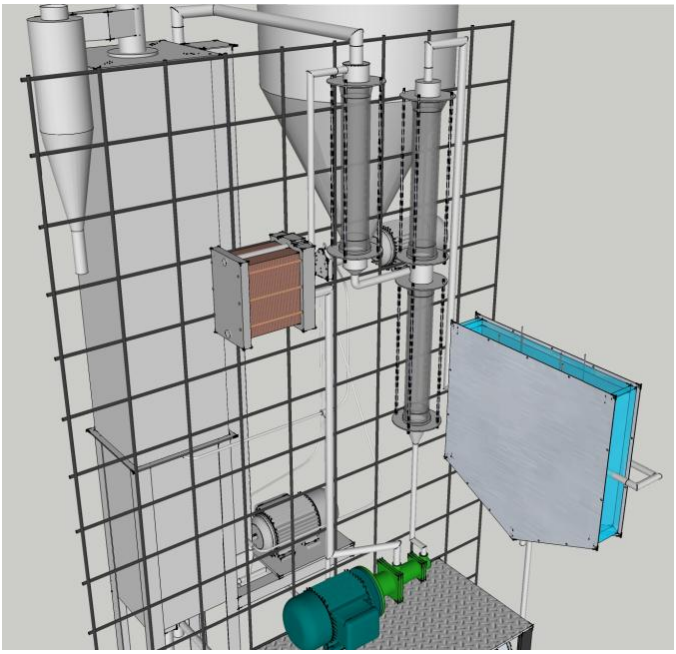

Figure 6.32: Complete design of quencher system, including the bio-oil pump, heat exchanger and electrostatic precipitator

6.7.3 Complete Pilot-Scale Design

The front view of the complete design for the pilot-scale system, including the environment in which it will be installed, is shown in Figure 6.33. The orange box shown on the left of the figure is the electrical cabinet for the system. The back view of the complete design of the pilot-scale system is shown in Figure 6.34.

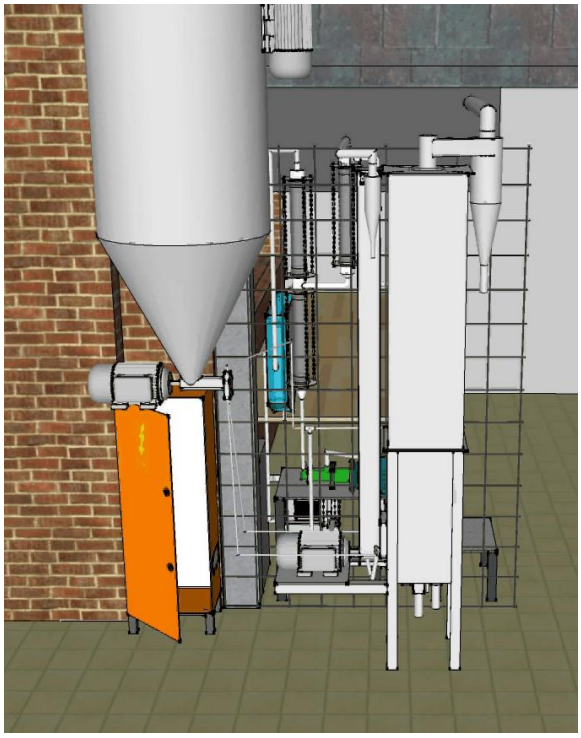

Figure 6.33: Front view of complete pilot scale system design

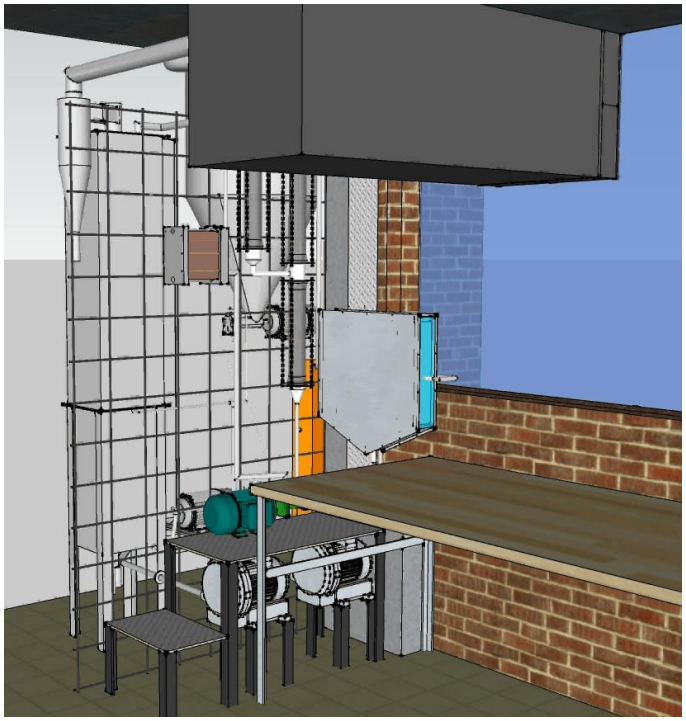

Figure 6.34: Back view of complete pilot scale system design

6.8 Conclusions

An overview of the design of the pilot-scale system that was built during the current project is provided in this chapter. The dual fluidised bed section of the system has a total height of 2.5 m and is composed of two rectangular fluidised bed reactors, namely the combustion and pyrolysis fluidised beds. Both beds are composed of several parts, which were designed to be easy to construct and assemble. The larger combustion fluidised bed is insulated with 25 mm of refractory and 25 mm of insulation wool on the inside of the mild steel shell of the bed and a further 25 mm of insulation wool on the outside of the shell. Due to the lower operating temperature of the smaller pyrolysis fluidised bed, the bed is insulated only with 25 mm of insulation wool on the outside of the mild steel shell of the bed. The shell of the combustion fluidised bed is divided into two sections, namely the bottom section and the freeboard section. These two sections can be separated to access the bed for maintenance purposes.

The quencher section of the pilot-scale system is composed of three parts, namely a quencher, a liquid cyclone and a demister part. All three parts are made from 500 mm long flanged glass pipelines, which are held in place by means of several stainless steel parts. These parts are held together with threaded rods. Cold bio-oil is sprayed into the quencher part by passing it through a small round opening in the stainless steel part above the quencher part. This opening can be reduced by changing the position of another threaded stainless steel part which fits into it. As a result, the degree to which bio-oil is sprayed into the quencher can be controlled. Most of the bio-oil condensed in the quencher is separated from the pyrolysis gases by forcing the mixture to the side of the liquid cyclone glass pipeline. This exerts a centrifugal force on the mixture which separates the bio-oil from the pyrolysis gases. The demister glass pipeline is densely packed with stainless steel wire which creates a surface on which the small bio-oil droplets left in the pyrolysis gas collect. The larger bio-oil droplets in the demister then drop down and are collected in the liquid cyclone part.

After the quencher section in the pilot-scale system, the pyrolysis gas still contains a fine mist of bio-oil, which is removed with the use of an electrostatic precipitator (ESP). The small biomass droplets in the gas are charged by means of a negative plate positioned in the centre of the ESP. The charged droplets are then attracted to two grounded plates positioned on the sides of the ESP, where they collect and fall downwards.

The hopper was designed to store approximately 160 kg of biomass, which allows 8 hours of operation at a processing rate of 20 kg of biomass per hour. A corkscrew-shaped agitator is positioned inside the hopper and is used to break up any clumps of biomass that may form. The biomass falls into a screw-conveyor positioned below the hopper, which is used to transport the biomass to the pneumatic conveyor part. Pyrolysis gas enters the pneumatic conveyor at the top of the part and forces the biomass into two small pipelines to the pyrolysis fluidised bed.

The flue gas from the combustion fluidised bed is fed to a large extraction box where the gas is mixed with a large volume of air in order to reduce the temperature of the gas before it is sent to atmosphere. An extraction fan is positioned at the end of the extraction box and is used to pull a slight vacuum in the box. Several pipelines from the extraction box are also positioned at different locations around the pilot-scale system; these are used to remove gas safely from the system in case of leakages.

CHAPTER 7: CONSTRUCTION

7.1 Introduction

The objective of the current project was to design a scalable dual fluidised bed system for the pyrolysis of biomass. A pilot-scale system of the suggested dual fluidised bed design was built at the University of Pretoria in South Africa. This was done to determine all of the design and construction considerations required for the system and to finalise the design of the system. In addition, several cold run experiments were also performed on the pilot-scale system to ensure that it would perform as expected and to identify any problematic areas in the dual fluidised bed design.

The purpose of this chapter is to provide an overview of the construction of the pilot-scale system. The observations made during the cold run experiments on the pilot-scale system are also discussed. Hot run experiments will be performed after the commissioning of the pilot-scale system, which does not form part of the current project.

7.2 Dual Fluidised Bed Section

The physical construction of the pilot-scale system is shown in Figure 7.1. The dual fluidised bed system is towards the front, the hopper at the top left-hand corner, the quencher section at the top centre, and the extraction box at the top left-hand corner of the figure. The freeboard section of the combustion fluidised bed can be taken off and has been placed next to the combustion fluidised bed. This allows access to the centre of the combustion fluidised bed for maintenance purposes. The combustion fluidised bed has been covered with polished mild steel which is used to hold the insulating wool on the outside of the combustion mild steel shell in place.

Figure 7.1: Physical construction of the pilot-scale system

The construction of the solids transfer mechanism used in the dual fluidised bed system is shown in Figure 7.2. The outlet from the overflow standpipe to the pyrolysis fluidised bed can be seen between the combustion fluidised bed and the pyrolysis fluidised bed. A three-phase motor is used to drive the screw-conveyor that is used to transport cold solids and bio-char back to the combustion fluidised bed.

Figure 7.2: Close-up of solids circulation system

The bottom plate and the outlet pipes used to remove solids from the combustion fluidised bed are shown in Figure 7.3. The bottom plate is bolted to the bottom mild steel shell of the combustion fluidised bed. Two gate valves are used to control the outlet of solids from the combustion fluidised bed due to their applicability in high-temperature applications. The inlet pipe for the LPG and air to the combustion fluidised bed is fed through the space between the outlet pipes. The thermocouples shown in Figure 7.3 are used to measure the temperature of the combustion fluidised bed at different positions in the bed.

Figure 7.3: Bottom plate and solids outlet on the combustion fluidised bed

The different layers used for the insulation and support of the combustion fluidised bed are shown in Figure 7.4. The inside of the combustion fluidised bed is surrounded by 25 mm of refractory, which is separated from the mild steel shell by 25 mm of insulation wool. The shell is 5 mm thick and is surrounded by another 25 mm of insulation wool, which is not shown in the figure. Polished mild steel is used to hold the outer layer of insulation wool in place and to improve the appearance of the system.

Figure 7.4: Refractory and insulating wool layers in the combustion fluidised bed

The inside of the combustion fluidised bed is shown in Figure 7.5. Solids continuously spill over into the entrance of the overflow standpipe which is shown on the left of the figure. A heating element is used during start-up to increase the temperature of the bed to 500°C. LPG is then combusted in the bed to achieve the operating temperature of 900°C. Three thermocouples are used to measure the temperature of the combustion fluidised bed accurately. One of these thermocouples is positioned on the heating element to ensure that it does not overheat during start-up.

Figure 7.5: Inside view of the combustion fluidised bed

The blowers used for the air flow to the combustion fluidised bed and the pyrolysis gas flow to the pyrolysis fluidised bed are shown in Figure 7.6. The air blower is the one towards the front of the picture and the pyrolysis gas blower is that towards the back.

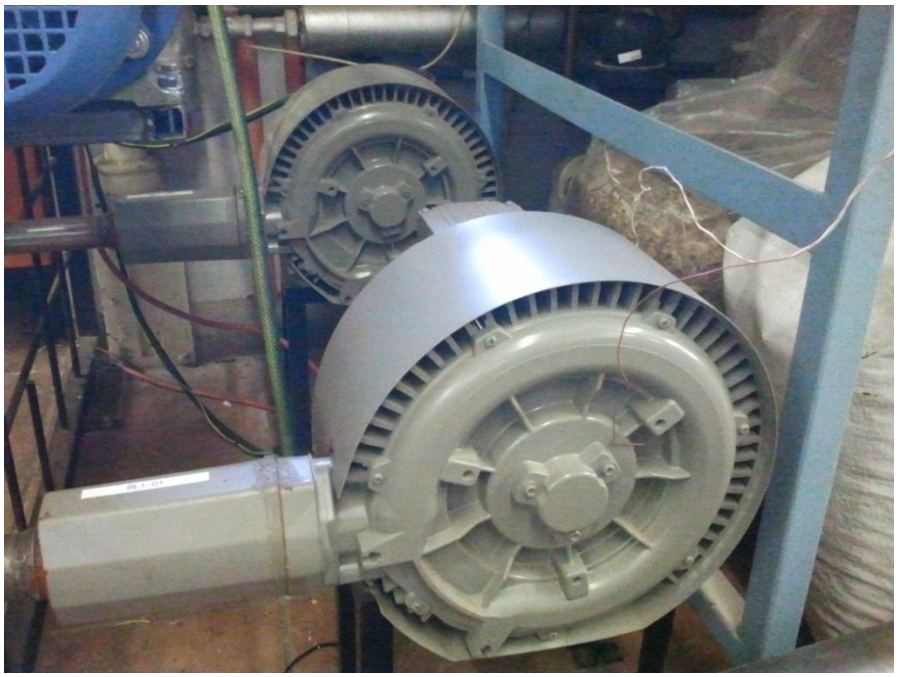

Figure 7.6: Pyrolysis gas and air blower

7.3 Hopper Section

The physical construction of the hopper used to store and feed sawdust to the dual fluidised bed system is shown in Figure 7.7. Polished mild steel was used for the construction of the hopper. The hopper is suspended from three load cells, which are used to calculate the rate at which sawdust is fed to the pyrolysis fluidised bed. The agitator inside the hopper is driven by means of a chain connected to the motor positioned at the top of the hopper shown in the figure. To balance the hopper the motor is positioned on the opposite side of the hopper to the motor that is used to drive the screw-conveyor at the bottom of the hopper.

Figure 7.7: Physical construction of hopper

The physical construction of the screw-conveyor and pneumatic injector that are used to transport sawdust to the pyrolysis fluidised bed is shown in Figure 7.8. The motor, screw-conveyor and pneumatic injector are all suspended from the hopper. A transparent Perspex plate was used for the face of the

pneumatic injector so that the flow of sawdust from the screw-conveyor into the injector could be observed.

Figure 7.8: Sawdust screw-conveyor and pneumatic injector

7.4 Quencher Section

The physical construction of the quencher section used in the pilot-scale system is shown in Figure 7.9. The steel parts of the quencher section are made from stainless steel to protect them from the high temperature and low acidity of the bio-oil formed. Standard flanged glass pipelines were used for the different parts of the quencher section. This section is supported on the steel grid shown in the figure. Not shown in the figure is the stainless steel wool that will be packed tightly into the demister part of the quencher section.

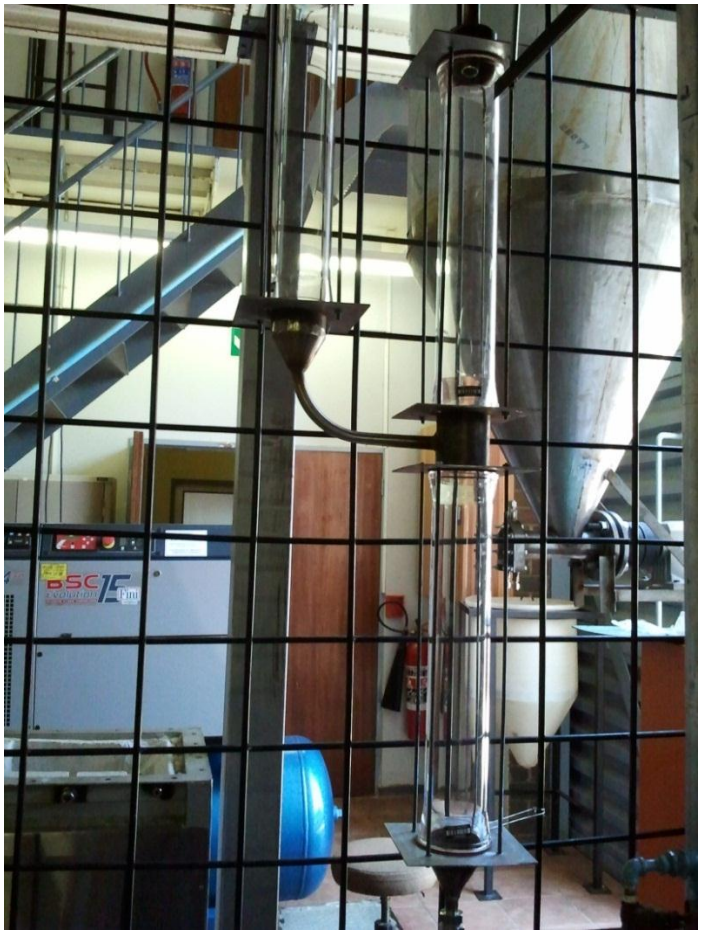

Figure 7.9: Physical construction of quencher section

7.5 Extraction Box

The physical construction of the extraction box is shown in Figure 7.10. The inlet pipe shown on the extraction box is used for the flue gas inlet. Several holes were cut into the side of the extraction box to allow air into the extraction box, which will dilute the flue gas, thus decreasing its temperature before it is sent to atmosphere. Flexible pipes were positioned in the holes to the extraction box, which were taken to several sections in the pilot-scale system. These pipelines are used to pull a vacuum around the system, which will help mitigate the effects of any gas leakages in the system.

Figure 7.10: Physical construction of extraction box

7.6 Cold Run Experiments

To ensure that the pilot-scale system would perform as required during operation, several cold run experiments were done. The response of the following three sections was observed during these experiments:

- The fluidisation of the bed of solids in the combustion fluidised bed
- The circulation of solids between the pyrolysis and combustion fluidised beds
- The flow of biomass from the hopper to the pneumatic conveyor

Complete fluidisation of the entire bed of solids in the combustion fluidised bed is necessary to prevent the formation of areas in which the solids are insufficiently mixed. These areas would create temperature spikes in the bed due to the exothermic combustion reactions taking place in the bed, which would create problems with controlling the dual fluidised bed system. In addition, it is important that the combustion fluidised bed can be operated in the bubbling fluidisation regime to ensure that the hot solids in the combustion fluidised bed will spill over into the overflow standpipe to the pyrolysis fluidised bed. Concerns about the fluidisation in the combustion fluidised bed were raised due to the shape of the bed, the design of the air distributor in the bed and the weight of the solids in the bed. For this reason an experiment was performed to evaluate the performance of the fluidisation in the combustion fluidised bed. At low flow rates of air to the combustion fluidised bed, small bubbles were observed at the centre of the bed. However, as the flow rate of air to the combustion fluidised bed increased, the entire bed of solids took on the appearance of a rapidly boiling liquid with large bubbles. The solids also spilled over easily into the overflow standpipe at these higher air flow rates. It was therefore concluded that the combustion fluidised bed could be fluidised as required during the operation of the pilot-scale system.

During the cold run experiments, it was observed that the solids that spilled over into the overflow standpipe flowed easily into the pyrolysis fluidised bed. In addition, it was also possible to transport all of the solids in the pyrolysis fluidised bed back to the combustion fluidised bed by means of the screw-conveyor positioned at the bottom of the pyrolysis fluidised bed. As the speed of the screw-conveyor was increased, the rate at which solids were transported back to the combustion fluidised bed increased, which increased the rate at which solids entered the overflow standpipe. It was therefore concluded that solids circulation between the combustion fluidised bed and the pyrolysis fluidised bed performed as required and could be easily controlled.

In order to evaluate the flow of biomass from the hopper to the pneumatic conveyor, the hopper was partially filled with sawdust. It was found that the sawdust flowed easily from the hopper to the screw-conveyor. Therefore it was concluded that the agitator effectively broke up any clumps of sawdust that formed in the hopper. The rate at which sawdust was transported to the pneumatic conveyor could easily be controlled with the screw-conveyor. The gas entering at the top of the pneumatic conveyor rapidly forced the biomass into the two pipelines to the pyrolysis fluidised bed at low gas flow rates. However, as the gas flow rate increased, the gas began to push the biomass back into the pneumatic conveyor. Therefore it is necessary to ensure that both the hopper and the screw-conveyor are air tight to prevent gas leakages and to equalise the pressure in the hopper and the pressure of the gas entering the pneumatic conveyor. This will ensure that the gas in the pneumatic conveyor flows to the pipelines to the pyrolysis fluidised bed rather than to the hopper.

7.7 Conclusions

An overview of the construction of the pilot-scale system and the observations made during the cold run experiments on the system was provided in this chapter. Both the combustion and pyrolysis fluidised beds are surrounded by a thin layer of polished mild steel, which is used to hold the insulating wool on the outside of the shells of both beds in place. A three-phase motor is used to drive the screw-conveyor at the bottom of the pyrolysis fluidised bed. Two gate valves are used at the bottom of the combustion fluidised bed to remove solids from the dual fluidised bed system. To measure the temperature in the combustion fluidised bed accurately, three thermocouples are fed into the bed through the bottom plate of the bed. One of these thermocouples is placed next to a heating element positioned inside the combustion fluidised bed and this is used to increase the temperature of the bed during start-up to 500°C before the LPG is fed to the bed.

The agitator inside the hoppers is driven by chain connected to a motor positioned on the side of the hopper. The motor is positioned on the opposite side of the hopper to the screw-conveyor motor positioned at the bottom of the hopper. This is done to balance the hopper which is suspended from three load cells. A transparent Perspex plate is used as the face of the pneumatic conveyor so that the flow of biomass into the pipelines to the pyrolysis fluidised bed can be observed.

The quencher section of the pilot-scale system is supported on a large steel grid. To prevent corrosion of the steel parts in the quencher section, these parts are made from stainless steel. A large inlet is positioned on the extraction box for the flue gas from the combustion fluidised bed. Flexible pipelines are attached to the extraction box and are used to draw a vacuum around the pilot-scale system and to allow the flow of air to the extraction box. This additional air helps dilute and cool the flue gas before it is purged to atmosphere.

Several cold run experiments were done on the pilot-scale system to ensure that it would perform as required during operation. It was observed that at sufficiently high flow rates of air to the combustion fluidised bed, the entire bed of solids was fluidised and bubbled violently. At these air flow rates, solids continuously spilled over into the overflow standpipe in the combustion fluidised bed. It was therefore concluded that the combustion fluidised bed could be fluidised as required during operation. The solids that spilled over into the overflow standpipe flowed easily into the pyrolysis fluidised bed. In addition, the solids in the pyrolysis fluidised bed could be easily transported back to the combustion fluidised bed at a controlled rate by means of the screw-conveyor at the bottom of the bed. It was therefore concluded that solids circulation between the combustion and pyrolysis fluidised beds performed as required and could be easily controlled. The agitator in the hopper effectively broke up any clumps of biomass that formed, which allowed the biomass to flow freely into the screw-conveyor below the hopper. At low flow rates of gas to the pneumatic conveyor, the gas rapidly carried the biomass at the end of the screw-conveyor into the pipelines to the pyrolysis fluidised bed. However, at high gas flow rates, a fraction of the gas flowed to the hopper, which pushed the biomass back into the screw-conveyor. It is therefore necessary to ensure that the hopper and the screw-conveyor are air tight to equalise the pressure in the hopper and the gas inlet to the pneumatic conveyor and to prevent harmful gas leakages.

CHAPTER 8: CONCLUSIONS AND IMPLICATIONS

8.1 Introduction

The objective of this project was to design, model and construct a scalable dual fluidised bed system for the pyrolysis of biomass. Included in this objective was the construction and testing of both a small cold unit and a 20 kg per hour pilot-scale unit of the dual fluidised bed design. The following tasks formed part of this project:

- A literature study on several areas of study pertaining to the current project, including biomass, pyrolysis and fluidisation.
- The design of a unique dual fluidised bed system for the pyrolysis of biomass, which included the block flow diagram, process flow diagram and process and instrumentation diagram of the system designed. The control system required for the pilot-scale unit also formed part of this task.
- The design and testing of a unique method for the circulation of solids between the pyrolysis fluidised bed and the combustion fluidised bed. This task involved the construction and experimental evaluation of a small cold unit of the proposed dual fluidised bed design.
- The detailed modelling and optimisation of the proposed dual fluidised bed design. This model included mass and energy balances, the hydrodynamics of the system and reaction kinetics.
- The design and 3D modelling of the pilot-scale dual fluidised bed system. This task involved the sizing of each part required in the pilot-scale system, as well as the design of all downstream process units from the dual fluidised bed section of the system.
- The construction and evaluation of the pilot-scale system. The objective of this task was to identify all design and construction considerations required for the system and to evaluate the unit during cold run experiments.

The objective of this chapter is to provide a summary of the important results obtained during each of the above tasks and the conclusions and recommendations obtained from these results.

8.2 Main Results and Conclusions

8.2.1 Literature Study

The pyrolysis of biomass is a relatively new area of study and involves several other branches of study, including the composition of biomass and fluidisation. During the pyrolysis of biomass, long polymers present in the biomass are split to form products of lower molecular weight. The main polymers present in wood are cellulose, hemicelluloses and lignin. Cellulose is the most abundant organic compound found in nature and makes up 40 to 50% of the organic constituents of both hardwood and softwood trees. It consists of a linear chain of glucose units linked together by β-glycosidic bonds.

There are several thermochemical processes for the conversion of biomass, namely combustion, torrefraction, pyrolysis and gasification. The combustion of biomass must take place in the presence of oxygen, while the last three processes take place in the absence of oxygen or in an oxygen-limited environment. These thermochemical conversion processes lead to the formation of four important products, namely heat in the case of combustion, and bio-char, bio-oil and syngas for the last three conversion techniques. Torrefraction, pyrolysis and gasification differ according to the temperature at which they take place and the main product formed during each process. The main product formed during torrefraction is bio-char, while the main products obtained from pyrolysis and gasification are bio-oil and syngas respectively.

The main product obtained from the pyrolysis of biomass is a liquid, transportable bio-oil. Bio-oil is a source of many high-value products and can be upgraded to form liquid bio-fuels, such as bio-diesel. The pyrolysis of biomass can be modelled with the use of a two-stage model in which the wood is first converted to bio-char, syngas and tar compounds. The tar compounds are gaseous compounds, which can be condensed to form bio-oil. These tar compounds undergo secondary conversion in the gas phase to form bio-char and syngas. Therefore it is important to condense the tar compounds rapidly to maximise the yield of bio-oil.

During the fluidisation of a bed of solids, a fluid is passed upwards through the bed, which exerts an upward drag force on the solids. When this upward drag force exceeds the gravitational force on the solids, the bed takes on properties similar to those of a fluid and is said to be fluidised. There are several fluidisation regimes, depending on the flow rate of the fluid through the bed of solids, namely fixed bed, bubbling fluidised, turbulent fluidised, fast fluidised and pneumatic conveying. In the last three regimes, solids are entrained from the bed and must therefore be replaced continuously. Bubbling fluidised beds take on the same appearance as a boiling liquid. In this regime, the fluid passes through the solids in the form of bubbles. A certain height must be provided above the bed of solids where the solids that are carried upwards with the gas can disengage from the gas and fall back down to the bed.

8.2.2 Dual Fluidised Bed Design

The reactor system chosen for the pyrolysis of biomass is a dual fluidised bed system. In this system, solids are heated by means of combustion in one fluidised bed and are then transported to a second fluidised bed where they provide the energy required for endothermic pyrolysis reactions. An overflow standpipe is used to transport the hot solids in the combustion fluidised bed to the pyrolysis fluidised bed, while a screw-conveyor, positioned at the bottom of the pyrolysis fluidised bed, is used to transport cold solids and a portion of the bio-char produced in the pyrolysis fluidised bed back to the combustion fluidised bed. The products obtained from the pyrolysis fluidised bed are pyrolysis gases and bio-char. The bio-char is separated from the pyrolysis gases, after which these gases are sent to a quencher where a portion is quenched to form bio-oil. A portion of the incondensable gases are then purged and the remaining gases are recycled to the pyrolysis fluidised bed to fluidise the bed. This is done to prevent any oxygen from entering the pyrolysis fluidised bed. Air is used both to fluidise the combustion fluidised bed and to provide the oxygen required for the combustion reactions. The fuel chosen for the combustion reactions is LPG. However, it is possible to replace the LPG with a quarter of the bio-char that is formed in the pyrolysis fluidised bed and with the purged pyrolysis gases. In this way, the system does not require additional fuel and is said to be self-sufficient. The products obtained from the combustion fluidised bed are flue gas and ash.

The biomass required for the pyrolysis reactions is stored in a hopper. A screw-conveyor positioned at the bottom of the hopper is used to control the rate at which the biomass is fed to a pneumatic conveyor, which is used to feed the biomass rapidly into the pyrolysis fluidised bed. This is done to prevent the back flow of heat from the pyrolysis fluidised bed to the hopper. The pyrolysis gas and bio-char mixture from the pyrolysis fluidised bed is fed to a cyclone which is used to separate the bio-char from the pyrolysis gases. The gases are then sprayed with cold bio-oil to condense the bio-oil oil present in the pyrolysis gases rapidly. The bio-oil is then separated from the incondensable pyrolysis gases with the use of a liquid cyclone, a demister and an electrostatic demister. Bio-oil is collected at the bottom of the liquid cyclone and the ESP. The bio-oil collected from the liquid cyclone is fed through a pump which pumps it through a heat exchanger where it is cooled before being recycled to the quencher. The ash formed in the combustion fluidised bed is separated from the flue gas by means of a cyclone. The flue gas is then fed to an extraction box where it is cooled and purged to atmosphere.

Five controllers are used to control the pilot-scale system, namely three pressure controllers and two temperature controllers. The first two pressure controllers are used to control the pressure drop over the orifice plates positioned on the air pipeline to the combustion fluidised bed and the recycled pyrolysis gas pipeline to the pyrolysis fluidised bed. The controlled variables used for these two controllers are the air blower speed and the pyrolysis gas blower speed. The third pressure controller is used to control the pressure in the freeboard of the pyrolysis fluidised bed. This is done through the control of a valve positioned on the pyrolysis gas purge line. The two temperature controllers are used to control the temperature in the combustion fluidised bed and the pyrolysis fluidised bed. The temperature in the combustion fluidised bed is controlled by adjusting the rate at which LPG is fed to the combustion fluidised bed, while the temperature in the pyrolysis fluidised bed is controlled by adjusting the rate at which the screw-conveyor positioned at the bottom of the bed feeds cold solids back to the combustion fluidised bed. This in turn will adjust the rate at which hot solids are fed to the pyrolysis fluidised bed from the combustion fluidised bed.

Mass and energy balances were also performed over the combustion and pyrolysis fluidised beds. It was found that more bio-char is produced in the pyrolysis fluidised bed than is required by the combustion reactions. All material and energy balances were found to balance and all unknown variables in the system, including the flow rate of bio-char and sand between the fluidised beds, were determined.

8.2.3 Solids Transport Mechanism

A relatively unique solids transport mechanism was chosen for the circulation of solids between the combustion and pyrolysis fluidised beds, i.e. unique when compared with most dual fluidised bed designs used for the pyrolysis of biomass. This mechanism uses an overflow standpipe for the transport of solids from the combustion fluidised bed to the pyrolysis fluidised bed, and a screw-conveyor to transport the solids back to the combustion fluidised bed from the pyrolysis fluidised bed. The entrance for the overflow standpipe is positioned at the splash zone of the combustion fluidised bed. This allows solids to spill over continuously from the combustion bed into the overflow standpipe. As additional solids are fed to the combustion fluidised bed by means of the screw-conveyor, the height of the combustion bed will increase, which in turn results in an increase in the rate at which solids spill over into the overflow standpipe. The solids transport mechanism selected therefore allows simple control of the solids circulation rate between the combustion and pyrolysis fluidised beds.

A small cold unit of the proposed dual fluidised bed design was built at the Agricultural Research Service in Wyndmoor, Pennsylvania, USA to test the performance of the solids transport mechanism. This cold unit was made from transparent Perspex so that the movements of solids in the beds could be observed. To test the performance of the system, several parameters were manipulated and the response of the system was recorded. The manipulated parameters investigated during these experiments were the speed of the screw-conveyor, the flow rate of the gas fed to the pyrolysis and combustion fluidised beds, and the amount of solids charged to the system. The following important observations and conclusions were obtained from these experiments:

- It was found that the pressure drops over the combustion and pyrolysis fluidised beds were not influenced by the speed of the screw-conveyor.
- The flow rate of gas to the pyrolysis fluidised bed had a negligible effect on the pressure drop over this bed. This is believed to be because of the gas flow through the overflow standpipe. The pressure drop over the pyrolysis bed is therefore dependent mostly on the flow of gas in the combustion fluidised bed due to its relatively higher flow rate.
- As the flow rate of gas to the combustion fluidised bed increased, the pressure drop over the combustion fluidised bed decreased and the pressure drop over the pyrolysis fluidised bed increased. This may be due to an increase in the flow rate of gas from the pyrolysis fluidised bed to the combustion fluidised bed through the standpipe.
- A change in the amount of solids charged to the system had a negligible effect on the response of the pressure drop over the combustion and pyrolysis fluidised beds, and on the height of the solids in the pyrolysis bed to changes in the combustion and pyrolysis gas flow rate and in the screw-conveyor speed.
- The height of the solids in the pyrolysis fluidised bed increased with increases in the pyrolysis and combustion gas flow rates, and decreased with increases in the screw-conveyor speed.

- An increase in the amount of solids charged to the system had a dampening effect on the rate of spills into the overflow standpipe. It also stabilised the response of the rate of spills to changes in the combustion gas flow rate.

In addition to these experiments, four requirements for the solids transport mechanism were identified, which would favour its suitability for the fast pyrolysis process. It was found that the solids transport mechanism selected during this project met all of these requirements.

8.2.4 Mathematical modelling of the pyrolysis of biomass

During the modelling phase of the project, a comprehensive model for the dual fluidised bed system was developed and optimised. This model included mass and energy balance considerations, the hydrodynamics of the system and reaction kinetics. It is planned to operate both the combustion and pyrolysis fluidised beds in the bubbling fluidised bed regime. A three-phase model was used to predict the hydrodynamics of the beds in this regime. This model makes provision for the fact that the reactions occur in the bubble, cloud and emulsion phase in the bed. Seven reactions were considered in the model for the combustion fluidised bed and the effects of particle shrinkage were also considered. The kinetics for these seven reactions was predicted with the use of the Arrhenius equation. The combustion fluidised bed was modelled in three steps, as follows:

1. Perform an energy balance over the pyrolysis fluidised bed.
2. Determine the total amount of bio-char and oxygen required in the combustion fluidised bed.
3. Determine the concentration profiles along the height of the combustion fluidised bed.

The pyrolysis fluidised bed was modelled with the use of a two-stage pyrolysis model. In this model, the wood is assumed to convert completely into three types of product, namely bio-char, syngas and gaseous tar compounds. The tar compounds then undergo a second reaction in the gas phase during which they are converted into bio-char and syngas. The kinetic parameters suggested by Chan *et al* (1985) were used for this model. The effects of heat transfer along the radius of the wood particles and the shrinking of the particles were also considered in this model.

The conclusions of other authors who had used the same concepts to model the pyrolysis of biomass were investigated. It was found that the two-stage pyrolysis model agrees well with experimental results. Hagge & Bryden (2002) reported that particle shrinkage has a significant effect on the gas product yield, the tar yield, and pyrolysis time

During the evaluation of the model developed for the dual fluidised bed system, it was found that the residence time required for the wood particles to reach complete conversion is 10 seconds. The maximum yield of bio-oil of 64% on a weight basis is obtained when the pyrolysis fluidised bed is operated at 500°C. The reduction in the amount of bio-oil obtained from the system due to the secondary conversion of the tar compounds was less severe than if the wood particles had been entrained from the bed before being fully converted. Therefore the velocity of the fluidising gas in the pyrolysis fluidised bed should be set low enough to ensure that complete conversion of the wood is obtained. For the pyrolysis fluidised bed modelled, it is suggested that this flow rate be set to approximately 0.28 m/s.

8.2.5 Physical Design of Pilot-Scale System

A complete 3D model of the pilot-scale system was developed to ensure that all design considerations were included in the design of the system and to help finalise the dual fluidised bed design. It was decided to use rectangular fluidised beds for both the combustion and pyrolysis fluidised beds to simplify both construction and the design of the solids transfer mechanism used between the beds. A total height of 2.5 m was chosen for the dual fluidised bed system due to the maximum height allowed by the environment in which the system was built and the height required above the system for maintenance. The dual fluidised bed system was broken up into several parts which were designed to be easy to construct and assemble. To reduce the temperature of the combustion fluidised bed from 900°C inside the bed to approximately 50°C on the outside of the bed, it was decided to insulate the bed with 25 mm of refractory and two 25 mm layers of insulating wool. The pyrolysis fluidised bed is insulated with only one 25 mm layer of insulating wool due to its lower temperature. The combustion fluidised bed was divided into a freeboard section and a bottom section, which can be separated from one another to gain entry into the combustion fluidised bed for maintenance purposes.

A quencher system was designed to condense and separate the bio-oil that is formed in the pyrolysis fluidised bed, which is composed of a quencher, a liquid cyclone and a demister. Flanged glass pipelines with a standard diameter of 75 mm and a length of 500 mm were selected for all three sections of the quencher system. The same glass pipeline design was used for all three sections to simplify construction and to make it easier to replace a section if it was damaged. The glass pipelines are held in place between steel parts by means of long threaded rods. An adjustable small round hole in the top steel part above the quencher section is used to spray cold bio-oil into the section with the pyrolysis gases to condense the bio-oil present in the gas. The mixture of bio-oil and gas is then fed to the side of the liquid cyclone, which separates most of the bio-oil from the gas by means of centrifugal force. Most of the smaller drops of bio-oil that are left in the gas are then separated from the gas by passing the gas through a dense bed of stainless steel wool in the demister section. The stainless steel wool provides a surface on which the bio-oil droplets can collect and drop downwards.

The small bio-oil droplets that remain in the gas from the demister section are removed from the gas by means of an electrostatic precipitator (ESP). This is done by charging the bio-oil droplets by means of a negatively charged plate in the centre of the ESP. The charged droplets are then attracted to two grounded plates positioned on the sides of the ESP, where they collect and fall downwards.

The hopper was designed to store sufficient biomass for 8 hours of operation at a processing rate of 20 kg of biomass per hour. To prevent any clumps of biomass from forming in the hopper, a corkscrew agitator is rotated continuously inside the hopper. The biomass is transported from the hopper into a screw-conveyor positioned below the hopper. The screw-conveyor is used to control the rate at which the biomass is transported to a pneumatic conveyor, which is used to inject the biomass into the pyrolysis fluidised bed.

An extraction box is used to dilute and lower the temperature of the flue gas from the combustion fluidised bed before it is purged to atmosphere. The extraction box is kept at a slight vacuum by means of an extraction fan positioned at the back of the box. Several pipelines from the extraction box are also positioned at different locations around the pilot scale-system; these are used to remove gas safely from the system in case of leakages.

8.2.6 Construction of Pilot-Scale System

The final objective of this project was to construct and test the pilot-scale system that was built at the University of Pretoria in South Africa. Polished mild steel is used to secure the insulating wool on the outside of the mild steel shell of the combustion and pyrolysis fluidised beds. Two gate valves are positioned at the bottom of the combustion fluidised bed to remove solids from the system. Three thermocouples are fed through the bottom of the combustion fluidised bed into the bed to measure the temperature inside the bed. A heating element is used to increase the temperature of the combustion fluidised bed to 500°C during the start-up of the system. Once the bed reaches 500°C, LPG is combusted inside the bed to increase the bed temperature to 900°C.

A chain is used to connect the corkscrew agitator inside the hopper to a motor positioned on the side of the hopper. The hopper is suspended from three load cells which are used to measure the rate at which biomass is fed from the hopper. The motor used for the agitator at the top of the hopper is positioned on the opposite side of the hopper to the motor used for the screw-conveyor in order to balance the hopper. A transparent Perspex plate is used as the face of the pneumatic conveyor so that the flow of biomass into the pipelines to the pyrolysis fluidised bed can be observed.

To ensure that the pilot-scale system would perform as required during the operation, three cold run experiments were performed. The performances of the following three areas of the pilot-scale system were evaluated during the experiments:

- The fluidisation of the combustion fluidised bed
- The solids circulation between the pyrolysis fluidised bed and the combustion fluidised bed
- The operation of the hopper and the pneumatic conveyor

At low flow rates of air to the combustion fluidised bed, small bubbles were observed in the centre of the bed. However, at higher air flow rates, the entire combustion fluidised bed bubbled violently and solids spilled over continuously into the overflow standpipe. These solids flowed easily from the standpipe into the pyrolysis fluidised bed and could also be easily transported back to the combustion fluidised bed by means of the screw-conveyor positioned at the bottom of the pyrolysis fluidised bed. The corkscrew agitator was effective in preventing the formation of any clumps of biomass in the hopper. Biomass could also be successfully transported to the pyrolysis fluidised bed by means of the pneumatic conveyor. However, if the flow rate of gas to the pneumatic conveyor was too high, the biomass was forced backwards into the screw-conveyor rather than into the pipelines to the pyrolysis fluidised bed. It is therefore necessary to ensure that the hopper and the screw-conveyor are air tight to equalise the pressure in the hopper and the gas inlet to the pneumatic conveyor and to prevent harmful gas leakages.

8.3 Conclusions on Research Problem

A large quantity of underutilised biomass is produced as a by-product in the forestry sector annually. The pyrolysis of biomass process allows the conversion of this biomass into high-value products, such as bio-char and bio-oil. However, little attention has been given to the design and optimisation of a feasible reactor system for the pyrolysis process. The objective of this project was to provide a feasible solution to this problem through the design, modelling and construction of a scalable dual fluidised bed system for the pyrolysis of biomass process.

The current research provides an overview of the theory, design, modelling, construction and evaluation of a proposed dual fluidised bed system for the pyrolysis of biomass. All of these aspects are summarised in Section 8.2. From these results, it was found that each sub-objective of the current project had been met and that the main objective of the project had been achieved. It is therefore concluded that the proposed dual fluidised bed system designed during this project offers a feasible solution the research problem.

8.4 Implications and Recommendations

This research has provided a preliminary design for a novel scalable dual fluidised bed for the pyrolysis of biomass. This design offers several advantages, which have particular implications for the forestry sector, as follows:

- The research results offer the opportunity for converting the large quantity of biomass in the forestry sector into high-value products, including bio-oil, bio-char and syngas. The bio-oil in particular is a source of many high-value chemicals and can be upgraded to form a liquid bio-fuel, such as bio-diesel. An alternative use is thus provided for the biomass arising in the forestry sector to applications such as pulp and paper making. It will be possible for the forestry sector to shift its focus from the production of traditional wood products to products such as specialised chemicals.
- The bio-oil produced in the dual fluidised bed system can be upgraded to form liquid bio-fuels, which can be used directly in the current infrastructure. The research results therefore offer an opportunity to produce renewable fuels, which may help reduce the dependence of the infrastructure on fossil fuels.
- The dual fluidised bed system allows the separation of bio-char from the pyrolysis products. As a result, it is possible to remove from the biomass the carbon that the biomass extracted from the environment. Therefore the proposed dual fluidised bed system provides a means of removing CO_2 from the environment and is considered to be a carbon-negative system. The large-scale operation of this system may thus help reduce the effects of global warming through the removal of greenhouse gases.
- The form of the bio-char collected from the system is particularly suitable for nutrient replacement in agriculture. Therefore an additional advantage of the separation of bio-char from the system is that the bio-char may be used in environmental management. This bio-char may be fed back to plantation floors in the forestry sector to add nutrients back to the soil and, as a result, aid the growth of further plantations.

Due to the implications and advantages explained above, it is recommended that the forestry sector allocate additional resources to the development and implementation of a large-scale dual fluidised bed system for the pyrolysis of the biomass produced in this sector.

8.5 Limitations

The objective of the current research was to design, model and construct a scalable dual fluidised bed system for the pyrolysis of biomass. As a result, further work is required before the research results can be implemented in large-scale operations. The following limitations formed part of the current research:

- The commissioning and therefore hot run testing of the pilot-scale dual fluidised bed system did not form part of the current project.
- Although the operation of the proposed dual fluidised bed system was designed to be scalable, only a pilot-scale system of the design was built. Therefore additional work is required to design and construct a unit for large-scale operation.
- The preparation of the biomass feedstock for the dual fluidised bed system, which includes the drying and size reduction of the feedstock, did not form part of the current research.
- Additional work is required to determine the economic feasibility of the dual fluidised bed system in large-scale operations.
- The further processing and upgrading of the bio-oil produced in the dual fluidised bed system did not form part of the current project.

8.6 Recommendations for Future Work

A comprehensive overview of the theory, design, modelling, construction and testing of a scalable dual fluidised bed system for the pyrolysis of biomass is provided in this dissertation. However, several limitations of the project were identified. The future work that is recommended for this project is aimed at overcoming these limitations and improving the feasibility of the proposed dual fluidised bed system for large-scale operations. The following future work is recommended:

- Commissioning and hot run testing of the pilot-scale system constructed during the current project must be undertaken.
- A large-scale version of the proposed dual fluidised bed system should be designed.
- An economically feasible method must be found for preparing the feedstock required for the dual fluidised bed system. This preparation must include the drying and size reduction of the wood chips used for the feedstock.
- The economic feasibility of the dual fluidised bed system in large-scale operations must be determined.
- A method must be found to process and upgrade the bio-oil formed in the dual fluidised bed system into a useable product.

8.7 Overall Conclusions and Recommendations

This chapter has summarised the research performed during the current project, including the main results and conclusions obtained from each task performed during the project. These results and conclusions were divided into the following sections:

- A literature study on the theoretical foundation of the current research
- The design of the dual fluidised bed system
- The solids transport mechanism used for the circulation of solids between the combustion and pyrolysis fluidised beds
- The modelling of the two fluidised beds, which included mass and energy balance considerations, the hydrodynamics of the system and reaction kinetics
- The physical design of a pilot-scale system of the proposed dual fluidised bed design
- The construction of the pilot-scale system

From these results and conclusions it was found that the objectives of the current project had been achieved. These objectives were aimed at finding a solution to the research problem of the current project, which was that little attention had been given to the design and optimisation of a reactor system for the pyrolysis of biomass. It was concluded that the proposed dual fluidised bed system designed during the current project offers a feasible solution the research problem.

The large-scale operation of the system design arrived at will offer several advantages, particularly within the forestry sector. These advantages have the following important implications:

- The research results offer the opportunity for the forestry sector to shift its focus from the production of traditional wood products, such as pulp and paper, to products such as specialised chemicals.
- The bio-oil produced in the dual fluidised bed system can be upgraded to renewable liquid fuels, which may help reduce the dependence of the infrastructure on fossil fuels.
- The dual fluidised bed system provides the opportunity for capturing and removing CO_2 from the atmosphere in the form of bio-char. It is therefore considered to be a carbon-negative process and may help reduce the concentration of greenhouse gases.
- The bio-char produced in the dual fluidised bed system can be used to feed nutrients back to plantation floors in the forestry sector, thereby aiding the growth of further plantations.

The objective of the current research was to design, model and construct a scalable dual fluidised bed system for the pyrolysis of biomass. Several limitations of the project were identified with regard to the additional work required before the dual fluidised bed system can be implemented in large-scale operations. The future work recommended for this project is as follows:

- Commissioning and hot run testing of the pilot-scale system constructed during the current project must be undertaken.
- A large-scale version of the proposed dual fluidised bed system should be designed.
- An economically feasible method must be found for preparing the feedstock required for the dual fluidised bed system. This preparation must include the drying and size reduction of the wood chips used for the feedstock.

- The economic feasibility of the dual fluidised bed system in large-scale operations must be determined.
- A method must be found to process and upgrade the bio-oil formed in the dual fluidised bed system into a useable product.

REFERENCES

Babu, BV and Chaurasia, AS (2004) "Heat transfer and kinetics in the pyrolysis of shrinking biomass particle" *Chemical Engineering Science,* 59(10), 1999–2012.

Bowyer, JL, Shmulsky, R and Haygreen, JG (2007) *Forest Products and Wood Science: An Introduction,* fifth edition. Blackwell Publishing, Iowa, USA.

Çengel, YA (2006) *Heat and Mass Transfer: A Practical Approach, third edition.* McGraw-Hill, New York, USA.

Chan, WR, Kelbon, M and Krieger, BB (1985) "Modelling and experimental verification of physical and chemical processes during pyrolysis of a large biomass particle" *Fuel,* 64(11), 1505–1513.

Demirbas, MF (2006) "Current technologies for biomass conversion into chemicals and fuels" *Energy Sources, Part A: Recovery, Utilisation, and Environmental Effects*, 28(13), 1181–1188.

Di Blasi, C (1996) "Heat, momentum and mass transport through a shrinking biomass particle exposed to thermal radiation" *Chemical Engineering Science,* 51(1996), 1121–1132.

Fengel, D and Wegener, G (1989) *Wood: Chemistry, Ultrastructure, Reactions*. Walter De Gruyter Inc, Berlin, Germany.

Göransson, K, Söderlind, U and Zhang, W (2010) "Experimental test on a novel dual fluidised bed biomass gasifier for synthetic fuel production" *Fuel*, 90(4), 1340–1349.

Hagge, MJ and Bryden, KM (2002) "Modeling the impact of shrinkage on the pyrolysis of dry biomass" *Chemical Engineering Science*, 57(2002), 2811–2823.

Karmakar, MK and Datta, AB (2010) "Hydrodynamics of a dual fluidised bed gasifier" *Advanced Powder Technology*, 21(5), 521–528.

Kaushal, P, Pröll, T and Hofbauer, H (2007) "Model development and validation: Co-combustion of residual char, gases and volatile fuels in the fast fluidised combustion chamber of a dual fluidised bed biomass gasifier" *Fuel*, 86 (17–18), 2687–2695.

Kaushal, P, Pröll, T and Hofbauer, H (2011) "Application of a detailed mathematical model to the gasifier unit of the dual fluidised bed gasification plant" *Biomass and Bioenergy*, 35(7), 2491–2498.

Kunii, D and Levenspiel, O (1991) *Fluidisation Engineering*. Butterworth-Heinemann, Jordan Hill, Oxford, UK.

Levenspiel, O (1999) *Chemical Reaction Engineering*. Wiley, New York, USA.

Meier, D and Faix, O (1997) "State of the art of applied fast pyrolysis of lignocellulosic materials – A review" *Bioresource Technology*, 68(1), 71–77.

Murakami, T, Yang, T, Asai, M and Suzuki, Y (2010) "Development of fluidised bed gasifier with triple-beds and dual circulation" *Advanced Powder Technology*, 22(3), 433–438.

Papadikis, K, Gu, S and Bridgwater, AV (2009) "CFD modelling of the fast pyrolysis of biomass in fluidised bed reactors: Modelling the impact of biomass shrinkage" *Chemical Engineering Journal*, 149(1–3), 417– 27.

Perry, RH, Green, DW and Maloney, JO (1997) *Perry's Chemical Engineers' Handbook, seventh edition*. McGraw-Hill, New York, USA.

Robbins, MP, Evans, G, Valentine, J, Donnison, IS and Allison, GG (2012) "New opportunities for the exploitation of energy crops by thermochemical conversion in northern Europe and the UK" *Progress in Energy and Combustion Science*, 38(2), 138-155.

Sinnott, RK (2005) *Chemical Engineering*, Volume 6, fourth edition. Butterworth-Heinemann, Jordan Hill, Oxford, UK.

Wang, X, Kersten, SRA, Prins, W and Van Swaaij, WPM (2005) "Biomass pyrolysis in a fluidised bed reactor. Part 2: Experimental validation of model results" *Industrial and Engineering Chemistry Research*, 44(23), 8786–8795.

Weimer, AW and Clough, DE (1981) "Modeling a low pressure steam-oxygen fluidised bed coal gasifying reactor" *Chemical Engineering Science*, 36(3), 548–567.

Zenz, FA and Weil, NA (1958) "A theoretical-empirical approach to the mechanism of particle entrainment from fluidised beds" *AICHE J.*, 4(4), 472–479.

Zhang, L, Xu, CC and Champagne, P (2010) "Overview of recent advances in thermo-chemical conversion of biomass" *Energy Conversion and Management*, 51(5), 969–982.

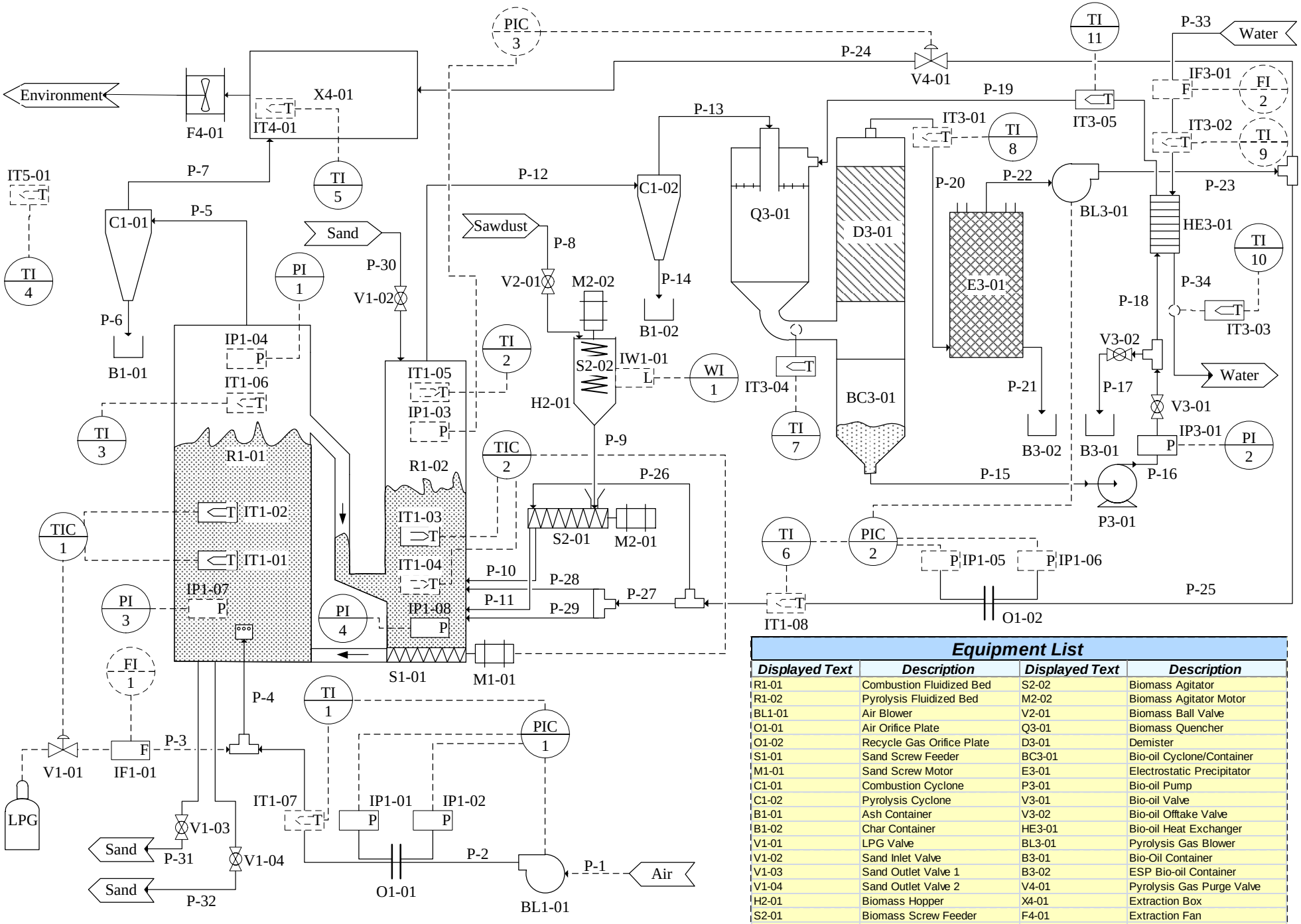

Equipment List

Displayed Text	Description	Displayed Text	Description
R1-01	Combustion Fluidized Bed	S2-02	Biomass Agitator
R1-02	Pyrolysis Fluidized Bed	M2-02	Biomass Agitator Motor
BL1-01	Air Blower	V2-01	Biomass Ball Valve
O1-01	Air Orifice Plate	Q3-01	Biomass Quencher
O1-02	Recycle Gas Orifice Plate	D3-01	Demister
S1-01	Sand Screw Feeder	BC3-01	Bio-oil Cyclone/Container
M1-01	Sand Screw Motor	E3-01	Electrostatic Precipitator
C1-01	Combustion Cyclone	P3-01	Bio-oil Pump
C1-02	Pyrolysis Cyclone	V3-01	Bio-oil Valve
B1-01	Ash Container	V3-02	Bio-oil Offtake Valve
B1-02	Char Container	HE3-01	Bio-oil Heat Exchanger
V1-01	LPG Valve	BL3-01	Pyrolysis Gas Blower
V1-02	Sand Inlet Valve	B3-01	Bio-Oil Container
V1-03	Sand Outlet Valve 1	B3-02	ESP Bio-oil Container
V1-04	Sand Outlet Valve 2	V4-01	Pyrolysis Gas Purge Valve
H2-01	Biomass Hopper	X4-01	Extraction Box
S2-01	Biomass Screw Feeder	F4-01	Extraction Fan
M2-01	Biomass Screw Motor		